Development of a numerical model for dynamic depositioning of non-Newtonian slurries

H.E. Van Es

Delft University of Technology

TU Delft Delft University of Technology

Challenge the future

Cover Image Source: http://www.niehs.nih.gov by Jiri Rezac

Development of a numerical model for dynamic depositioning of non-Newtonian slurries

by

H.E. (Hugo) Van Es

in partial fulfillment of the requirements for the degree of

Master of Science
Offshore & Dredging Engineering

at the Delft University of Technology,

public version

Student number:	4111117	
Supervisor:	Prof. dr. ir. C. van Rhee	TU Delft
Thesis committee:	Prof. dr. ir. J. C. Winterwerp,	TU Delft and Deltares
	Dr. ir. A. M. Talmon,	TU Delft and Deltares
	Ir. L. Sittoni,	Deltares

Deltares
Enabling Delta Life

TU Delft
Delft University of Technology

Preface

This masters thesis has been written for the Offshore and Dredging masters track from Delft University of Technology with specialization dredging. The project has been carried out at and under the supervision of Deltares.

I would like to thank my committee for supervising and supporting me throughout this project. Cees van Rhee for being the chairman and helpful feedback. Han Winterwerp for his critical look and expertise on mud and fine particles. Arno Talmon for his close involvement and interest in this project and in depth knowledge of all processes for both the university as at Deltares. Luca Sittoni for guiding me through the process and helping me putting all the pieces together. Also thanks to employees at Deltares, mainly Jan van Kester and Adri Mourits for guiding me with through the numerical process and Jill Hanssen for a good physical introduction in the subject. My parents and brothers for their support during my entire study and feedback on my writings. Finally i would like to thank my fellow students from Deltares for creating such a nice working environment and good conversations.

H.E. Van Es
Delft, March 2017

Abstract

This study aims to improve the predictive capabilities of flow pattern and depositional behaviour of non-Newtonian, high concentration sand and fines mixtures. The depositional behaviour influences the geometry of the deposit and the distribution of sand and fines particles, which in turn influence the strength and consolidation performance of the deposit. Ultimately this affects the area reclamation targets from the mining industry. In this study an existing numerical model, Delft3D (a three-dimensional, open source flow model from Deltares utilized world-wide in various hydrodynamic and sediment transport studies), is extended with the physics that describe non-Newtonian rheology and sand settling in shear flow. The rheology determines the yield stress and viscosity of a fluid. Shear induced sand settling occurs for fluids with a yield stress. Sand settles under shear whereas smaller particles stay suspended, producing segregation. Segregation leads to non-uniformity in deposit composition (e.g sand and fines dominated areas). Rheology and sand settling mutually interact, directly influencing deposition patterns. This study is a continuation of the work of [Hanssen, 2016], who included specific rheology and sand settling formulation in a one-dimensional version of Delft3D (i.e. 1DV). As part of this work, further verification of this one-dimensional model has been performed and the model has been extended to two-dimensional vertical (i.e. 2DV in a longitudinal cross section). The extended model has been tested in 2DV with deposition over a 400 meters slope. A sensitivity analysis is performed to consider the effect of different solid contents and rheological properties. The model is also tested on specific oil sand applications and data, such as tailings deposition down a beach, mutual interaction of tailings with different rheology or strength and a characterization of fines capture compared with data. This study proved that the extended version of Delft3D can simulate a 2DV non-Newtonian high density flow including sand settling. However there are still some physical processes where the model needs improvements or further research is needed, such as laminar-turbulence regime; transition to 3D and the motion of sand layers. Further model verification and development goes hands in hands with a good data set. Specifically important are flume/field tests with rheology data and its variation with time, especially for polymer added tailings, to verify the model.

Contents

Executive Summary

While providing valuable resources for the society, the mining industry (including oil sands), puts significant pressure on the surrounding environment. After extraction of the desired ore (e.g. iron, gold, bauxite and bitumen) a dense fluid waste product that consists of sand, silt, clay, water, polymers and ore residuals, is often stored in large ponds so solids can settle and water can be recycled. These waste mixtures that are discharged into the pond are called tailings. The problem with this storage process is that the surface area for storage needs to be large and in certain cases (oil sands) the fluid fine tailings do not consolidate to trafficable soil, keeping that area from being reclaimed. These problems, together with the high expenses that are coupled to the use of large quantities of water, have pushed the industry to use less water in tailings. This have shifted these tailings to behave more visco-plastic or non-Newtonian. When tailings are discharged and flow towards the pond, long beaches are produced, generating large deposits with often segregation of sand and fines. The sand settles and forms the beach deposit, whereas the fines remain suspended and form fluid fine tailings, which accumulate in the pond. The fluid fines do not consolidate and need to be retreated. Areas dominated by fines consolidate differently than areas dominated by sand, with repercussion in strength development and reclamation time. Assessment in prediction of depositional and segregating behaviour is therefore critical to best manage tailings deposit (i.e: geometry, beach slope and segregation). A numerical tool that can aid to predict deposition of tailings is currently not available. This thesis intends to work on the development of such a tool.

The objective of this study is to continue the work of [Hanssen, 2016], on the development of a numerical dynamic depositional model. This model should be able to simulate non-Newtonian flow and sand segregation for a broad range of different tailings down a slope. Furthermore the model should be verified against laboratory or field data.

In this thesis some typical physical characteristics of non-Newtonian slurries are incorporated and tested in Delft3D, which is a numerical hydro-morphological model developed and maintained by Deltares. This model is utilized world wide to model river systems, water flows and sediment transport. In this thesis Delft3D is extended with rheology for non-Newtonian flow and shear settling, to be able to simulate the dynamic flow depositional behaviour of different tailings down a slope.

This thesis focuses on two main physical processes, rheology and shear induced settling, which directly influence flow behaviour. These processes and other relevant theory, such as, slope prediction, channelization and lobes formation are described in Chapter 2. Rheology is important because it describes the strength and viscosity of a fluid. Shear induced settling is important because it can be considered the main settlement mechanism in non-Newtonian thick flows. The coupling of rheology and shear induced settling creates a typical tailings flow profile that is critical for rheology and sand settling and therefore also for the deposition. This flow profile consists of three layers:

- Plug player
- Shear layer
- Bed layer

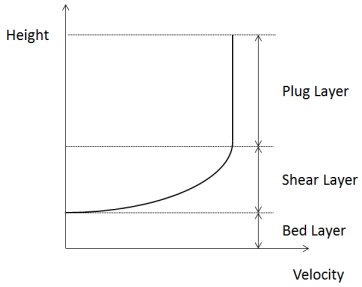

Figure 1: Flow profile of a non-Newtonian mixture with the three layers indicated

The plug layer is the upper part of the flow, here the yield stress of the slurry is larger than the shear stress in the fluid. In thick fluids sand particles stay suspended in the plug layer. The shear layer is the middle part of the flow where the shear stress is larger than the yield stress of the slurry and sand particles start to settle through the fluid due to shear. The bed layer is the bottom part of the flow where sand particles accumulate and form a bed layer with a relative high sand content. Rheological and shear settling formulas in terms of concentration values have already been created and tested in a one-dimensional version of Delft3D in the thesis from [Hanssen, 2016].

In Chapter 3, data on oil sand tailings is provided. This data focuses on fines capture percentages for sand rich tailings. Fines capture represents the amount of fines that are captured within the deposited beach. The capture of fines is a positive effect as the fines that are not captured flow towards the pond producing non-settling fluid fine tailings, which is one of the main reasons for long timescales before tailing basins reclamation. The data set is helpful to test the depositional behaviour of the model, the processes that interact between slurry flow and deposit beaches in the model are to-date still under development. Therefore the match between data and the model can only be qualitative.

The one-dimensional model (1DV version of Delft3D) is used to test the newly added rheology and sand settling processes in the vertical direction. After validation these processes are included in Delft3D, parallel to this work. This is described in Chapter 4. In Delft3D the model is tested in 2DV (i.e. a longitudinal cross section of a beach), for a first estimate of depositional behaviour. The test scenario includes a beach with a 1 % slope and 400 m length before it enters a pond. Eventually the model will be used with a 3D grid and the spatial processes become important for the depositional behaviour. The model to-date focuses on the laminar regime.

The rheological properties of these slurries are calculated with equations that use sand and fines concentrations and empirically determined parameters depending on the characteristics of the slurry. The empirical constants can be determined from rheological measurements of a slurry. Three rheological empirical parameter sets are created in this thesis which are described in the end of Chapter 4. These rheological sets represent different types of tailings.

Chapter 5 includes some numerical improvements to the model necessary to guarantee stability. These improvements are first tested in 1DV. Disturbances in the calculation of the viscosity and depletion of the plug layer are overcome by changes in the numerical calculation scheme. An upwind scheme has been applied to the calculation of yield stress and viscosity to make the solution monotone. The solution retrieves information from the cell beneath, which can only be justified by the fact that the sand fluxes are only downwards, as in laminar regime there is no turbulence or re-suspension mechanism. The numerical switch changes the upwind scheme direction in the plug layer, so only information from the cell above is retrieved. This way the thickness of the plug layer remains unchanged.

Results of the 2DV model and can be found in Chapter 6, which provides the results of flow down a slope for the test beach scenario. A sensitivity analysis is performed to visualise the effects of changes in: solid concentrations; particle size; and rheology properties. From the depositional behaviour it can be observed that most sand particles are settling at the bottom of the slope. The comparison of the 1DV and 2DV model indicate a good agreement in rheology and shear induced settling behaviour. For a definite validation the 2DV model needs to be compared against 2DV flume tests or analytical 2DV solutions. The 1DV model is missing important longitudinal gradients, no one-on-one comparison on deposition behaviour can be made between 1DV and 2DV. A qualitative comparison of the 2DV model with the data set on fines capture is also made. Certain conclusions can not be made based upon these results due to the lack of detailed information (i.e. rheology of fine dominated tailings) and missing focus on flow-bed interaction processes in this thesis. Finally some conceptual attempt results on flow behaviour, when two tailings with different strengths flow over each other, are provided. Strong over weak tailings and weak over strong tailings are presented on the same beach scenario as the other results. The behaviour at the moment is largely dominated by the density differences, mixing processes would also be relevant for future research.

Nomenclature & Abbreviations

General Parameters

$\frac{3V}{H}$	Bulk Shear Rate $[m/s]$
a	Power Constant (Anisometric parameter, reflecting non-sphericity) [-]
A_μ	Viscosity Constant [-]
A_{clay}	Activity Clay [-]
A_y	Yield Constant [-]
B_μ	Viscosity Power Constant [-]
B_y	Yield Power Constant [-]
c	Solid concentration by weight $[\%]$
c_0	Initial Concentration of Solids by Mass $[-]$
$C_{u,clay}$	Undrained Shear Strength Of The Carrier Fluid [Pa]
C_u	Undrained Shear Strength Of The Mixture [Pa]
d	Diameter Of A Sand Particle $[m]$
d_{50}	Median grain size $[m]$
$F_{y,p}$	Upward Force Of The Fluid Its Yield Stress $[N]$
g	Gravitational Acceleration $[m/s^2]$
H	Height of the slurry $[m]$
K	Viscosity index [pas]
k	layer number [-]
k_{visc}	Viscosity Constant Thomas [-]
k_{yield}	Yield Constant Thomas [-]
m	Input parameter that defines slope of flow curve at low shear rates $[s]$
M_p	Mass Of A Particle $[kg]$
M_{SD}	mass of sand particles in the beach deposit $[kg]$
M_{SS}	mass of sand particles in the slurry $[kg]$
n	Flow Index [-]
n_f	Fractal Dimension [-]
P	Power Constant Thomas [-]
PI	Plasticity index [-]
q	Specific Discharge $[m/s^2]$

R_H Hydraulic Radius $[m]$

Re Reynolds number [-]

SFR_D Sand to fines ratio beach deposit [-]

SFR_S Sand to fines ratio slurry [-]

t Time $[s]$

u Horizontal Flow Velocity $[m/s]$

V Mean Velocity $[m/s]$

W Width $[m]$

w Water content [-]

w_{cf} Water Content Of The Carrier Fluid [-]

w_s Fall Velocity of a particle $[m/s]$

z/h Relative Thickness Height $[-]$

α Empirical coefficient for shear settlement $[-]$

α_{cr} Empirical Settling Parameter $[-]$

α_{form} and β_{form} Form Parameters For Segregation [-]

β_v Linear Sand Coefficient for yield stress[-]

β_y Linear Sand Coefficient for viscosity [-]

$\dot{\gamma}$ Shear Rate [1/s]

λ Linear Sand Concentration [-]

μ (Plastic) Viscosity [Pa s]

$\mu_{a,cf}$ Apparant Viscosity of the Carrier Fluid $[Pas]$

μ_a Apparent Viscosity [Pas]

$\mu_{carrrierfluid}$ Viscosity Of The Carrier Fluid [Pas]

$\mu_{mixture}$ Viscosity Of The Carrier Fluid [Pas]

μ_w Viscosity Of Water $[0.001Pas]$

ϕ_{cl} Volume Concentration clay [-]

ϕ_{fines} Volume Concentration Total Fines, Clay or Clay+Silt [-]

$\phi_{sand,max}$ Maximum Sand Concentration [-]

ϕ_{sa} Volume Concentration sand [-]

ϕ_{si} Volume Concentration silt [-]

ϕ_{solids} Volume Concentration Total Solids [-]

ρ_{cf} Density of Carrier Fluid $[kg/m^3]$

ρ_{solids} Density Solids $[kg/m^3]$

ρ_w Density Water $[kg/m^3]$

τ Shear Stress $[Pa]$

τ_0 Bottom Shear Stress

τ_y Yield Stress $[Pa]$

θ Slope angle $[^\circ]$

Abbreviations and Definitions

1DV One-Dimensional Vertical

2DV Two-Dimensional Vertical

BAW Beach Above Water

BAW Beach Below Water

Beach Sand deposition of tailings

COSIA Canada's Oil Sands Innovation Alliance

CT Composed Tailings

Delft3D-Flow Original Three dimensional Numerical Flow Model from Deltares

Delft3D-Slurry Adapted Three dimensional Numerical Flow Model from Deltares with rheological and shear settling equations.

ETF External Tailings Facility

FFT Fluid Fine Tailings

Fines Clay and Silt Particles

fMFT Flocculated MFT

FOFW Ratio of Fines over Fines and Water

M1 Rheological Model 1

M2 Rheological Model 2

M3 Rheological Model 3

MFT Mature Fine Tailings

NST non-Segregating Tailings

Plug A layer in the top of a slurry where the yield stress is larger than the shear stress. All non-cohesive particles stay suspended as they are carried by the carrier fluid, it has a uniform velocity profile so no shear rate.

Segregation Sand particles settle out of a slurry leaving fine particles suspended

SFR Sand to Fines Ratio

Slurry Mixture of sand, fines and water

Tailings Disposed slurries in the mining industry

TRO Tailings Reduction Operations

TT Thickened Tailings

WT Whole Tailings

1

Introduction

1.1. Problem Definition

The mining and dredging industry produce, dispose and manage large volumes of slurry. A slurry is a fluid mixture of sand, silt, clay, water and often polymers. Clay and silt are finer material, defined as fines, they play an important role in the behaviour of slurries. In the mining industry these slurries are called tailings and are a waste product. They are often deposited and stored in large ponds next to the mining facility. In the dredging industry thousands of cubic meters of slurry are moved and deposited to suit human activities. In nature mud flows or land slides are dangerous phenomena that claim multiple lives every year.

Especially in the mining industry a lot of water is used to process all the solid material and extract the product. Although most of the water is recycled it creates large volumes of stored material. This leads to a negative impact on the environment because large natural areas are used for water storage that contain lots of fines and possible toxic left overs from bitumen, minerals and chemical processing. This water problem is pushing the industry towards working with higher density slurry, thus containing more solids and less water. Slurries have specific properties which make the fluid behave differently than water. A slurry is more viscous and has a yield strength unlike water. This is called non-Newtonian behaviour. The focus area of this thesis will be on the oil sands mining industry. Thus a more in depth introduction into mine tailings will be given.

A pipeline discharges the tailings mixture near the pond. The tailings will then flow down a slope towards the pond creating a delta and a beach-like profile of settled sediment. Hereafter it enters the pond so the solids settle and the water on top can be removed/recycled. Environmental regulations demands for improving strength performance of the deposit and water reduction. This has caused the tailings to become thicker, more paste like. These tailings are non-Newtonian fluids, mainly due to the presence of cohesive fines. These fines are the subject of problems in tailing management. When tailings are flowing towards the pond, sand settles and accumulates at the bottom. The sand particles settle much faster than the finer particles and the different particles are separated from each other. This process is called segregation. Segregation produces a sandy bottom layer and leaves a mixture of water with suspended fines, (fluid fine tailings), on top of the flow in which fines do not settle. Once the tailings reach the pond, the top layer consists of these fluid fine tailings. The ponds need to be reclaimed after the end of its life time. The problem is that the pond retains to much water because evaporation estimations of large pond areas are not reached. The evaporation rate is reduced to almost nothing as the top layer of mud dries out and forms a crust that entraps the water and fines beneath. This keeps the pond in a weak and muddy stage, delaying or even preventing the land from being reclaimed.

Before the industry activities scaled up and expanded it was estimated that the mining ponds could be reclaimed after 5-10 years. However with the actual experience gained this period has increased to up to 40 years or more. In recent years governments and activist organizations have emphasized on

environmental issues. Industrial activities should have a minimum impact on the environment. This has led to a large investment in research on minimizing the volume of fluid fine tailings. Intensive technology research is conducted on:

- Thickened tailings (TT). Chemicals are added to fluid fine tailings to speed up the consolidation process. Solid contents that are normally achieved under gravitational forces in periods of up to 5 years are now reached in 30 minutes.

- Non-segregating tailings (NST). Deposition in a way there is no/almost no segregation of sand. Thickened tailings are mixed with existing tailings to create mixtures with high sand content, reducing its volume and increasing the deposit's strength.

- Pumping old water-fines mixture in the sand bed as a kind of storage where the bed captures the fines.

Tailings flow behaviour and the sand segregation process critically influence the geometry and geotechnical characteristics of a deposit, such as areas of high sand or fines content. This dramatically influences the long term consolidation performance and final topography and therefore reaching the targets of reclamation. Understanding of the behaviour and deposition is important:

- To optimise industrial activities and apply the technologies mentioned above.

- To keep the required area for deposited tailings as small as possible and to achieve the best and quickest way to reclaim the land after mining activities. Thus keeping a small environmental footprint.

- for the financial side, costs can be reduced with better management of tailing storage and faster reclamation of ponds.

- It also is important safety wise, as better risk management can be adapted to prevent failure of dams of the ponds that can flood a large area with toxic material from mining activity.

When sand segregates during deposition, fines flow free in the middle of the pond. These fines are not "captured". Fines can be captured by sand trapping fines between the pores of the settled sand. In this case there will be fewer fines that reach the pond and remain suspended in water, which prevents the large ponds from being reclaimed for decades. Fines capture is therefore an important variable.

The 3D effects in tailing deposition are also very interesting. Spatial variations across the surface are present and include processes as channel formation, width, migration and beach slope. This is matter of ongoing research. After being discharged and able to flow free, slurries tend to form beaches. These beaches are very similar to river deltas, even though they are of very different scale. Major differences are the solid content, this is much higher for slurries and the main reason for non-Newtonian behaviour and fines dominance.

A reliable understanding of the behaviour and flow of these slurries is not yet available; a robust model that can improve the management of these tailings is still missing. In this thesis a better understanding of slurries and the entire system process will be the basis for the improvement of an existing numerical model (Delft3D-Flow) to allow for prediction of slurry flow and deposition.

1.2. Objective

The objective of this study is to continue the work on the development of a numerical dynamic depositional model (Delft3D-Flow). This model should be able to simulate non-Newtonian flow and sand segregation for a broad range of different tailings down a slope. Furthermore the model should be verified against laboratory or field data.

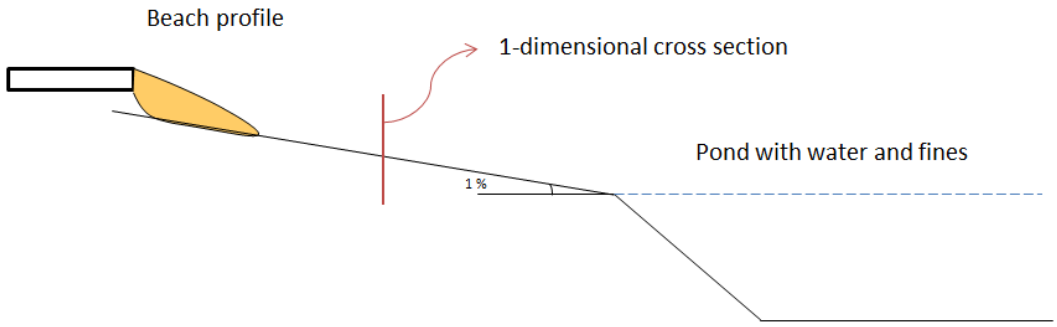

Figure 1.1: Sketch of the 2DV situation, a pipeline that discharges slurry, beach profile and pond are depicted. This thesis focuses on the process of the slurry that take place on deposition of the slurry on the beach.

1.3. Approach

So far there are no models that can predict these slurry flows and associated segregation process. Basic settlement equations have been modelled and tested with flume data but a complete simulation of tailings flow is not possible before this thesis, because the described mechanisms for slurry deposition were not complete. The basic idea is to use the existing morphological model of Deltares, Delft3D-Flow and extend/adapt it to use for slurry deposition. Delft3D-Flow is numerical open-source software that has been validated on the capability to model entire river delta deposits in alluvial environments. This can be very useful regarding the channelization and other morphological characteristics of these slurries.

In a previous study, flow behaviour and sand segregation was studied with a one dimension vertical version of Delft3D-Flow [Hanssen, 2016]. Some adaptions have been made: rheology and shear induced settling have been incorporated in the one dimensional model to simulate the non-Newtonian behaviour of tailings.

In this Thesis the following has been done:

1. Improved the one-dimensional model with a better fitted numerical scheme. This is done because it had instabilities and was not running for high sand contents.
2. Included the new formulation for rheology and segregation to Delft3D-Flow standard (done by Deltares). The performance of this transition is verified by comparison with one dimensional profiles.
3. Carried out a sensitivity analysis to test robustness of the model. This is done for different rheological properties and sand-clay concentrations.
4. Verification against oil sands data for fines capture, to test the depositional behaviour in a two-dimensional environment. This data set does have its ”gaps”. There are no details provided on rheological properties.
5. Tested on oil sands applications, to get a feeling for application of the model.

2

Theory

2.1. Composition Slurries

2.1.1. Basic Classification

Sediment mixtures are composed of three types of solids: sand, silt and clay. A combination of the three gives the ratio of material that determines the characteristics of the soil. This is often done in triangle diagrams, a classification introduced by [van Ledden et al., 2004] and shown in Figure 2.1. Both structural and granular properties of the mixture determine the various characteristics. Percentages are described by weight. The structural effect depends on water content (also pore volume), in respect to clay content. Dashed lines are different pore volumes. The transition between cohesive and non-cohesive material is indicated by the solid line. A mixture can be cohesive or non-cohesive. The transition varies per type of clay. In this case, this is at 7.5% clay and indicated by the solid horizontal line.

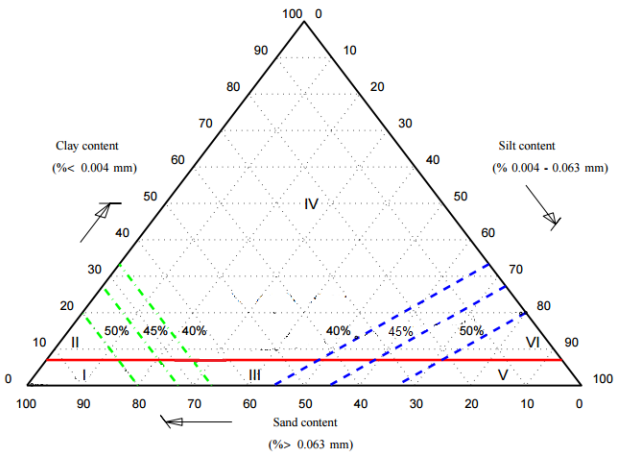

Figure 2.1: Sand–silt–clay triangle with transitions for cohesion and network structure. I=non-cohesive sand-dominated, II=cohesive sand-dominated, III=non-cohesive mixed, IV=cohesive clay-dominated, V=non-cohesive silt-dominated, and VI=cohesive silt-dominated network structure. Source [van Ledden et al., 2004]

Slurries can be separated in two mixtures that define the characteristics.

- The carrier fluid & The entire mixture

The carrier fluid is the medium in which particles are suspended. For slurries this consist of water and fines (clay and maybe silt) that are homogeneously distributed. The entire mixture is, as the name says it, everything. So carrier fluid including sand particles if they are present. The carrier fluid determines whether sand particles stay suspended or settle in static situation and the entire mixture determines the strength and viscosity of the fluid.

2.1.2. Oil Sands

In the oil sands industry many different names for tailings exist, depending on their sand, fines, water content and polymer treatment. In this section some more insight in these tailings and what their role is in oil sands industry is given. A classification of the tailings is given by putting them in perspective in the solid percentage triangle. The differences in tailings depend on solid content, FOFW (Fines Over Fines+Water ratio), SFR (Sand to Fines Ratio) and rheology (which depends on the type of clay). Some important tailings are described below.

- Whole tailings (WT): This is the slurry that is deposited on the beach after separation of bitumen. It contains sand, fines and water from original sand plus recycled water from the mining process. Solid content is about 50% by weight. After deposition the sand will settle and form a beach together with about half of the fines. Note that this is an estimation by the industry.
- Fluid fine tailings (FFT): Thin tailings that are left after whole tailings are segregated. They consist of water with suspended fines that do not segregate, solid content is about 8% by weight. These tailings accumulate at the center of the pond.
- Mature fine Tailings (MFT): Consolidated fluid fine tailings. After a few years the fluid fine tailings have settled and reached about 30% solid content by weight. Further consolidation to increase solid content can take centuries.
- Thickened Tailings (TT): Tailings that underwent thickening process, resulting in less water content. It has a higher sand content but is subjected to sand segregation.
- Non-segregating tailings (NST) or composite tailings (CT): Tailings that are fine-enriched by recycling and mixing FFT with sand and fines to enhance strength that form a paste like material. These tailings are designed not to segregate.

The tailings types that are listed here above may be placed in a ternary diagram (figure: 2.2 from [Sobkowicz et al., 2014]). Their place is based on characteristic solid content, fines content and FOFW. Note that the axes differ from the basic composition shown in figure 2.1, but this gives a good idea of tailings composition. Also the de-watering target for end products from the industry is depicted. Solid concentrations go all the way to 70-80% in these targets.

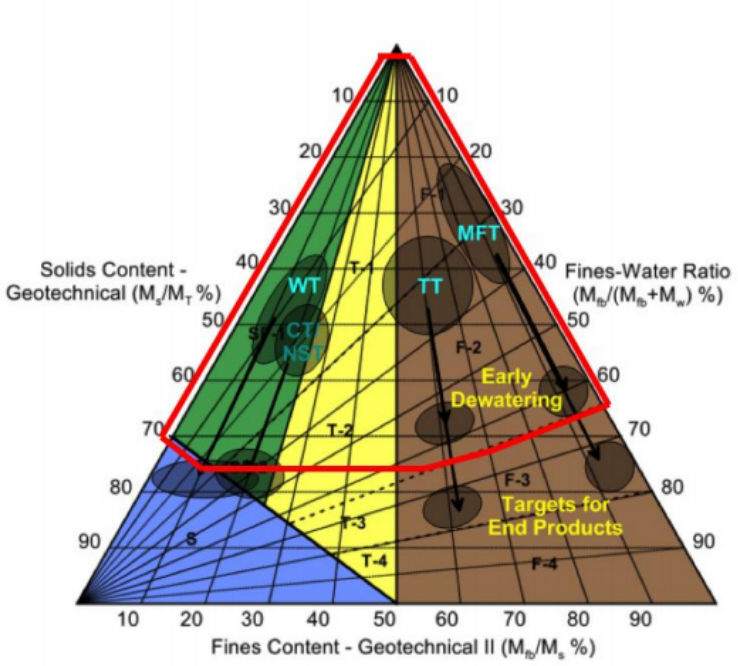

Figure 2.2: Ternary diagram including different oil sands tailings based on their specific characteristics. The blue area is sand dominated and represents sand tailings. The green area is sandy mud and represents sandy-fine tailings (SFR ≥3). The yellow area is muddy sand and represents transition tailings (3 > SFR > 1). The brown area is mud and represents fine tailings (SFR ≤1). The notations T1 to T4 and F1 to F4 are zones that depend on FOFW ratio, they differ in static segregation boundary and plastic limit. S is sand. Source [Sobkowicz et al., 2014]

2.1.3. Tailings Storage Facility

An overview of the tailings storage process is given in Figure 2.3. The figure shows a cross section of a tailings storage facility including volumetric quantities. Tailings are discharged on top of a dyke from a pipeline. Once the tailings enter the pond they will flow towards the centre. The tailings will loose sand as they flow towards the centre. The settling sand forms the beaches and fluid fine tailings remains on top. The FFT consolidate into MFT in the centre of the pond. The figure shows a pond that has been filled completely. In operational conditions this will not be the case and the beach comes out of the water, or in other words the water level is lower.

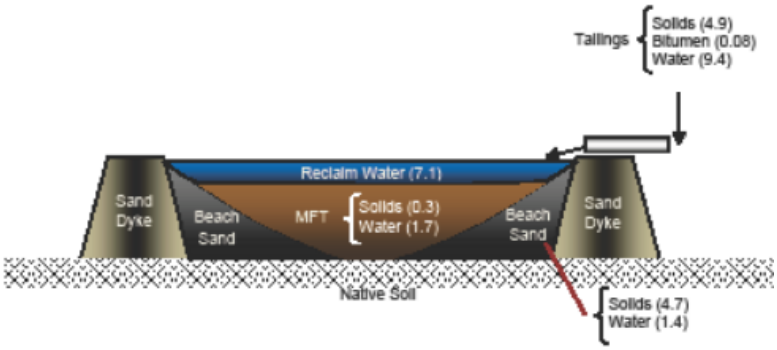

Figure 2.3: Schematic overview of tailing management, depicted is a cross section of a storage facility. Including an indication of volumetric solid and water quantities. Source [BGC Engineering Inc, 2010]

2.2. Rheology

Rheology is defined as the study of the deformation and flow of fluids. Rheology determines the relation between shear stress and shear rate, which is the deformation of the fluid. This is very important because tailings are non-Newtonian fluids. Non-Newtonian fluids have specific rheological behaviour, these fluids have a yield strength and a higher viscosity compared to water.

A rheogram such as Figure 2.4 is the best way to visualise the effect of yield strength and viscosity on the behaviour of a fluid. A rheogram shows the flow curves of a fluid and plots strength and/or viscosity against shear rate. There are different types of fluids that can be divided into the categories:

- Newtonian
- Pseudo-Plastic
- Dilatant
- Fluid with a yield stress
  (a) Bingham
  (b) Hershel-Bulkley

They all have their representative mathematical model that can be found in Table: 2.1. τ is shear stress, μ is viscosity index, $\dot{\gamma}$ is shear rate, n is flow index and τ_{yield} is yield stress.

Table 2.1: Fluid types and rheological models

No yield	**Apparent viscosity**	**Yield strength**	**Rheological model**
Newtonian	Constant	= 0	$\tau = \mu\dot{\gamma}$
Pseudo-plastic	Decreases for increasing shear; 0 <n <1	= 0	$\tau = \mu\dot{\gamma}^n$
Dilatant	Increases for increasing shear; n >1	= 0	$\tau = \mu\dot{\gamma}^n$
Yield stress			
Bingham	decreases to a constant asymptote	>0	$\tau = \tau_y + \mu\dot{\gamma}$
Hershel-Bulkley	Decreases for 0 <n <1 Increases for n >1	>0	$\tau = \tau_y + \mu\dot{\gamma}^n$

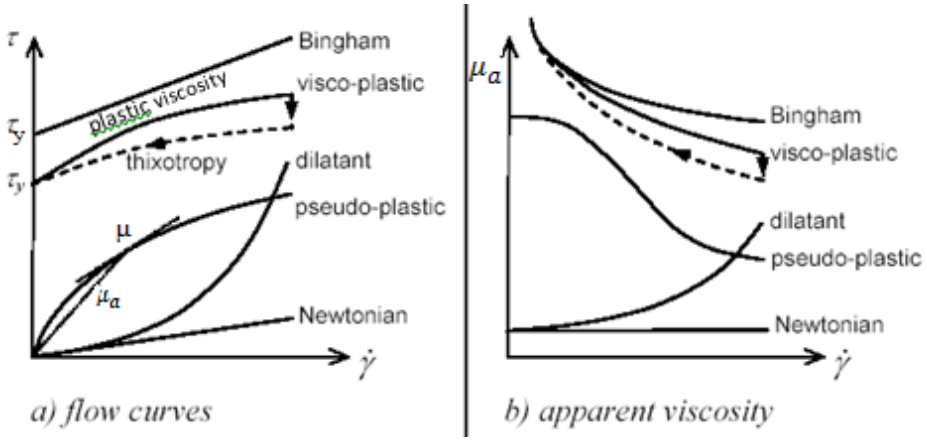

Figure 2.4: Rheograms for: a) shear stress and b) Apparent viscosity. yield stress is τ_y and μ_a is the apparent viscosity. The different fluid types from Table 2.1 are depicted. Source [Talmon, 2016]

The viscosity μ is the tangent of the flow curve and describes the thickness of a fluid at a specific shear rate. The apparent viscosity μ_a is the angle from origin to a certain point on the flow curve, also shown in Figure 2.4 and Eq 2.1. Water has a low dynamic viscosity: $10^{-3}[Pas]$, whereas the magnitude for a non-Newtonian fluid can be of three orders of magnitude higher 10^0. Fluid particles will start moving with respect to each other when shear is applied. This gives a transfer of momentum and thus acts as a force on the particles. The viscosity is the feature of a fluid that gives resistance to this forcing due to the internal friction of layers. The rheological parameters of a fluid are microscopic and difficult to determine; the use of a roto-viscometer or slump test is necessary.

$$\mu_a = \frac{\tau}{\dot{\gamma}} \tag{2.1}$$

2.2.1. Three Rheological Models

In this section there will be a description of three different analytical rheological models. These three models are needed for this study and can be found in [Talmon et al., 2016] and [Hanssen, 2016]. The three existing rheological models describe non-Newtonian fluids in different fields of expertise. The retrieved equations give the possibility to calculate yield stress and viscosity based on solids and water content. All three models have a basis in a Hershel-Buckley fluid for shear stress determination:

$$\tau = \tau_y + \mu\dot{\gamma}^n \tag{2.2}$$

For Model 1 the flow index n ranges from $0 < n \leq 1$ so viscosity is shear dependent. In Model 2 and 3 the flow index $n = 1$ inducing a constant plastic viscosity, so called Bingham models. The symbol ϕ indicates a volumetric concentration. ϕ_{cl} is the volumetric concentration of clay, ϕ_{sa} is the volumetric concentration of sand, ϕ_{sasi} is the volumetric concentration of sand and silt (non-cohesive particles), ϕ_{fines} is the volumetric concentration of fines (cohesive particles), ϕ_{solids} is the volumetric concentration of total solid particles, ϕ_{water} is the volumetric concentration of water and $\phi_{sa,max}$ is the maximum volumetric concentration of sand. The symbol ρ is density, ρ_w is the density of water and ρ_{solids} is the average density of the solid particles. n_f is the fractal dimension, a parameter that describes the coagulation of clay particles. B_y and P are power coefficients needed for the computation of the yield stress. The parameters a and B_μ are power coefficients for the computation of the viscosity. Model 2 has parameter A_{clay}, which is the clay activity. In Model 1 and Model 2 the presence of non-cohesive particles is described by: λ, the linear sand concentration (described in Section 2.4) and β, a coefficient for sand influence. In Model 3 constants k_{yield} and k_{visc} are correlating parameters to account for non-cohesive particles. A_y and A_μ are model coefficients for yield and viscosity respectively.

Table 2.2: The three rheological models

#	Based on work of	Type
Model 1	Winterwerp & Kranenburg	Power-law
Model 2	Jacobs & van Kesteren	Bingham
Model 3	A.D. Thomas	Bingham

Model 1 is based on a clay colloid theory that incorporates self-similarity and fractal dimension theory, described in [Kranenburg, 1994]. This can be found in [Winterwerp and van Kesteren, 2004].

$$\tau_y = exp(\beta_y \lambda) A_y \left(\frac{\phi_{cl}}{1 - \phi_{sasi}} \right)^{\frac{2}{3-n_f}} \tag{2.3}$$

$$\mu = exp(\beta_v \lambda) \left[\mu_w + A_\mu \left(\frac{\phi_{cl}}{1 - \phi_{sasi}} \right)^{\frac{2(a+1)}{3}} \left[\frac{1}{\dot{\gamma}} \right]^{\frac{(a+1)(3-n_f)}{3}} \right] \tag{2.4}$$

Model 2 is based on theory by [Jacobs et al., 2011]. Jacobs modelled the rheology of slurry as a function of water content to the fines, which is practically identical to the ratio of water content w and plasticity index PI, which is a function of solids and clay volume. This model has been used for thick non-segregating tailings in the oil sands industry before.

$$\tau_y = exp(\beta_y \lambda) A_y \left(\frac{\rho_w}{A_{clay} \rho_{solids}} \frac{1 - \phi_{solids}}{\phi_{cl}} \right)^{B_y} \tag{2.5}$$

$$\mu = exp(\beta_v \lambda) \left[\mu_w + A_\mu \left(\frac{\rho_w}{A_{clay} \rho_{solids}} \frac{1 - \phi_{solids}}{\phi_{cl}} \right)^{B_\mu} \right] \tag{2.6}$$

Model 3 is a model based on the work of [Thomas, 1999]. Thomas created a rheological model based on fitted data points using ratio's of slurry over fines characteristics. He found that there is a relation between plastic viscosity and sand volume concentration over maximum sand concentration. This model was developed for mineral mine tailings. The data from his paper was used to calibrate the rheological empirical parameters in his model. The rheological parameters for Model 1 and 2 are also tested on this data set.

$$\tau_y = A_y \left(\frac{\phi_{fines}}{\phi_{water} + \phi_{fines}} \right)^P \left[1 - \frac{\phi_{sa}}{k_{yield} \phi_{sa,max}} \right]^{-2.5} \tag{2.7}$$

$$\mu = exp\left(A_\mu \frac{\phi_{fines}}{\phi_{water}} \right) \left[1 - \frac{\phi_{sa}}{k_{visc} \phi_{sa,max}} \right]^{-2.5} \tag{2.8}$$

2.3. Laminar-Turbulent Transition

The flow state of a fluid can be:

- Laminar. The flow appears in parallel layers with no mixing or disruption of layers.
- Turbulent. A very dynamic flow that is characterized by eddies. It exhibits abrupt changes in flow speed and mixing between vertical layers.
- Transition region. The flow state in between laminar and turbulent flow.

Non-Newtonian fluids in open channels have distinct models for laminar and turbulent flow, and some will be reviewed in Appendix A. In the mining and oil sands industry, slurries tend to flow slowly down the slope in the laminar regime. This is due to lack of re-suspension or upward mixing forces. This causes problems as sand settles out of the slurry in an early phase resulting in a flow with suspended fines for the remaining route. The combination of fluids with strong rheological parameters and slow flow conditions give low Reynolds numbers. However there are many records that report turbulent

flow of tailings, especially in diluted oil sand tailings. For non-Newtonian open channel flow no general accepted model exists for the transition between laminar and turbulent flow. The transition region differs from Newtonian fluids and is not yet completely understood. This has been researched by [Haldenwang, 2003], Haldenwang formulated empirical models for non-Newtonian open channel flow and observed that the transition point for non-Newtonian fluids is lower than for Newtonian fluids. The transition point lies around the order of Re ~ 700 instead of 2100. For this thesis the Reynolds number for laminar non-Newtonian open channel flow from [Slatter, 2013] is considered most important and given in Eq 2.9. This formulation of Reynolds number is most accurate for non-Newtonian laminar open channels, as it has incorporated the rheological properties. This has been described in more detail in Appendix A. In Eq 2.9 ρ is density, V is the mean velocity and $\frac{3V}{R_H}$ is the bulk shear rate where R_H is the hydraulic radius. n is the flow index and is equal to 1 for Bingham models.

$$Re_4 = \frac{8\rho V^2}{\tau_y + \mu_a\left(\frac{3V}{R_H}\right)^n} \tag{2.9}$$

2.4. Sand Influence

The introduction of sand particles in the carrier fluid has an effect on the fluid. It introduces a friction force as well as a non-cohesive particle. The sand particles augment the yield stress and viscosity of mixture. This is called the solids effect, which enhance the rheological properties of the slurry mixture. The presence of sand particles introduces resistance, increasing the total stress in the fluid mixture. This effect was first described for Newtonian fluids by Einstein. One of the first to quantify it with experiments was [Bagnold, 1954]. Bagnold derived a mathematical expression (Eq. 2.10) for the friction factor of sand particles, λ, based on the ratio of particles diameter and distance between the particles. λ is dependent on solids content and can be written in terms of a specific maximum sand content.

$$\lambda = \frac{1}{(\phi_{sand,max}/\phi_{sand})^{1/3} - 1} \tag{2.10}$$

The solids effect for non-Newtonian fluids can be described in the same way, keeping in mind the difference between carrier fluid and entire mixture. This effect essentially is a multiplication factor to convert carrier fluid rheology to mixture rheology.

$$Solids\ effect = \frac{Rheological\ properties\ mixture}{Rheological\ properties\ carrierfluid} \tag{2.11}$$

Some empirical solids effects are based on:

- Krieger-Doughetry type of function described in [Thomas, 1999]

$$\frac{\mu_{mixture}}{\mu_{carrierfluid}} = \left(1 - \frac{\phi_{sa}}{k\phi_{sa,max}}\right)^{-2.5} \tag{2.12}$$

- Exponential function on undrained shear strength with Bagnold friction by [Jacobs et al., 2011]. With C_u is the undrained shear strength of the mixture and $C_{u,clay}$ is the undrained shear strength of the carrier fluid.

$$\frac{C_u}{C_{u,clay}} = exp(\beta\lambda) \tag{2.13}$$

The influence of sand can be visualized by plotting yield stress against w_{cf}, which is the water content of carrier fluid. Different sand to fine ratios are plotted in the graph. The rheological parameters are calculated with use of ”rheological Model 2” and ”Set REF”, see (Section 2.2.1 and Table: 4.3). Both axes are in log scale.

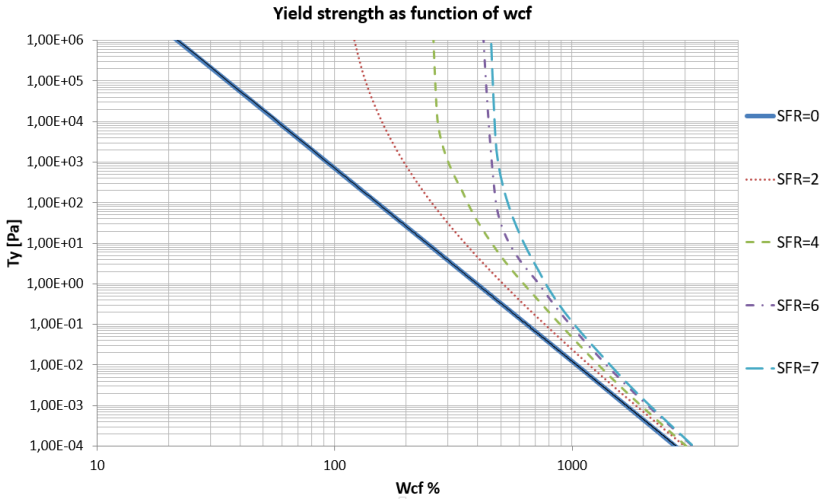

Figure 2.5: Influence of sand on yield stress plotted against the W_{cf}, based on the output of the one-dimensional model. Parameters from rheological Bingham model "Model 2" for Set "REF", (Section 2.2.1 and Table 4.3). Different lines are different SFR's.

2.4.1. Shear Induced Sand Settling

When a fluid is at rest and the gravitational force of a particle in a non-Newtonian fluid is less than the yield stress, the particles will stay suspended in the carrier fluid. However if the fluid is not at rest the carrier fluid is sheared and this will enhance sand settlement. If this shear layer is on a large scale compared to the particle size, the apparent viscosity of the fluid is determined by the shear rate rather than the initial viscosity of the carrier fluid. The apparent viscosity by shear rate is larger than the the initial viscosity of the carrier fluid. This is why the settling of sand particles is enhanced by shear. This process is called dynamic settling or shear induced sand settling.

Here the mechanism for sand settling for a single particle is described. The force balance or settlement criteria (Eq. 2.16) is made by the reduced mass of a particle M_p and the yield stress of the fluid that exhibits an upward force $F_{y,p}$. α_{form} and β_{form} are parameters describing the form of a particle. ρ_s is the density of solids and ρ_{cf} is the density of the carrier fluid. g is the gravitational acceleration constant. d is the sediment diameter.

$$M_p = \alpha_{form}\frac{1}{6}\pi(\rho_s - \rho_{cf})gd^3 \tag{2.14}$$

$$F_{y,p} = \tau_y \beta_{form}\pi d^2 \tag{2.15}$$

$$M_p > F_{y,p} \tag{2.16}$$

In a static situation (i.e no flow) this would lead to a settlement criteria (Eq 2.17) with the empirical parameter α_{cr} ranging from 0.048-0.2 based on a literature survey by [Chhabra, 1993]

$$\tau_{yield} \leq \alpha_{cr}(\rho_s - \rho_{cf})gd \tag{2.17}$$

In a shear flow however the force balance is different due to co-rotating of particles with the shear. The shear stresses acting on a particle in a shear flow are assumed to be equal to the shear rate of the fluid per area, see Figure 2.6. The settling velocity and rotation of the particle influence the direction of the shear stresses. This process is described in details in [Talmon and Huisman, 2005].

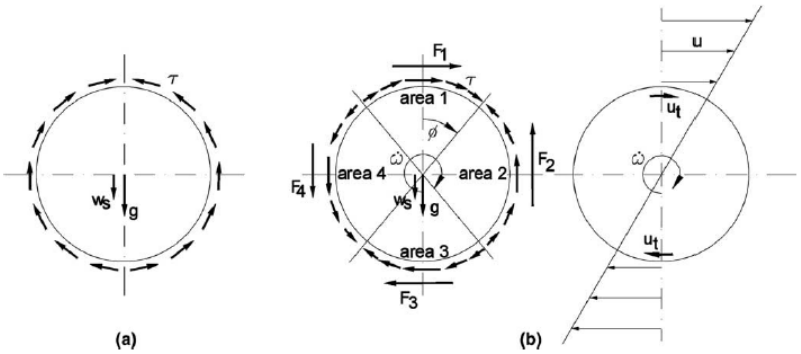

Figure 2.6: Schematized shear stress distribution acting on a particle in static situation (a), with gravitational force and fall velocity. In sheared flow (b), with gravitational force, fall velocity, rotation speed $\dot{\omega}$ and force vectors on different areas. Source [Talmon and Huisman, 2005].

This gives a new force balance with a settling velocity for non-Newtonian fluids w_s similar to the Stokes equation 2.18, where α is an empirical coefficient and $\mu_{a,cf}$ the apparent viscosity of the carrier fluid. This is the settling velocity of a particle that will settle if the internal shear stresses in the fluid are larger than the yield stress.

$$w_s = \alpha \frac{1}{18} \frac{(\rho_s - \rho_{cf}) g d^2}{\mu_{a,cf}} \tag{2.18}$$

There also is the effect of hindered settlement. When many sand particles settle in the same area, those particles will hinder each other. This hindrance can be accounted to different physical processes, some more dominant than the other. The effects of buoyancy and return flow are accounted for. Eq. 2.18 already has the viscosity enhancement and dynamic effects of carrier fluid. Buoyancy effect gives reduction to fall velocity due to the presence of particles. Return flow gives reduction to fall velocity because settling fraction is limited regarding to the minimum porosity. The two hindered settlement effects can be defined in terms of volume concentration following work of Dankers [Dankers and Winterwerp, 2007].

$$Buoyancy : (1 - \phi_s) \tag{2.19}$$

$$Return\ flow : (1 - \frac{\phi_{sa}}{\phi_{sa,max}})^2 \tag{2.20}$$

Equations 2.18, 2.19 and 2.20 together make the fall velocity equation complete:

$$w_{s,eff} = (1 - \phi_s)(1 - \frac{\phi_{sa}}{\phi_{sa,max}})^2 \alpha \frac{1}{18} \frac{(\rho_s - \rho_{cf}) g d^2}{\mu_{a,cf}} \tag{2.21}$$

The requirement for shear settling of particles in non-Newtonian fluids is that the shear stress in the fluid has to be larger than the yield stress. Equation 2.22 shows this requirement. The entire shear settling process is given by equations 2.21 & 2.22.

$$If\ \tau < \tau_y\ Then\ w_{s,eff} = 0 \tag{2.22}$$

The larger sand particles that are affected by shear induced settling have a high fall velocity compared to the fines in a slurry (In this thesis fall velocity for fines is even neglected). This means the sand and fines particles will get separated when the sand settles. This process is called segregation and this will be important further on in this work.

2.4.2. Bed Formation

Once the fluid is moving and sand has started to settle there will be a formation of a sand bed on the bottom. This bed has a higher density than the mixture because of a higher sand content. It can either be granular sand dominant Newtonian flow, or ”gelled” non-Newtonian. In the latter case, introduced by [Talmon and Mastbergen, 2004], the sand particles in the bed do not make contact with the bottom, so there is no Coulomb friction. A granular bed will not flow, forming a stationary bed. A gelled bed

will keep flowing, at a slower rate. These two bed types and the interaction with the bottom are given in Figure (2.7). The maximum solid concentration in the bed before it turns into a loose packed bed is taken around 60% volumetric concentration. Gelled beds have been observed with solid content by volume ranging from 20 to 40 %.

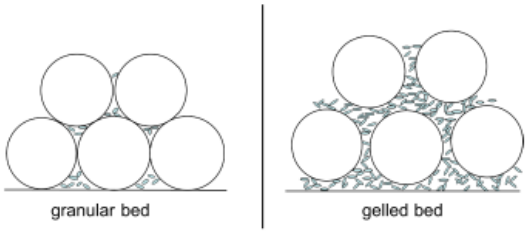

Figure 2.7: Granular bed and gelled bed, schematization of fluid-bed interaction. Source [Talmon et al., 2014]

2.5. Introduction to Flow Down a Slope, (Focus on 2DV)

In this section the processes of rheology and segregation are transferred to a 2DV environment of flow down a slope. non-Newtonian velocity and concentration profiles will be brought to attention. Earlier research and experiments on this topic are covered and some beach deposition profiles are given.

2.5.1. Typical non-Newtonian and Plug Flow

The shear induced settling of sand leads to a deposit at the bottom. This creates a so called beach. Tailings run over this sloped beach while being forced by gravity and discharge. The non-Newtonian behaviour gives a velocity profile that increases concave-up from the bottom until it reaches a point where the velocity will be uniform until the top interface. This layer is the ”plug” layer, and this is a layer where the yield stress of the slurry is larger than the internal shear stress. The consequence is that sand particles will not settle in this layer. The yield stress therefore stays constant in the plug and the velocity does not change here. Essentially the flow consist of three layers. The plug layer, the plug layer is the top part with a uniform velocity profile. A shear layer, this shear causes deformation in the slurry. Depending on settle velocity and time this shear layer will be depleted from sand particles decreasing the yield stress of the slurry in the shear layer. At the bottom the sand particles accumulate and form a bed layer.

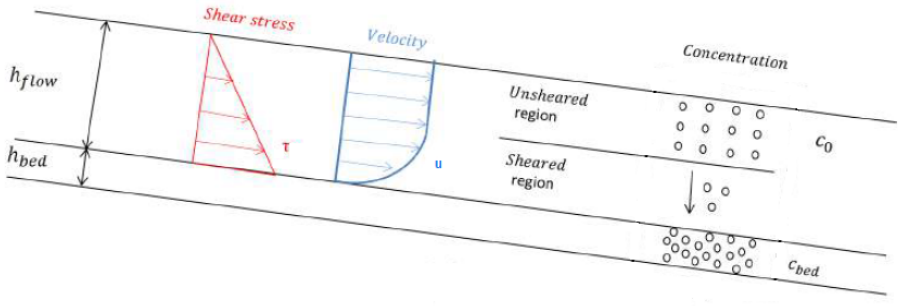

Figure 2.8: Sketch of the three different layers in a non-Newtonian fluid, Bed layer, Shear layer and Plug layer. The profiles for shear stress and velocity are also given and these combine the theory with practise, providing the segregation process for $\tau_y < \tau$

2.5.2. Interaction of Rheology and Segregation on Deposition

The interaction of non-Newtonian behaviour and segregation causes a distinct concentration profile that is constant in the plug layer, then decreases in the plug layer before it increases rapidly when it hits the bed layer. As the bed layer continuous to grow the shear layer will become depleted of sand. After this it becomes interesting, will the plug layer collapse on shear layer or will it continue to flow with constant velocity and concentration. This coupling of behaviour has been researched with experiments in flumes and by analytical approaches.

There are only few physical experiments described in literature that report good detailed non-Newtonian flow and sediment profiles in open channels. These include experiments that are conducted in a half open pipe or a flume. Larger scale experiments are expensive and slurry tailings flow is difficult to measure due to the high concentrations that are present. [Sanders et al., 2002] performed tests in a half open pipe with 15 % volume of fines and two different sand types ranging from 4 to 8 % volume. The fluid had Bingham behaviour and showed the presence of a plug and shear induced settling.

[Spelay et al., 2006] and [Spelay, 2007] used the same flume as Sanders but extended it in length and used different fines and sand concentrations. Spelay described that sand segregation is affected by the velocity in two ways: faster velocity means higher shear that leads to more segregation but when velocity becomes too high flow changes to turbulent regime and segregation is less due to mixing, re-suspension and erosion.

[Pirouz et al., 2013] performed tests on mine tailings, characterized as Hershel-Bulkley fluids in a rectangular flume. Pirouz found typical non-Newtonian velocity profiles with constant plug velocity, the concentration profile did not indicated a shear layer with settling solid content. He did experience the formation of channels inside the flume. This was also the case for flume experiments performed in the [Sisson et al., 2012] report. Sisson developed an analytical model for non-Newtonian fluids that focuses on shear segregation of a power-law fluid. The objective of this model is to get more insight in the prediction of the segregation of sand. With this model the effect of changing input parameters as mixture characteristics and deposition method could be investigated. Experiments were carried out to validate the model. The model calculates the flow velocity and sand concentration profile in time. The model simulates the flow being advected down a beach by using a time-place transformation in a depth average longitudinal direction. It does not model the bed layer, but only the flowing slurry (i.e.: the shear and approximate plug layer). What can be seen is a decreasing sand concentration above the bed layer. The model is strictly speaking valid for a low SFR or very low sand concentration tailings, but it is applied to industrial level sand concentrations. Figure 2.9 shows the theoretical suspended concentration deposition for a flow index of n=0.05. The concentration profile is given by Eq. 2.23. Where c is solids concentration by weight, c_0 is initial solids concentration and z/h is the relative height. The y-axis is the vertical distance divided by total slurry height and the x-axis shows the ratio of actual over initial solid concentration. The time-dependent one-dimensional results are advected with flow down the slope. The time is made dimensionless with 2.24. The multiple lines in the graph show a solid concentration in one-dimensional following a control volume of flow along the beach.

$$\frac{c}{c_0} = \left(t^+ \frac{1/n - 2}{(1 - z/h)^{2-1/n}} + 1 \right)^{\frac{n-1}{1-2n}} \tag{2.23}$$

$$t^+ = \frac{w_s t}{h} \tag{2.24}$$

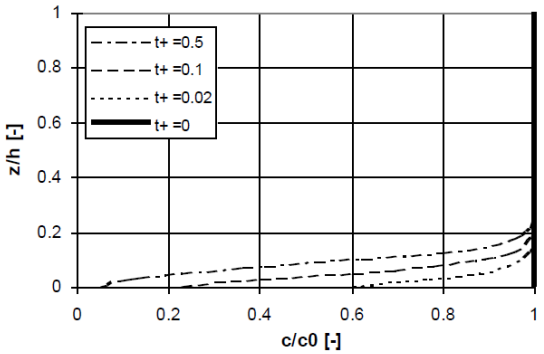

Figure 2.9: Suspended sand concentration profile development in time. Output comes from the analytical Sisson model. Source [Sisson et al., 2012]

2.5.3. Beach Profile Characteristics and Fines Capture

A slurry that has not reached the pond yet, has a flowing front and a distinct profile over longitudinal cross section. There is the morphological moving boundary model (MMB model) described in [Swenson et al., 2014]. They set up a simple one-dimensional model (in length direction) to visualise slurry dynamics with focus on the interaction of fluid with bed layers. It gives Predictions of flow thickness and horizontal propagation time. This model is based on the lubrication theory. The main assumption is that the slurry remains in equilibrium by balance of bed shear stress with yield stress. This gives an indication of what the front of the slurry looks like for different yield stresses. Other processes like segregation and more sophisticated dynamics are not taken into account.

When sand settles and segregates from the other solids, a bed is formed on the bottom. Theories on the shape of this beach profile is given by [Morris, 2004]. The best known profile is a concave beach profile that decreases in thickness towards the pond. In Literature some examples of deposited beaches have been documented. This can be helpful to get a feeling of quantities like height and length of beaches with more realistic dimensions than documented flume experiments. Beach profiles retrieved from [Charlebois, 2012] and [Soleimani et al., 2013] can be found in Appendix B.

Fines capture

Fines capture is a variable used in the oil sands industry. Fines capture quantifies the amount of fines that are captured in the deposited beach with respect to the total fines in the initial deposited slurry. The fines can be captured in between the pores of the larger sand particles. This is dependent on sand void ratio or size of the pores, FOFW or strength of the slurry and flow regime. Fines capture is important because fines that are not captured in the beach are responsible for the MFT inside the pond.

There are two methods to define fines capture, a direct (Eq. 2.25) and a semi-indirect method (Eq. 2.26):

- The direct method quantifies fines capture in terms of mass of fines. Mass of fines in deposited beach $M_{F,beach}$ divided by mass of fines in initial slurry $M_{F,slurry}$ per unit beach volume (Eq. 2.25). Measurements of beach characteristics are performed by gathering of core samples over beach length and determining the solid composition. This method is independent of runoff material and uses average initial and beach characteristics as density, solid content and SFR. Measurements can be more specific if smaller time intervals are used for initial slurry or if the samples spacing of the beach is smaller.

$$Fines\ Capture = \frac{M_{F,beach}}{M_{F,slurry}} \tag{2.25}$$

- The semi-indirect method is not based on direct measurement of fines in beach, but calculates the fines in the beach by subtraction of the initial mass of fines in the slurry with the mass of fines from the MFT that are measured in the pond (Eq. 2.26). This method is more reliable than the direct method as it is independent from beach volume, density and fines content. However it does require the amount and characteristics of the MFT in the pond, which are not always monitored and sampled.

$$Fines\ Capture = \frac{(M_{F,slurry} - M_{F,mft})}{M_{F,slurry}} \tag{2.26}$$

The pore capture model from C. Marsh, (described in [AMEC, Environmental & Infrastructure, 2013]), is able to simulate fines capture for beaches above water. It is a very simple that calculates fines capture based on: slurry density, porosity, SFR of the beach and fines content of the slurry. The main conclusion of his findings are that

- A higher slurry density increase the fines capture.
- Increasing the fines content decreases the fines capture.

2.6. 3D Processes of Flow Deposition

Some interesting morphological behaviour and characteristic of deposition of non-Newtonian slurries in a 3D environment are given. Formation of channels and lobes will be covered as well as other related research and experiments.

2.6.1. Beach Slope Prediction

Depositional systems environments, where a natural or man-made sediment/water mixture fills a broad receiving basin, tend towards concave-up beach slopes over long timescales. This fact is primarily attributable to the gradual removal of sediment from the mixture during transit across the beach, thereby reducing the ratio of sediment to fluid. The progressively thinner, or less sediment containing, mixture therefore requires a progressively shallower slope to maintain transport. While this process is relatively straightforward and predictable for Newtonian fluids, such as those found in most natural river deltas, the range of behaviour common in non-Newtonian tailings slurries complicates predictions of beach slope.

Therefore one of the most researched issues is the prediction of beach slope of the beach above water. The deposition pattern plays a role here and will be treated in subsections. Besides the theory from [Morris, 2004], experiments and models have been set-up to study this phenomenon. Physical experiments that describe the deposition and formation of beaches are mainly performed by Fitton. He mainly studied slope prediction but also the physics and geometry of channels. [Fitton et al., 2007] describes a 3D stacking model that simulated non-segregating slurry channel flow that would end in a diverging sheet flow at the bottom of a channel. Once the resistance of sheet becomes too large a new channel path would form as it takes the path of least resistance. The model produced concave beach profiles due to operational and rheological effects. He also found that the cross section of channels did not have much influence.

[Thomas and Fitton, 2011] created a new beach slope prediction method based on pipe flow physics for three situations, laminar, turbulent heterogeneous and homogeneous. It consist of simple equations that give reasonable estimations on beach slope.

[Fitton and Slatter, 2013] gave an improved beach slope prediction based on rheological properties and plug flow. It incorporates more dense slurry characteristics with higher yield stress and viscosity. This changed the sediment transport mechanism used in his earlier work. Based on a different velocity profile and rheological properties a new formula for slope prediction is derived with more accuracy. It also suggest the effect of laminar flow of tailings and the mechanism behind channelization.

2.6.2. Channel Formation

Beside tailings deposition in sheet flow there is deposition by self-formation of channels. In sheet flow the tailings will flow in a thin layer, spread over a large area, possible stacking up. When tailings run in channel flow speeds are higher and the cross section is much smaller. Channelization was observed in experiments by [Williams, 2001], [Pirouz et al., 2005] and [van Kesteren et al., 2015]. As said in the introduction, this behaviour is similar as in natural alluvial environment, where the flow follows the path of least resistance. There are two issues discussed in this section.

- What is happening with the channels and how are they formed
- What are the characteristics of the channels.

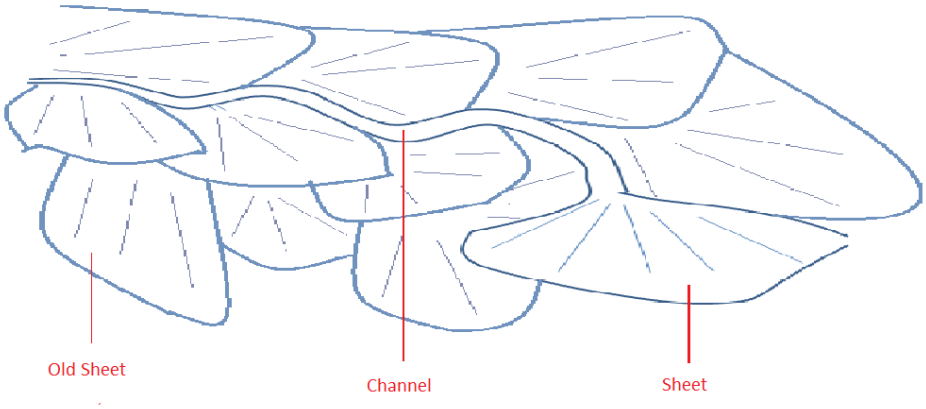

Figure 2.10: Channel deposition schematization

On a tailings beach a (laminar) flowing channel runs down a slope. As it flows down it loses sand in the shear layer at the bottom. The channel rises over time and build its banks higher due to the settling of sand and slowing down of the fluid due to wall friction. Eventually the sheet deposition at the end of the channel builds up too much resistance and somewhere upstream the channels breaks a bank causing the flow to continue in a new direction forming a new channel [Fitton and Slatter, 2013]. The process is shown in figure 2.10

Research to the cross sectional area of a channel has been performed by [Fitton et al., 2007]. He took an analytical approach to test impact of various artificial channel cross sections on slope prediction. Then compared it with actual measured channels (measured at a gold mine) using variable width to depth ratio. He concluded that a different cross section did not have a significant effect on slope prediction but that the best artificial cross section was a parabolic cross section with a 5.5 width to depth ratio.

2.6.3. Lobes

Non-Newtonian slurries that flow down a slope towards a basin, preferable deposit in the upper part of the slope. In the top part a slurry has more sand particles that are able to settle before the slurry is depleted of solids. This leads to steepening of the effective slope, which in turn leads to a higher velocity and deposition further down the slope. The slurry is now transported over a longer distance until the slope reaches a new equilibrium adjusting the slope. This process repeats itself, driving the slurry further and further down the slope. As said before, there are multiple forms of deposits, it can stack up with high yield stresses or flow in channels that are either laminar or turbulent depending on their slope and energy. Besides the rheology or strength of the slurry and beach slope, the volumetric discharge rate influences the deposit. [Charlebois, 2012] observed different depositional regimes during research. He constructed a regime map that indicates depositional regimes for MFT treated with polymers (Flocculated MFT), depending on yield stress and the kinetic energy of the flow (Figure 2.11). Weak slurries tend to channelize and strong slurries tend to stack up one another. When looking a the width of these deposit the stacks are much wider and therefore have a lower flow energy. A channel is

relatively small, and has considering the same amount of material is passing through the cross section, the energy is higher in channels. These stacking can be seen as lobs, already seen in Figure 2.10.

There likely is a cyclical process of lobe to channel to lobe deposition. This process will ultimately adjust the slope of the entire basin to the point that relatively long channels will extend many hundreds of metres, allowing the lowest topography to be filled by lobes. As the deposits evolve over time, the basin floor that a flow will encounter upon entering the basin will become increasingly complex and marked by previous deposition. For example, if a relatively established channel path exists across the existing deposit, subsequent slurry flow may tend to follow this course. So pre-existing low spots (between lobes) or channel paths would tend to focus flow. Thereby increasing its energy, which encourages channelized flow.

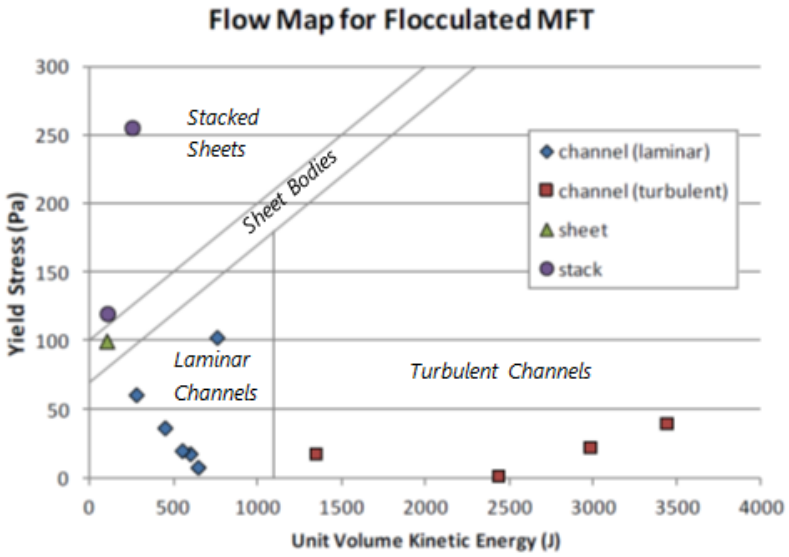

Figure 2.11: Regime map of depositional behaviour observations for flocculated MFT at TRO depending on yield stress and kinetic energy of the flow. Source: [Charlebois, 2012]

2.7. State of the Art

Research in mud and cohesive sediment has been a priority since the new millennium. The main focus for depositional behavior of slurries is on rheology, flocculant behaviour and segregation. These topics are already covered in [Hanssen, 2016]. Latest developments mainly focus on analytical and numerical modelling with beach slope prediction as the main researched issue. Themes as laminar/turbulent transition for non-Newtonian flow, channelization and geometry of flow, thixotropy and consolidation are hot research topics as well. A start of a numerical model has been made in [Spelay, 2007], a one-dimensional environment was used to test the behaviour of coarse particles and the sand settling mechanism in laminar flow. It uses shear-induced diffusion theory and shear settling, transport of solids is described by diffusion fluxes. Results of simulations show the typical plug layer and shear layer but no continuation on this has been made as far known.

The newest development is to make the combination of non-Newtonian flow behaviour and sand settling into Deltares' morphological Delft3D model. Work of [Sittoni et al., 2015] showed the propagation and deposition of different type of tailings on a 400 m beach, including segregation. No specific rheological formulation was used though. Analytical rheological formulas were created to make three different rheological models and they were tested in a one dimensional environment by [Hanssen, 2016]. The next step is to bring the new formulation into Delft3D-Flow and again validate the procedure. Focus will still be on rheology and the segregation process. 3D effects like channel formation and deposition form are for follow-up work.

Recently a 2DV model for thick slurry depositional behaviour has been developed with including rheology and particle settling by work from [Treinen et al., 2010] and [Treinen and Jacobs, 2015]. This 2DV model seems to aim at the same principles as the model being developed in this thesis, although different analytical rheological and settling models have been used. It is very interesting to compare the works of both models and to further improve the development of these depositional models.

2.8. Conclusions on Theory

- Different types of oil sand tailings exist. They can be classified on their solid content, FOFW and fines percentages.
- Laminar-turbulent transition for non-Newtonian fluids often occurs at lower Reynolds numbers than for Newtonian fluids. There is no explicit number for the onset of turbulence for non-Newtonian open channel flow like for Newtonian fluids.
- Sand increases strength of the mixture but at the same time introduces a non-cohesive particle that decreases strength. The gaining in strength is dominant, same as a mortar that becomes stronger with gravel in it.
- Tailings are subjected to segregation due to shear induced settling. A sandier beach layer is formed at the bottom.
- Up to date there is no accurate or widely used numerical model available that is able to simulate high density non-Newtonian flow with included formulations for rheology and segregation.
- This thesis focuses on Section 2.1 to 2.5 and leaves the 3D effects from Section 2.6 for further development.

3

Data on Fines Capture

In this chapter the available data sets will be described and explained. The data subsist of three technical reports, which all review or study the effects on and of fines capture. Objectives of these studies are: to figure out what the main effect of initial concentration of slurry on fines capture is; to examine the effect of adding polymers on fines capture; to investigate what operational aspects influence fines capture, like discharge method and bottom geometry. With the data on fines capture the depositional behaviour of model can be evaluated.

All of the three reports cover a beaching study on oil sands. One of the reports is public and is a review of old and existing commercial oil sand ponds. The other two are confidential and describe experiments performed in a flume and field tests performed next to a larger pond. Preliminary conclusions are made solely based on the data.

3.1. Review on Fines Capture; Studies on Multiple Case Records

In this study [AMEC, Environmental & Infrastructure, 2013] a summary on fines capture of existing commercial tailing ponds (also called external tailings facility, ETF) and performed flume or field tests is given. This will be named the COSIA data set. Research in depositional behaviour and the reduction of total volume of fluid is often performed at locations next to a ETF, at a tailings reduction operations (TRO). Only segregating slurries are considered here. No detailed mass balance for any of the records is available, only global data on fines capture and sand to fines ratios are presented. Since a detailed mass balance is lacking, all the cases compute fines capture with a rewritten version of the direct method. Eq. 3.1 is valid, this is essentially the same as Eq. 3.2.

$$Fines\ Capture = \frac{SFR_S}{SFR_D} * \frac{M_{SD}}{M_{SS}} \tag{3.1}$$

Where SFR_S = sand to fine ratio of the slurry, SFR_D = sand to fine ratio of the beach deposit. M_{SD} is the mass of sand particles in the beach deposit per unit volume and M_{SS} = mass of sand particles in the slurry per unit volume. This can also be written as:

$$Fines\ Capture = \frac{SFR_S}{SFR_D} * sand\ capture \tag{3.2}$$

In the Tables 3.1 and 3.2 the different case records are listed including the resulting fines capture. Table 3.1 categorises all the field tests and gives the operator and the names of the different cases. Table 3.2 gives the belonging SFR for discharged slurry and deposited beach. Combining the SFR of the slurry and the beach with Eq. 3.2 the fines capture can be calculated. In the last column the beach lay-out is given. It tells whether the deposition of a slurry in a facility or test occurs in open air, in a submerged area or both. This is important as it influences the settlement of particles. Commercial scale ponds can have beaches, BAW is beach above water and BBW is beach below water. Small scale flume or field do not qualify for the definition of a beach. These test are indicated with sub-aerial and sub-aqueous. Hereafter a few conclusions on the report will be given.

Table 3.1: Case records, operator, location and year

Operator	Facility/Test	Year	Number
Commercial Scale ETF			
Suncor	Tar Island	Early 1990	1a
Syncrude	Mildred Lake Settling Basin (MLSB)	1st 2002	1b
Suncrude	Auora Settling Basin (ASB)	2000-2009	1c
Shell	Muskeg River Mine ETF overall (MRM)	2003-2011	1d
Shell	Muskeg River Mine north east beach	2008-2011	1e
Canada natural	Horizon Mine ETF	2008-2012	1f
Flume tests and field trials			
Syncrude	Küpper field trials at (MLSB)	1988	2a
Syncrude	Contained 1200 m long beaching trials	1989/1990	2b
OSLO	Contained 100 m long beaching trials	1991	2c
Syncrude	Contained 300 m long spiking trials	1993	2d
Syncrude	Field monitoring	2004	2e
Total	Contained flume test	2011	2f

Table 3.2: Case records, fines capture and beach layout. The layout is mentioned in beaches for large scale facilities and in sub-aerial/aqueous terms for flume and field tests.

number	SFR_S	SFR_D	Fines capture [%]	open air/submerged
1a	7.4	11.7	63	BAW&BBW
1b	3.88	6.6	62	BAW&BBW
1c	4.15	5.34	77	BAW&BBW
1d	4.54	6.5	70	BAW&BBW
1e	2	3	65	BAW
1f	3.53	6.2	57	BAW&BBW
2a	2-4	10-20	20	Sub-aerial
2b	4.3	6.7	64	Sub-aerial&Sub-aqueous
2c	3-4	10	30-40	NA
2d	3-7	13-14	20-30	NA
2e	4	12	37	Sub-aerial
2f	4-17	10-35	40-60	Sub-aerial

The conclusion of flume tests and the operational ponds with respect to fines capture is that beaches below water have a significant larger fines capture than beaches above water. This is due to a lower flow speed and hydraulic gradient, so there is less energy present in the system at beaches below water. Less energy leads to less segregation. Because the study was very general and mainly focused on fines capture, there is no further specific information for every case on discharge, slope or concentration input other than sand to fine ratio's. No specific data on rheology is given.

3.2. Flume Tests from 2011

In 2011 a study was performed on the capabilities of a sand bed to capture fines. The objective of this study was to evaluate the concept of storing fines in the voids of sand when oil sand tailings are deposited as a beach. The report investigates the initial assumption from the industry that 50 % of the total input fines by weight is captured in the initial beach. The benefits of the addition of more MFT to slurry is also evaluated. This is done to increase strength of the slurry and lower segregation. In the study three types of coarse sand were used and one fines dominated mixture. The sands were characterized by their SFR ratio, based on their original ore grade. Sand is considered as all particles larger than 44 micron.

1. High grade (HG); SFR = 18
2. Medium grade (MG); SFR = 9

3. Low grade (LG) SFR; =6

4. Mature fine tailings (MFT); SFR = 0.01

The setup of the experiment was to create a deposit in a flume with the three different tailing sands. The flume dimensions were: Length 8 m, Width 0.25 m, Height 0.5 m and a 1 % slope. When the deposit was formed, samples of the deposit were taken. The weight of the sand and fines fractions were measured and compared with the slurry feed. This way fines capture could be computed, which is done with Equation 3.3 where $M_{F,beach}$ is the mass of fines in beach and $M_{F,slurry}$ is the mass of fines in the slurry feed. This is also a form of direct method for calculating fines capture.

$$Fines\ capture = \frac{M_{F,beach}}{M_{F,slurry}} \tag{3.3}$$

Before the slurry was pumped into the flume, the mixture was completely homogenized in a mixing tank with a volume of 1500 L and a mixer with two impellers. The mixed slurry had a volume of 600-800 L. To achieve the best homogeneous result only 400 L of the slurry was used to avoid inadequate mixing or entrain air. Then the mixture was poured into the flume with a 25 mm diameter pipe and at an angle of 45 degrees from the top of the flume, so 0.5 m above flume bottom. The drainage of the slurry was done by slowly opening the rubber plugs at the end of the flume, located a little above the bottom (not exactly described). This drainage could have led to erosion of the settled beach but no erosion was assumed. After the drainage, the beach was allowed to settle for 24 hours before final samples were taken. So consolidation occurred. Table 3.3 shows the feed input variables of the slurry. Experiments used different feed mixtures; mixtures with only one of the sand types, mixtures with sand and MFT and mixtures with sand, MFT and chemicals. MFT is added to some samples to simulate the effects of thickening the tailings this was done in various amounts. Chemicals were added to look at the effect of flocculation of clay particles on fines capture. The addition of MFT and chemicals have their effect on initial concentrations and therefore on the SFR.

Table 3.3: Flume tests from 2011; Slurry feed input

Experiment ID	**System**	**Density [kg/m^3]**	**SFR**	ϕ_{sand}	ϕ_{clay}
C1	HG only	1511	16.4	0.29	0.018
D1	HG + MFT	1469	6.1	0.24	0.041
D7	HG + MFT x 2	1525	5.9	0.27	0.047
D8	HG + MFT x 2 + chem	1360	4.6	0.18	0.040
C2A	MG only	1477	9.3	0.26	0.029
D2	MG + MFT	1478	6.4	0.25	0.040
D4	MG + chem	1473	6.5	0.25	0.039
D6	MG + MFT x 2	1435	3.8	0.21	0.056
D5	MG + MFT + chem	1445	5.4	0.23	0.043
C3	LG only	1436	7.7	0.23	0.031
D3	LG + MFT	1499	7.1	0.27	0.038

The tests were set up by pumping approximately 400 L into the flume with a discharge of 100 L/min. No more than five minutes were needed to fill the flume and after one hour the flume was drained. The runoff was separated and analysed. Then the slurry was allowed to settle for 24 hours. There were three moments of measuring, directly after discharge, two hours after discharge and 24 hours after discharge, when the beach had settled.

The measurements consisted of: four depth gauges to measure beach profile, located 1, 2.6, 4.4 and 6.4 m from the flume inlet; two ”gamma radiation” meters to measure concentration profiles, located 2 and 6 m from flume inlet. These gamma meters can measure the concentration over the entire vertical profile and give a better understanding of beach consistency and density. After 24 hours, four core samples from the beach were taken at the same location of the four depth measurements. These core samples were split into two so there will be eight samples in total. The samples were subjected to the following analyses.

- Wet sieving + laser diffraction (Particle size distribution)
- Composition (solids, water and bitumen)
- Methylene Blue Index analysis (clay content)
- Permeability and void ratio

The outcome variables of the beach are listed in Table 3.4. What can be seen is a relative high volumetric concentration of sand and low volumetric concentration of fines. This gives high SFR's and probably low rheological parameters, but no further information on them is given. Note that the boundary at the end of the flume is initially closed and later opened so the flume could be drained. The start boundary is affected by pit deposition. The input feed of slurry concentrations is a good indication for oil sand tailings consistency. The fines capture percentages give an indication of the amount of fines that are "not captured", don't settle and are the cause for fluid fine tailings and MFT.

Table 3.4: Flume tests from 2011; Slurry Beach output

Experiment ID	**Density [kg/m^3]**	**SFR**	ϕ_{sand}	ϕ_{clay}	**Fines Capture [%]**
C1	1890	35.4	0.54	0.015	**45.83**
D1	1860	12.3	0.49	0.040	**54.97**
D7	1881	19.8	0.53	0.027	**40.63**
D8	1577	10.0	0.34	0.034	**76.92**
C2A	1850	18.2	0.50	0.028	**56.69**
D2	1815	10.8	0.47	0.043	**64.29**
D4	1919	13.7	0.54	0.039	**63.76**
D6	1884	14.4	0.51	0.036	**17.27**
D5	1639	7.7	0.36	0.046	**88.41**
C3	1860	20.1	0.52	0.026	**53.01**
D3	1858	16.1	0.51	0.032	**50.63**

Notice that the fines capture in this study is not computed by dividing the slurry SFR with beach SFR but actual mass measurements. Conclusions of these tests are: if there is mainly coarse sand in the system, as in experiments C1,C2A and C3, the solids settle very quickly since the carrier fluid has few to no fines. If looked at the deposited beach profile, the first part of the flume has a large deposit whereas the second part almost has no beach.

The influence of MFT addition is visible, more MFT means a higher FOFW ratio and therefore a higher yield stress of the carrier fluid. This causes a more uniform deposition of sand particles and more possibilities of the beach to capture fines. However this is not always the case, in experiment D6 the fines capture is significant lower than all other cases. Even though more MFT has been added to this experiment. Probably there are other factors to which the fines capture is more sensitive than only initial feed concentrations and polymers. Another effect of MFT that can be seen is that if two times as much MFT is added, the fines capture decreases. This probably has to do with the relative small length of the flume and the ability of stronger slurry to carry more particles. There is an optimum for FOFW content which lies between 10-13%. If the FOFW increases, higher than 15%, it has a negative effect on fines capture in this study as a high amount of fines remained suspended and were lost when the flume was drained.

The effect of the chemicals or polymers caused an increase in fines capture. Because fines coagulate easier with chemicals, they are more subjected to settlement. The beach slope is even more uniform. When comparing the three different types of used sand, HG sand is able to capture more than MG and LG. Due to more settling particles that can capture the fines between the voids. This is not seen in fines capture percentage and can be confusing, but this is caused by the fact that the initial fines concentration was lower with HG sand.

3.3. Beaching Trial for Oil Sands

This is a report based on four field test completed in an oil sands mine. The objectives of the tests were to study the effect added polymers to the tailings and to test the discharge method. The polymer is ”alum”, a chemical to bind the clay particles together to enhance rheological properties and settling of fines. The discharge method is either a series of ten smaller (8 inch) pipelines named ”spigots”, that create a uniform flow down the slope. Or one large 26 inch open pipe that allows fluid and material to form sheet flow down the slope.

The four test areas were constructed by pushing sand to the sides and to the discharge end to create a berm or dyke. At the far end of the area there was no berm, so it could be considered open-ended. Although there was an open end, the different bottom geometry of the four areas still caused some form of containment in the longitudinal direction. This containment has the affect that the slurry is hold back or slows down. The containment effect was most significant for Area 4.

Table 3.5 gives general input information like discharge method, added polymers yes or no, discharge rate, running time and distance travelled by the slurry or the length of beach deposition. Table 3.6 gives information on input slurry, density and concentration of sand and fines.

Table 3.5: Field tests input information parameters

	Discharge Method	**Polymers**	**Q [m^3/s]**	**Time**	**Beach length [m]**	**Level of Containment**
Area 1	Spigots	No	1.47	1h 13m	75	Medium
Area 2	Spigots	Yes	1.35	2h 28m	180	Low
Area 3	One large pipe	Yes	1.33	2h 53m	85	Medium
Area 4	One large pipe	Yes	1.2	2h 08m	155	High

Table 3.6: Field tests slurry characteristics of concentrations

	Density [kg/m^3]	**solid content [%]**	ϕ_{sand}	ϕ_{clay}	**SFR** $_S$
Area 1	1599	60.8	0.31	0.055	5.8
Area 2	1657	64.3	0.36	0.040	9.3
Area 3	1628	62.6	0.33	0.052	6.8
Area 4	1590	60.2	0.32	0.047	6.9

After deposition, the beach characteristics are determined. Average run time is about 2h 15m, then the beach SFR is determined by in-situ testing and laboratory tests. Fines capture is calculated with Equation 3.2, so again the direct method. Results are shown in Table 3.7.

Table 3.7: Field tests output information of beach concentrations

	Dry Density [kg/m^3]	**SFR**$_D$	**Sand captured [%]**	**Fines captured [%]**
Area 1	1537	11.8	78	38
Area 2	1547	12.1	58	45
Area 3	1584	11.5	35	21
Area 4	1581	12.6	98	54

Conclusions from the report were that Area 4 had the highest fines capture due to the containment effects. This is a highly positive effect for fines capture because it allows the fluid to slow down and decrease the amount of energy in the system which increases the fines settlement. This effect outweighs the negative effect on fines capture when using one large diameter discharge pipe that will cause a sheet flow in upper part of area. Spigots give a more uniform flow and better environment for fines to settle. Area 3 has the lowest fines capture, probably affected by the use of one large diameter pipe instead of spigots, considering that the containment effects between Area 1, 2, 3 are not that different. The difference between Area 1 and 2 probably is the effect of added polymers but can also be addressed to other effects.

3.4. Overview of the Data Sets

To get a better feeling for the differences in fines capture all field tests, experiments and pond data are bundled together in a graph. Two field tests have been given a trend line. These are the Küpper and OSLO field tests. These two performed experiments with different slurries but in similar topography conditions. This gives the ability to compare the individual test by slurry input with each other without significance effects on containment. Figure 3.1 provides all the discussed cases from the three reports. Fines capture on the vertical axis and SFR of the input slurry on the horizontal axis. Figure 3.2 provides the fines capture percentage against actual fines in the initial slurry. This way a more physical definition of fines capture is described. This fines capture rather depends on the ability of the slurry to form a flocculated clay structure and the amount of clay concentration. Not all records have enough detailed information to retrieve clay content and some case record do not comply cohesive requirements. Three data points are not in the cohesive regime, one from the flume tests 2011, one from Kupper and OSLO field tests. The other data points are assumed to be beyond gelling point so a clay network structure can be formed. This graph does not provide a relation between the initial clay concentration of the slurry, which will determine rheological properties, and fines capture.

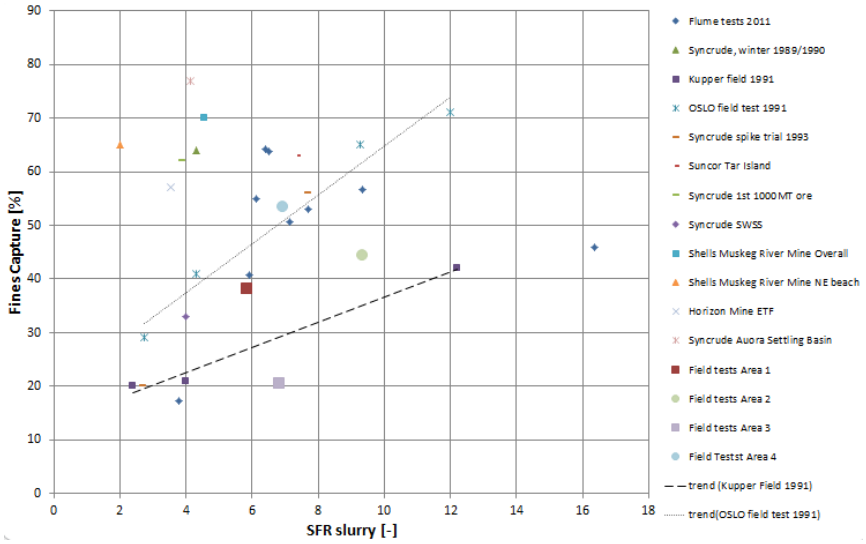

Figure 3.1: Case records; Fines capture plotted against input slurry SFR

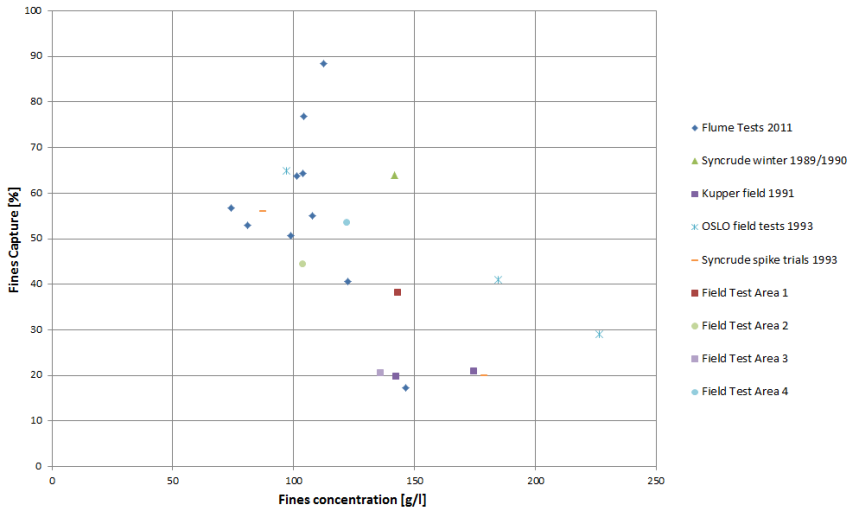

Figure 3.2: Case records; Fines capture plotted against initial fines content of the slurry

3.5. Conclusions on the Data Sets

- Overall no consistent conclusion can be drawn upon the graphs with fines capture relationships.
- Tests with same bottom topography characteristics (Küpper and OSLO field tests) do show a trend. Higher SFR in slurry means more sand to capture fines so higher fines capture but also less fines in material to begin with.
- There are no rheological properties in the entire data set.
- Containment is a very important factor for fines capture. Independent from the input SFR the geometry has a large influence on depositions. This is due to a lower kinetic energy in contained areas which leads to lower flow speeds and improved settlement. This is also the mechanism for BAW and BBW. A BBW has less energy, so a better settlement of sand.
- Increasing the density of the slurry means an increase in fines capture. This is achieved by increasing sand content, as an increase in fines content yield to a decrease in fines capture due to a large bearing capacity.
- For the comparison with a slurry model, only field tests are of importance, the flume experiments performed in laboratory are too specific at this point and the commercial ponds do not have enough information or are not described in enough detail. Field test often only have a BAW which limits the complexity of retrieved data. These are therefore more favourable than tests with both BAW and BBW.
- The review on fines capture is very general and not into the details. Some individual reports from these cases were found and they contain more information. At this point the most interesting case that was found is Küpper. Because it showed different tests with similar topography, this means that changes in fines capture do depend on other factors like initial concentration and rheological properties of the fluid. This report is used later on in the thesis.

4

Models Background and Approach

In previous studies, [Van De Ree, 2015] and [Hanssen, 2016], research towards high density non-Newtonian slurries was performed and the start was made for the creation of a predictive slurry flow model. Summarizing the findings in proceeding research, relevant physical processes are computed and described in [Talmon et al., 2014]. Rheology and shear induced settling of slurries have been examined and formulations for these processes form the backbone of the new slurry model. The beginning of modelling these processes was made in one dimension, in a vertical cross section. This will be referred to as the 1DV model. In this chapter this 1DV model will be discussed and the transition to Delft3D-Flow, to form a three-dimensional model, will be described. Furthermore a typical set-up is provided that functions as a test case to validate the behaviour in the extended Delft3D-Flow model.

4.1. Description of the 1DV Model

The 1DV model describes a single flow profile in vertical direction, therefore one-dimension vertical model. The 1DV model is suited for the investigation of vertical processes. Therefore it is a great way to study new processes and equations in rheology and sand settling. The model starts flowing with a homogeneous mixture, consisting of sand, water, clay and possibly silt, at time zero. The fluid is forced by a changing horizontal pressure gradient due to a gravitational force and discharge rate. As the 1DV model propagates in time it is possible to approximately simulate a flow down a slope. The slurry travels with an average longitudinal velocity if this is multiplied with time, an estimation for covered distance can be achieved. Obviously this is not realistic. However it does give the ability to study a typical situation. This situation is illustrated in Figure 4.1. A slurry is flowing down the slope, forming a shear layer where the yield stress is surpassed by the shear stress and a plug layer where the yield stress of the fluid is larger than shear stress. In the shear layer the slurry loses sand, forming a bed layer on the bottom with accumulated sand particles. The shear layer will be completely depleted of sand particles after time. The plug thickness does not change because the sand particles stay suspended here and therefore the yield stress of the slurry in the plug does not change. If a bed is formed, the flow height will increase because the model keeps the same specific discharge rate over the vertical. This means that a bed layer at standstill and same plug velocity give an increased thickness of the slurry.

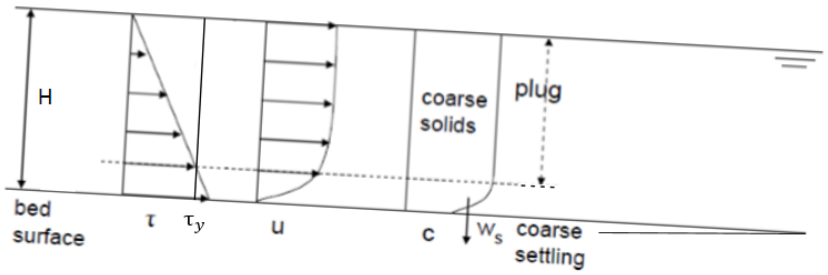

Figure 4.1: Schematic overview of flow along slope including sand settling mechanism. When the yield stress τ_y is larger than the shear stress τ there will be no shear rate and therefore no sand settling. This indicated the plug layer. H is the height of the flow, u the horizontal velocity profile and c the concentration profile.

4.1.1. Main Processes in the 1DV Model

Delft3D-Flow is a model that is based on the shallow water equations derived from the Navier-Stokes equations to simulate alluvial systems and river delta's. The main equations are documented in the Delft3D Manual [Deltares, 2016] and they are summarised in Appendix D. In the 1DV model the shallow water equations are adapted and simplified, only the vertical direction is considered. This is already documented in [Hanssen, 2016] and also summarised in Appendix D

The slurry is characterized by a carrier fluid and entire mixture. The carrier fluid consist of water and fines. It can carry the sand particles when strong enough in a static situation. When the slurry is moving it is subjected to shear and this influences the settlement.

Implemented Rheological Models and Sand Settling Equation

There are no general models for different types of rheological behaviour. Analytical rheological models are based on different theories and efforts. The choice between rheological models was made based on multiple considerations: described rheology, available information and the expertise of local contacts that could provide lots of background information. Multiple analytical rheological models have been analysed and three of them have been selected to be represented in the new slurry model. Two of these models are Bingham models, the other is a power-law model that simulates the effect for Hershel-Bulkley fluids. The latter is based on fractal dimension theory of flocks. For the definition of the rheological models see Section 2.2.1 or [Hanssen, 2016] and [Talmon et al., 2016]. The properties of the entire slurry will determine what rheological model should be used in a simulation. Some slurries behave like a Bingham fluid so a Bingham model is favourable, others are behave more like Hershel-Bulkley fluid so rheological Model 1 is favourable.

- Rheological Model 1 (M1): Fluid with Hershel-Bulkley behaviour
- Rheological Model 2 and 3 (M2 and M3): Fluid with Bingham behaviour

Depending on the structure of the carrier fluid: water, water and clay or water clay and silt, the general rheological equation (Eq. 2.3 to 2.8) will slightly differ. This is dependent on the silt fraction that can be part of the carrier fluid but can also act as a non-cohesive particle.

A segregation model is included based on work done by [Talmon and Huisman, 2005]. This is described in Section 2.4.1. The boundary layer at the bottom is considered as a gelled bed, based on work by [Talmon and Mastbergen, 2004], [Pennekamp et al., 2010] and [Talmon et al., 2014]. This means that there is no mechanical interaction between individual particles or particle and bottom interaction, so there is an absence of Coulomb friction.

Validation of the 1DV Model

The 1DV model was compared to one of the few public available and detailed data in [Hanssen, 2016]. The mentioned data is original flume data by [Pirouz et al., 2013]. A simulation was performed with the same input parameters as that of one of the experiments. The velocity profiles of the simulation and the experiment were compared and they corresponded. This experiment was performed in a 10

m length flume. This made the simulation very short, only 6 seconds. In reality a slurry can flow for multiple hours along a 500-1000 meter sloped beach. In this study the larger data set based on actual field data from Chapter 3 will be used as new step in the verification of the model.

4.1.2. Main Assumptions of the 1DV Model and Composition of Slurries

To get an overview, the main assumption of the 1DV model are listed below:

- **Shallow water equations**, the vertical pressure distribution is hydrostatic.
- **Laminar flow state**, because slurries with high solid concentrations moves rather slow and the transition to turbulent flow for non-Newtonian open channel flow is not yet consented on.
- **Homogeneous carrier fluid**, meaning that there will be no settlement of clay particles. The time scales in these tailings flows are not that long so settlement of clay particles can be neglected.
- **Only shear induced settling of particles is regarded**. The static settlement of particles is neglected because it is assumed orders smaller than shear induced settling.
- **Uniform sand particle size**, as it is used as input in the segregation equations.
- **A no-slip condition is present at bed boundary**, which means that the velocity at the bottom is zero.
- **No thixotropy is considered**. This is the strengthening of material over time. This is definitely present in slurries and should be looked at in a later stage.

For the 1DV model three slurries have been defined. This is done to further test the model and to validate the rheological and sand settling equations.

- **Slurry I** does not contain sand and only has 10 % clay content by volume. This slurry is a general case with only carrier fluid. This is done to be certain of the rheological behaviour and flow profile.
- **Slurry II** has low sand content (4 % by volume) and high clay content (16 % by volume). This slurry has the original concentration used in the thesis report of [Hanssen, 2016]. It was composed to create a relative large shear layer to properly notice the effect of segregation.
- **Slurry III** has high sand content (36 % by volume) and low clay content (7.5 % by volume) concentration. This slurry is composed to achieve a higher Sand to Fine Ratio (SFR) which is more common in recent tailings and the oil sand industry. This phenomenon is caused by the de-watering of tailings. Also it gives a view of the broad range of possible tailings to simulate.

Slurry II and III were used in simulations from the paper [Sittoni et al., 2016]. Important parameters of the three slurries are listed in Table 4.1. c Is the solid concentration by weight and d_{50} is the median grain size . The density of water is taken as 1000 kg/m^3, also for the rest of the report. The yield stress and plastic viscosity are based on the entire slurry.

Table 4.1: Input parameters for the three different slurries in the 1DV model.

	I No sand	**II** SFR 0.25	**III** SFR 5
Discharge q $[m^2/s]$	0.1	0.1	0.1
Slope [-]	0.01	0.01	0.01
Time [s]	0-3000	0-30000	0-10000
ρ_{sand} $[kg/m^3]$	2650	2650	2650
ρ_{clay} $[kg/m^3]$	2600	2600	2600
$d_{50,sand}$ [μm]	250	250	250
$d_{50,clay}$ [μm]	0.08	0.08	0.08
$\rho_{mixture}$ $[kg/m^3]$	1160	1322	1720
c [%]	22.4	39.5	67
ϕ_{sand} [-]	0	0.04	0.36
ϕ_{clay} [-]	0.1	0.16	0.075
τ_y mixture $[Pa]$	2	37.5	20
μ mixture $[Pas]$	0.75	4	5

4.2. Description of Delft3D-Flow

Delft3D is open source software from Deltares, see `http://oss.deltares.nl/`. It allows 3D modelling to investigate water hydrodynamics, sediment transport and morphology. The main module is Delft3D-Flow which couples hydrodynamics and sediment transport processes in time in a 2D or 3D environment.

Delft3D has lots of experience in modelling deltas and river dynamics. This can be a useful attribute, because tailings deposition show similar morphological behaviour. Tailings flow down a slope and form a deposit. This deposit can differ and range from: spreading sheet flow to self-formed meandering channels through existing deposits.

4.2.1. Extension to Delft3D-Slurry

Delft3D-Slurry has its origin in Delft3D-Flow. This model is being extended in such a way that it can deal with slurries. This extension is called Delft3D-Slurry. The basic idea of this slurry model is to extent the standard Delft3D-Flow code with rheological properties and shear induced settling of sand particles.

Once the 1DV model has been tested and all the processes described earlier are working correctly, the next step can be made: implementing the code that describes rheological properties of the fluid and sand segregation into Delft3D-Flow. Basically this means that Equations 2.3 through 2.8 for rheological properties and Equation 2.21 for shear induced settling are implemented in Delft3D-Flow. The transition of these equations from 1DV to Delft3D-Flow has been performed by Deltares employees and tested by the author.

4.2.2. Delft3D-Slurry, a 2DV Model Approach

The Delft3D-Slurry model is priorly tested in a 2D environment before moving on to 3D. Effectively it is modelled in Delft3D but only with one cell width and a number of choice for longitudinal and vertical cells. This means it is two-dimensions vertical, therefore it is named as a 2DV model. To verify the transition from the 1DV to Delft3D-Slurry model, 1DV results are compared with 2DV results and later on with data from the available data set. Many data is based on flume tests, this is essentially a 2DV environment, so this makes it a logical step to first test a 2DV case.

4.2.3. Typical Set-Up in 2DV

To test the output of the model similar conditions as the 1DV model are used. The layout of the cross section is as in Figure 4.2. This figure describes a generic cross sectional view of a slope, which will be the main format in the model simulations. The top boundary where the slurry is discharged from a pipeline is called the ”CELL” which is a small horizontal zone that account for pit forming effect. A long beach follows, where tailings flow towards the pond. Beach slope angles are usually around 1%. This section is called the ”Beach Above Water” or BAW. After this section, the tailings flow into the pond. The pond has a steeper beach, with slopes around 4 %. This is called the ”Beach Below Water” or BBW. Finally the slurry reaches the lowest part of the pond which is a horizontal zone with MFT and water on top. This is called the ”pond centre” or PC.

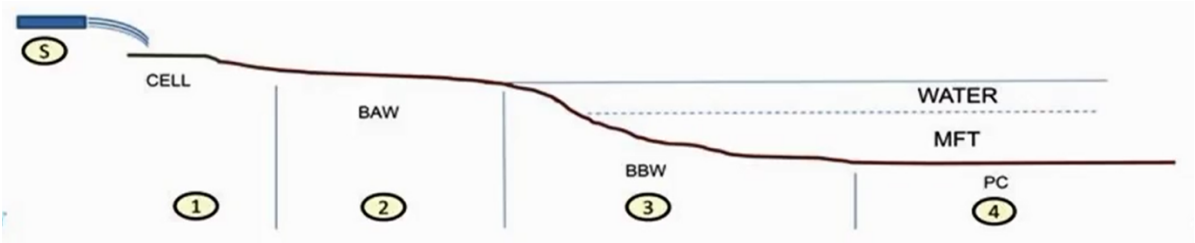

Figure 4.2: Schematic overview of flow along slope. S = slurry, 1 (Cell) is discharge pit, 2 (BAW) is beach above water, 3 is beach below water and 4 is the pond centre.

To get a feeling for the dimensions of this cross section some more estimations of distances and given. The length of the cell is approximately 10 - 20 m. The length of BAW ranges from 400 - 1000 m with

a slope of 1 %. The BBW ranges from 40 - 100 m with a slope of 4 %. The distance to pond centre has a length of approximately 200 m.

4.2.4. Boundary Conditions in 2DV

In the typical set-up from Figure 4.2 the boundary conditions are of high importance. The imposed boundary dictate how the solution will look like. The 2DV set-up has a begin boundary and end boundary. At the begin boundary the slurry is being discharged. At the end boundary the slurry has reached the pond and this pond is being sustained at a certain water level. It is an open boundary where fluid can leave the computational grid.

Begin and end Boundaries

The discharged slurry at the top of the slope consist of a mixture of water and solids. This can be the same over entire time interval but can also be different at specific time intervals. (i.e the discharged can be turned on and off). Both the velocity and concentration distribution start uniform. The pond at the bottom of the slope has been imposed with a fixed water level. Excess fluid can be drained off out of the computational grid. It is a weakly reflective boundary. This means that short waves or instabilities can cross the open boundary without being reflected. These short waves are likely at the start of a simulation. Because the flow runs over a dry beach, there is no connection between the two boundaries at the start. This creates some instabilities or short waves before the solution will converge to a steady solution. Described in detail in [Deltares, 2016]. The reflection parameter is set at 100.

Bottom Boundary

The adhesion of the fluid is of importance when modelling viscous fluids. The adhesion of a slurry at a solid boundary is makes it stick to the boundary, the cohesion force makes the fluid stick to itself. If this adhesion effect is larger than the cohesion is sticks to the bottom and effectively this means that at the bottom the velocity is zero, a no-slip boundary. In the 1DV model the bottom roughness is switched off and the vertical viscosity term changes, directing the flow at bottom to zero. In the Delft3D-Slurry model this cannot be modelled the same, due to different numerical approaches. A different way to model a no-slip boundary is implemented in the Delft3D-Slurry code. The velocity in a fictive cell bottom cell (k_{max+1}) has the same magnitude but opposite direction of the velocity at the bottom cell (k_{max}). This means the velocity at the bed has a zero velocity gradient and the velocity at the bottom is being languished. This is modelled as:

$$u_{kmax} = -u_{kmax+1} \tag{4.1}$$

Eq. 4.1 should be give the same desired effect, however it does not for the slurry fluids. The standard Delft3D-Flow model has a ”slip” boundary condition based on the roughness the bed. To still simulate a no-slip boundary, the bottom roughness or friction coefficient is made very large. The used friction relation is Chezy, Eq 4.2. A low Chezy number gives large friction. This pushes the velocity to at the bottom to zero and once the first sand particles settle, this roughness effect does not not matter anymore.

$$\frac{\lambda}{8} = \frac{g}{C^2} \tag{4.2}$$

A relation between yield strength to account for the stickiness or adhesion with a solid boundary is needed, this can be seen as a Bingham law-of-the-wall. This creates a slipping fluid but at low velocities. For now the method with low Chezy number is used, but this is an temporary solution.

4.2.5. Rheological Parameters

The parameters for rheological equations 2.3 through 2.8 depend on rheological measurements. The 1DV model uses a rheological parameter set that is based on experimental data on a mineral sand tailing from A.D Thomas [Thomas, 1999]. The values for M3 are determined in this paper. Subsequently the rheological parameters for M1 and M2 are derived at a shear rate of 1 $[1/s]$. In Table 4.2 the original rheological input parameters from Thomas are listed. Note that the original viscosity constant coefficient was fitted on data in $[mpas]$. This data set has been adapted to be represented in $[Pa]$. These parameters can be used in the three rheological equations from Section 2.2.1. These parameters are needed to compute the rheological properties of the slurry and give yield stress and viscosity.

Remarks regarding M1: the viscosity parameter is determined at a shear rate of 1 $[1/s]$. M2: the clay activity was not incorporated yet, but the ratio of water density over solid density · clay activity (ρ_w over $\rho_{solids} \cdot A_{Clay}$) is taken as 1. With the estimation that ρ_w over ρ_{solids} are 1000 and 2650 kg/m^3 the clay activity is effectively taken as 0.378 so this ratio stays 1. The clay activity is therefore practically left out of the equation for now, but literature indicates a value around 0.5 - 5.0 for clay activity.

To make the numerical computation of shear stress and viscosity in the plug possible, a modification for shear stress can be used, similarly as work from [Papanastasiou, 1987]. This is also described in more detail in [Hanssen, 2016]. Eq. 4.3 comes from [Mitsoulis and Zisis, 2001] and gives this modification, parameter $m[s]$ is an exponential coefficient that defines the slope of the flow curve for low shear rates. A higher m gives a closer approximation of Bingham behaviour but stays an approximation nonetheless.

$$\tau = (1 - exp(-m\dot{\gamma}))\tau_y + \mu\dot{\gamma} \tag{4.3}$$

Table 4.2: Rheological input parameters, based on data set from [Thomas, 1999]. With viscosity in [Pa s]

M1		M2		M3	
ϕ_{max}	0.6	ϕ_{max}	0.6	ϕ_{max}	0.6
A_y	7.3E+05	A_y	6.72E+04	A_y	7.45E+05
n_f	2.64	B_y	-4.75	P	5.61
β_y	0.275	β_y	0.275	k_{yield}	1.5
A_μ	9.32	A_μ	2.51	A_μ	-44.5
a	3.65	B_μ	-2.64	k_{visc}	1.25
β_v	0.275	β_v	0.275	m	5E+03
m	5E+03	m	5E+03		

To get a better feeling for the rheological behaviour like shear stress, plastic and apparent viscosity the flow rheograms for this parameter set is given in Figure 4.3. The applicability of shear range for these slurry flows is from 0 to 30 $[1/s]$. In the apparent viscosity rheogram the two Bingham models are flattened for higher shear rates, axes are on log log scale. The shear stress rheogram is almost horizontal which indicates a low plastic viscosity and is on normal scale.

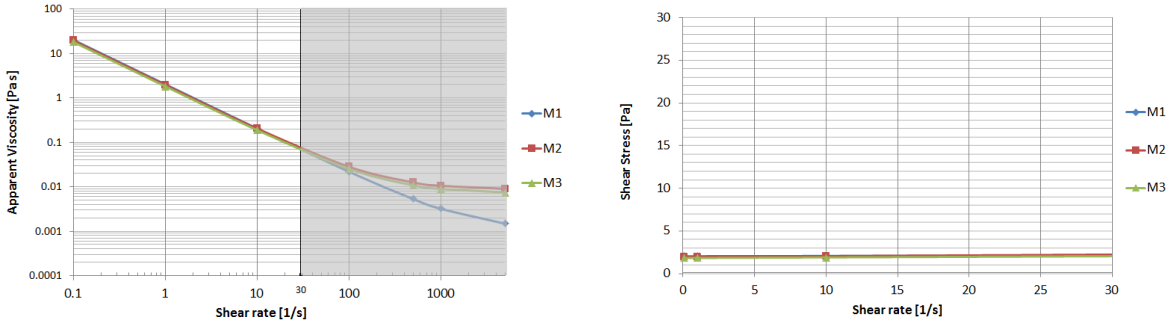

(a) Rheogram for the apparent viscosity of the parameter set from Table 4.2. The shear rate range that is applicable is the white area, higher shear rates are unrealistic and are indicated by the grey area.

(b) Rheogram for the shear stress of the parameter set from Table 4.2

Figure 4.3: Rheograms for apparent viscosity and shear stress from Table 4.2

In the report of [Hanssen, 2016] page 63 it states that the overall viscosity was increased by a factor 100. This was done because otherwise the was no visible shear layer, since there was no range for possible solutions. The rheogram is almost horizontal because of a very small plastic viscosity. There was no room for different solutions at the specific shear rates. For rheological models M1 and M2 the viscosity is changed by multiplying the actual viscosity constant coefficient with 100, in M3 the viscosity coefficient is an exponential function and therefore changes by a different factor. In Table 4.3

the parameters for the increased viscosity are given. This is done in order to make everything explicit. This parameter set is used for all simulations in the 1DV model, so for the calculation of the yield stress and viscosity from Table 4.1. This rheological parameter set will be referred to as **Set REF**.

Table 4.3: Rheological input parameters, Set REF for all three rheological models. With an increased viscosity by factor 100.

Set REF (Based on [Thomas, 1999]), Enhanced Viscosity					
M1		M2		M3	
ϕ_{max}	0.6	ϕ_{max}	0.6	ϕ_{max}	0.6
A_y	7.3E+05	A_y	6.72E+04	A_y	7.45E+05
n_f	2.64	B_y	-4.75	P	5.61
β_y	0.275	β_y	0.275	k_{yield}	1.5
A_μ	932	A_μ	251	A_μ	-3.03
a	3.65	B_μ	-2.64	k_{visc}	1.25
β_v	0.275	β_v	0.275	m	5E+03
m	5E+03	m	5E+03		

The rheograms for this increased plastic viscosity are given in Figure 4.4. The increased plastic viscosity mainly affects the Bingham rheological models M2 and M3. M1 with Hershel-Bulkley behaviour is less affected by the increased plastic viscosity due to the present shear rate in the calculation of shear stress and plastic viscosity. This enhanced viscosity gives more possibilities for solutions.

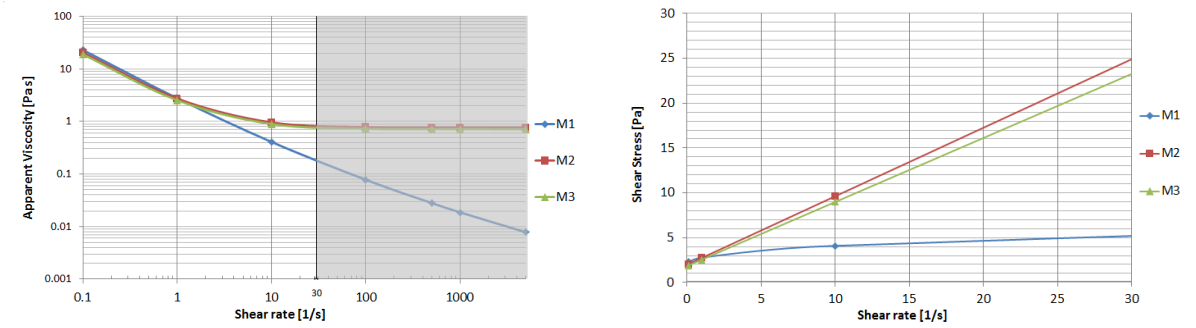

(a) Rheogram for the apparent viscosity of the parameter set from Table 4.3. The shear rate range that is applicable is the white area, higher shear rates are unrealistic and are indicated by the grey area.

(b) Rheogram for the shear stress of the parameter set from Table 4.3

Figure 4.4: Rheograms for apparent viscosity and shear stress from Table 4.3

The effect of increasing the plastic viscosity with a factor 100 does not only influence the flow state by increasing the shear layer, it also influences the fall velocity of particles. The fall velocity of sand particles is dependent on the apparent viscosity of the carrier fluid. This apparent viscosity will not be a hundred times larger but does have its influence on the total segregation of sand particles. To keep a realistic view on the segregation process, the particle diameter can be enlarged by a factor that is equal to ratio of the apparent viscosity of the increased slurry viscosity over the original slurry viscosity. This is still an idea and not yet used in the calculations/simulations further in this report.

4.2.6. Rheological Parameters Oil Sands

To make a comparison with the data set from Chapter 3 there is a need for different rheological input parameters, other than used in the 1DV model. The rheological parameters listed in Tables 4.2 and 4.3 are specific for a mineral sand tailing. In order to model oil sands the rheological input parameters for these kind of slurries need to be determined. Compared to other mine tailings the oil sands have different properties in shear stress and viscosity. The rheological parameters for oil sands are based on a project done by Deltares [Personal communication], (named as oil sand Case A) and determined in Appendix E. This Case A was the one of few available data set for oil sands present at Deltares. Now that there is a feeling for rheological parameters that represented oil sands, the parameters can

be tuned in a way that they represented specific tailings like MFT treated with polymers (flocculated MFT - fMFT) and TT. These different parameter sets are finally compared with fitted data from case records that represents these tailings. For fMFT a public case is available: [Diep et al., 2014], for TT a confidential case from Deltares is available: Case B, [Personal communication]

Table 4.4 shows the two different rheological sets:

- **Rheo Set 1**, can be seen as values for fMFT and is compared with fitted rheological data from [Diep et al., 2014]
- **Rheo Set 3**, can be seen as de-watered TT and is compared with fitted rheological data from project Case B.

Note that the parameters are only given for M1 and M2. M3 is not included because it has very similar behaviour to M2 and has been determined empirically on data from a mineral sand tailing by (A.D Thomas). Also the plastic viscosity has a higher coefficient than realistic values, for the same reasons stated before. This is not exactly a factor 100, but in the same range. The rheograms that compare the rheological parameter sets with case records show that this is still in range of possible solutions.

Table 4.4: Rheological input parameters oil sands. Set 1 and 3 for rheological Model 1 and 2.

Rheo Set 1 "fMFT"				Rheo Set 3 "TT"			
M1		M2		M1		M2	
ϕ_{max}	0.6	ϕ_{max}	0.6	ϕ_{max}	0.6	ϕ_{max}	0.6
A_y	1.1E+04	A_y	1.725E+04	A_y	5.1E+04	A_y	2.0E+05
n_f	2.3	B_y	-3.2	n_f	2.38	B_y	-4.0
β_y	0.58	β_y	0.58	β_y	0.2	β_y	0.2
A_μ	150	A_μ	20	A_μ	965	A_μ	130
a	2.6	B_μ	-1.6	a	2.6	B_μ	-1.6
β_v	0.54	β_v	0.54	β_v	0.36	β_v	0.36
m	5E+03	m	5E+03	m	5E+03	m	5E+03

The rheograms for the oil sand tailings are compared with fitted data from industrial activities. The rheological parameter sets were fitted on these data lines so they do not match completely. However they lie in the range of possible outcomes, indicated by the dashed lines that give a boundary by a limited fractal dimension for these kind of slurries, $2 \leq nf < 3$. From these rheograms it can be seen that the parameter sets chosen to represent the oil sands are in correct range, but depending on the behaviour of the slurry matches Bingham M2 or Hershel-Bulkley M1. The initial yield stress for fMFT (60 Pa) is slightly higher than the data fit by Diep et al (25 Pa). but expected is de-watering of the material which makes the fitted data stronger eventually. The initial yield stress for TT seems in range of the data fit at (90 Pa).

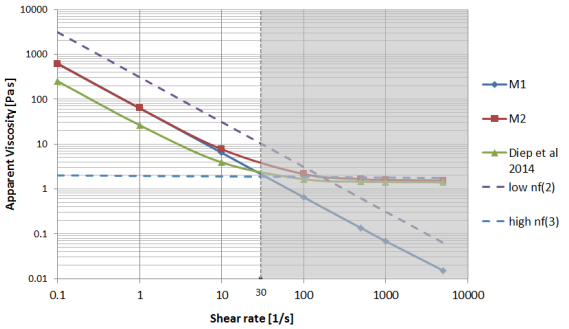

(a) Rheogram for the apparent viscosity of the parameter set from Table 4.4 for Set 1 "fMFT". The shear rate range that is applicable is the white area, higher shear rates are unrealistic and are indicated by the grey area

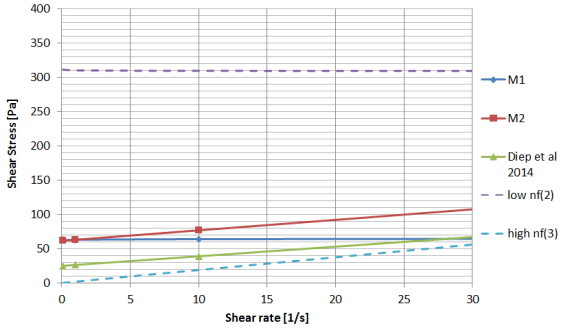

(b) Rheogram for the shear stress of the parameter set from Table 4.4 for Set 1 "fMFT"

Figure 4.5: Rheograms for apparent viscosity and shear stress from Table 4.4 for Set 1: "fMFT".

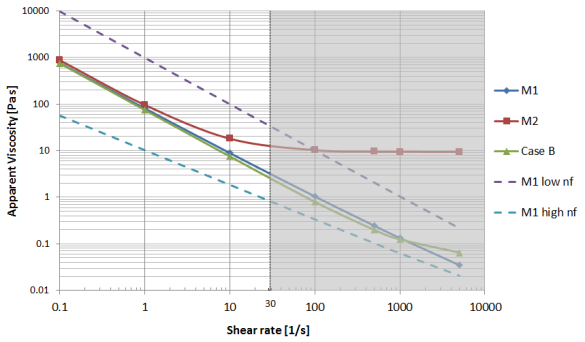

(a) Rheogram for the apparent viscosity of the parameter set from Table 4.4 for Set 3 "TT".The shear rate range that is applicable is the white area, higher shear rates are unrealistic and are indicated by the grey area

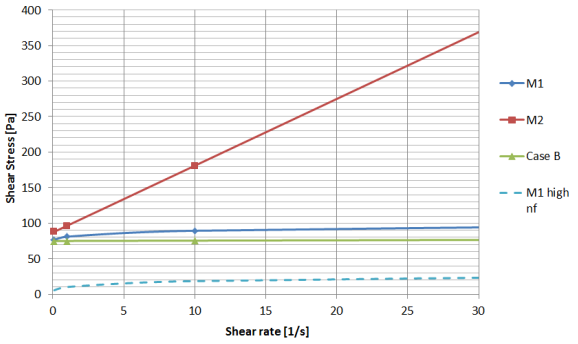

(b) Rheogram for the shear stress of the parameter set from Table 4.4 for Set 3 "TT". The low nf boundary line is at higher shear stresses and not shown to keep the other lines distinctive.

Figure 4.6: Rheograms for apparent viscosity and shear stress from Table 4.4 for Set 3: "TT".

To get a feeling of what the different sets do with strength of the slurry, a relation between yield stress and sand content is given. The original rheological parameter Set REF is also included, see Figure 4.7. The graph is made with a clay or fines content of 10 %.

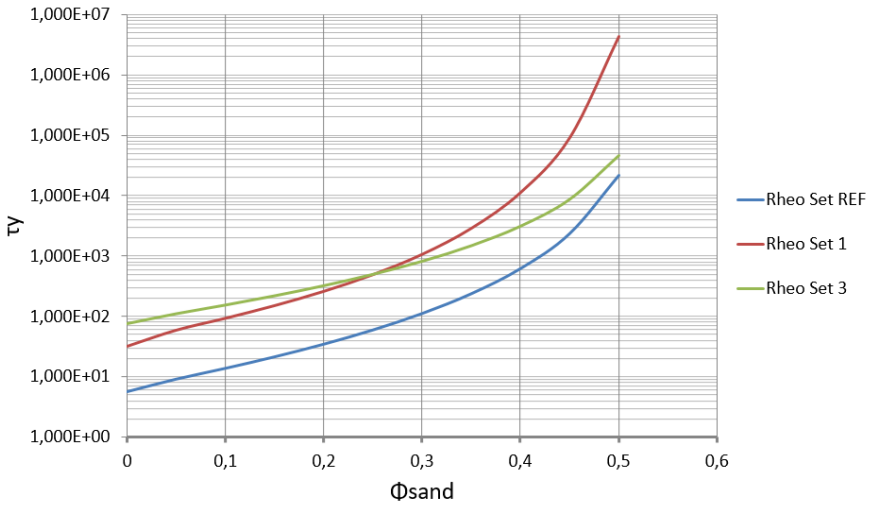

Figure 4.7: Relation between yield stress and sand content by volume for the three different rheological parameter sets. The Set are given in Tables 4.3 and 4.4 Applied is rheological Model 2 and a clay content of 10 % is used.

4.3. Conclusions on the 1DV and Delft3D-Slurry Approach

- The 1DV model can use the three different rheological models from Section 2.2.1. One Hershel-Bulkley model that has non-linear strength dependency on shear rate and two Bingham models that have a linear strength dependency on shear rate.
- The rheological and shear induced settling equations have been implemented in Delft3D-Flow to form a Delft3D-Slurry module. This was done by Deltares.
- The Delft3D-Slurry model is used in a 2DV form for initial test cases.
- The typical set-up is: tailings are discharged on top of a slope and flow down over a beach towards a model pond.
- Rheological properties have a significant influence on tailing properties. Three different sets of rheological parameters are defined to compare different sort of tailings, Set REF, Set 1 and Set 3.

5

Improvements of the 1DV Model

In this chapter the 1DV model of Delft3D-Flow is reviewed. Improvements that are made with respect to the 1DV model, described in detail in [Hanssen, 2016], are documented and the characteristics of the model that require attention are pointed out.

5.1. Comparison 1DV Model with Analytical Results

To confirm the correctness of the rheological equations that are implemented in the model a validation is needed based on analytical work. Slatter [Slatter, 2013] described an explicit expression for the bulk shear rate of non-newtonian fluid, see equation 5.1, based on earlier work from [De Kee et al., 1990] describing non-Newtonian flow on inclined plane. K is the viscosity index and τ_0 the bottom shear stress.

$$\frac{3V}{H} = \frac{3nK}{\tau_0(2n-1)}\left(\frac{\tau_0}{K}\right)^{\left(\frac{n+1}{n}\right)}\left(1-\frac{\tau_y}{\tau_0}\right)^{\left(\frac{n+1}{n}\right)}\left(1+\left(\frac{n}{n+1}\right)\frac{\tau_y}{\tau_0}\right) \tag{5.1}$$

For a Bingham fluid (n=1), Eq. 5.1 reduces to:

$$\frac{3V}{H} = \frac{1}{K}\left(\tau_0 - 1\frac{1}{2}\tau_y + \frac{t_y^3}{2\tau_0^2}\right) \tag{5.2}$$

When the rheological parameters of a fluid, yield stress and viscosity index, are known a solution can be obtained. Together with the Equations 5.3 and 5.4 for τ_0 and a constant specific discharge q the solution for slurry height H and velocity V will be an iterative solution. θ is the angle of the slope.

$$\tau_0 = \rho g H sin(\theta) \tag{5.3}$$

$$V = q/H \tag{5.4}$$

Both the equilibrium height and mean velocity are plotted against clay content. This is done for the 1DV model result as well as Slatter's analytical solution. The results in this section only contain clay, so it can be considered as carrier fluid only. Figures 5.1a and 5.1b show the results, the horizontal axis represent clay content by volume and the vertical axis height or velocity. From the three rheological models only M2 is used for comparison. This is done because a Bingham model is required since flow index n = 1 so M2 or M3. Rheological Models 2 and 3 are very similar and don't show much differences between each other. M2 is preferred over M3 in this case because it has a wider background.

The analytical solution and the model solution agree quite well. A minor deviation for the mean velocity at small clay contents can be observed. This can be explained by the large flow speeds which are unrealistic to appear in a laminar situation. When looking at pure carrier fluid, so no sand in the mixture, the 1DV model provides good results. It may be concluded that the basic equations that describe rheology are correct. The next step is to see what happens when sand is added to the mixture.

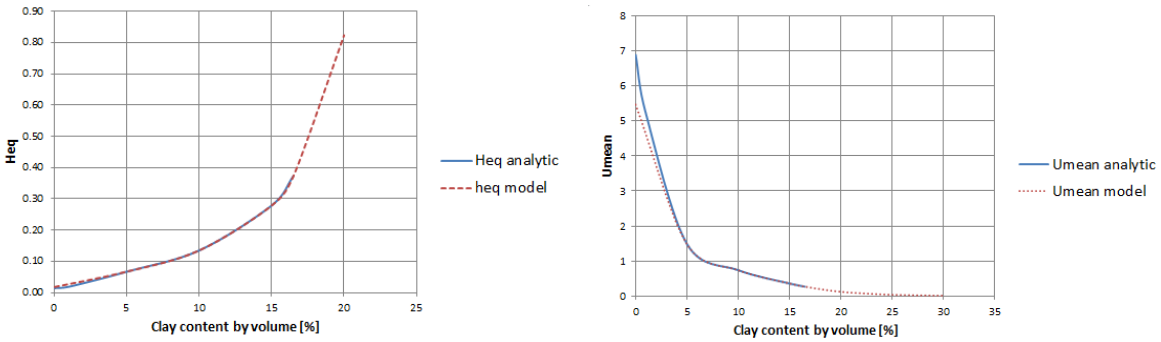

(a) Equilibrium height plotted against clay content by volume for M2.

(b) U_{mean} plotted against clay content by volume for M2.

Figure 5.1: Analytical results vs results with rheological model M2

5.2. Wiggles in 1DV

The 1DV model did have an uncertainty; as time and sand concentration were increasing, an instability was created in the bed region. This instability caused sudden sharp gradients in viscosity, velocity, shear stress, fall velocity and concentration. These instabilities or ”wiggles” kept forming over a long time span. This was caused by a positive feedback loop where each process affected each other and eventually themselves, see Figure 5.2.

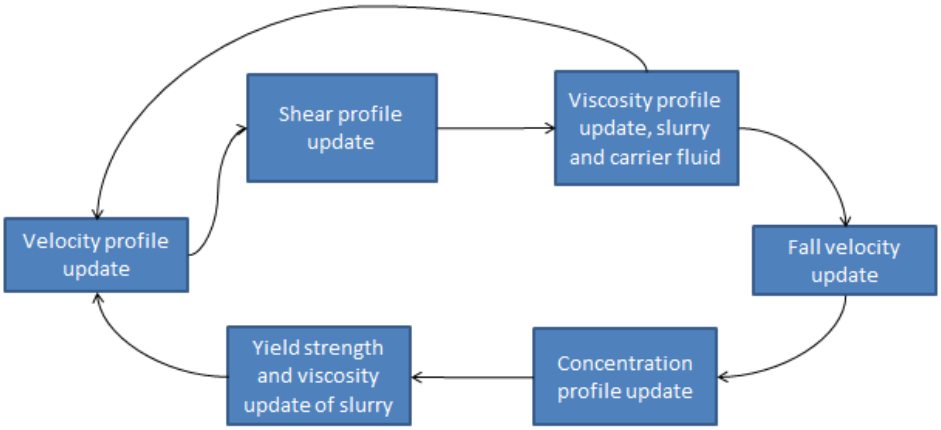

Figure 5.2: Influences aan feedback loop of the 1DV model main processes

The discretization of the model is done with the central difference method. This is a second order accurate method but also subjected to non-physical oscillations or so called ”wiggles” [Gresho and Lee, 1981]. These wiggles are a phenomenon caused by steep gradients close to or near boundaries. In the 1DV model the wiggles start forming in the bed region. At high concentrations and high density the slurry is forming an almost stationary bed region. This creates steep gradients at the interface between bed and flow layer, however these gradients at the bottom boundary are averaged by the central difference method and hence overlooked. The model doesn’t correct itself and the wiggles continue to exist throughout the upcoming solutions.

The easiest way to correct for the wiggles is to make use of an upwind scheme. This makes the solution monotone and gives a smooth solution. However the solution is damped and only first order accurate. It makes the solution stable but introduces a truncation error in the form of a second order artificial viscosity [Vreugdenhill, 1989]. This may well be visually attractive but the outcome can be deceptive [Gresho and Lee, 1981].

In Delft3D-Flow a staggered grid is used, the concentration constituents are located in the cells centre and flow velocity, fall velocity, viscosity and turbulence fluxes on the cells interface. These interface values are fluxes through the cells boundary and affect the value in the cells centre. The yield stress and viscosity are calculated with concentration values of the sand and fines constituents. Initially these values were computed at the interface, herefore the concentration values were mediated to the interface by Eq. 5.5. With c is the concentration, dz is cell thickness and k is cell number.

$$c_{(k+1/2)} = (c_{(k)} * dz_{(k+1)} + c_{(k+1)} * dz_{(k)})/(dz_{(k+1)} + dz_{(k)}) \tag{5.5}$$

Central difference uses two cells to get an average interface value, whereas upwind only one cell is used in upwind direction. In the upwind scheme the information is obtained directly from the next grid cell its centre. The change in calculation scheme is given in Figure 5.3.

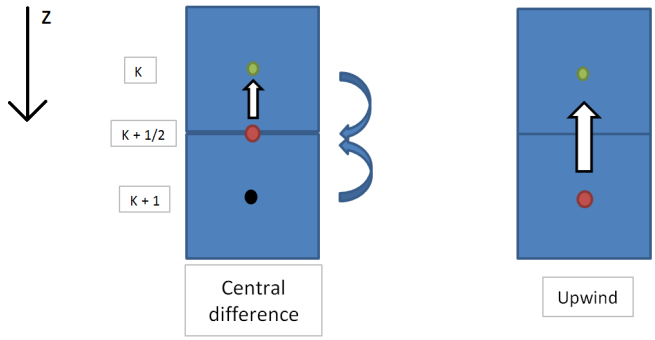

Figure 5.3: Central difference scheme vs upwind scheme for calculating yield stress and viscosity. With k representing the layer number. The green dot is the cell that needs to be calculated and the red dot is the point where it gets its information. Either a mediated value at the interface of the cell is used or the value of the next cell its centre

In the 1DV model an upwind scheme is already used for the hindered settlement calculation. This was implemented in order to avoid that the value for sand concentration exceeded its theoretical maximum value. The upwind scheme is now also used for the calculation of the mixture yield stress and mixture viscosity. Since the model operates in a vertical medium and everything is falling due gravity, extra focus on the cells below is much more important than the cells above. This makes the computed cell feel more resistance when entering the bed layer due to higher sand concentration values in these cells. This defines more realistic behaviour of the fluid. This is the reason that the use of an upwind scheme can be justified and it is not just a way to make the solution look more elegant. When the upwind procedure is applied to the calculation of the slurries viscosity, the wiggles disappear. Both yield strength and viscosity are therefore calculated with the upwind scheme. The averaged values can be left out of code, see Appendix F. A good calculation of the viscosity is of extreme importance since the viscosity of the carrier fluid, which is affected by the clay volume concentration, affects the sand segregation. The new viscosity of the slurry, which is dependent on the sand concentration, affects the hydraulic gradient.

Upwind schemes are accurate if the numerical diffusion is significantly less than the physical diffusion. The physical diffusion in the 1DV model however is set to zero, however some molecular diffusion is present though. This means that every numerical diffusion will affect the solution. To check the influence of the upwind scheme on the solution, the simulations II and III for SFR=0.25 and SFR=5 (from Table 4.1) are compared by using the central difference scheme and upwind scheme separately. Simulations I with clay only is not needed because the instabilities only arise in slurries with sand included. The instabilities occur in every model but differ depending on elapsed time. Because it occurs for every rheological model only the results from M3 are reported here. The rheological parameters come

from Table 4.3. This comparison is provided in Figures 5.4 to 5.7. These figures give the velocity and concentration profiles for both the central difference scheme as the upwind scheme at four different time instances; after 0, 1,000, 5,000 and 30,000 seconds for SFR = 0.25 and after 0, 1,000, 5,000, 10,000 for SFR = 5. The vertical axis represents height in $[m]$ and the horizontal axis either velocity in $[m/s]$ or sand concentration in $[g/L]$.

Almost no differences can be distinguished in the SFR = 0.25 comparison. In the bed layer in the central difference simulation an instability is indicated in a red circle. This occurrence is after 30,000 seconds and is not present in the upwind code. All other profiles are similar.

In the SFR = 5 comparison, a total different result can be is seen. When a certain bed layer is present the profiles in Figure 5.6 are dominated by "wiggles", which are not present in figure 5.7. The problem here is that also the flow height or thickness of the slurry has changed. This difference is can be explained. In Figure 5.6 a plug layer, a shear layer that is depleted of sand particles and a bed layer can be seen. In Figure 5.7 only a depleted shear layer and a bed layer are present. This explains a larger flow height for the upwind scheme. But it also introduces an error, namely a depletion of the plug layer, which should not occur. The upwind scheme amplifies this problem but it is already present in the central difference scheme. This problem will be further addressed in Section 5.3

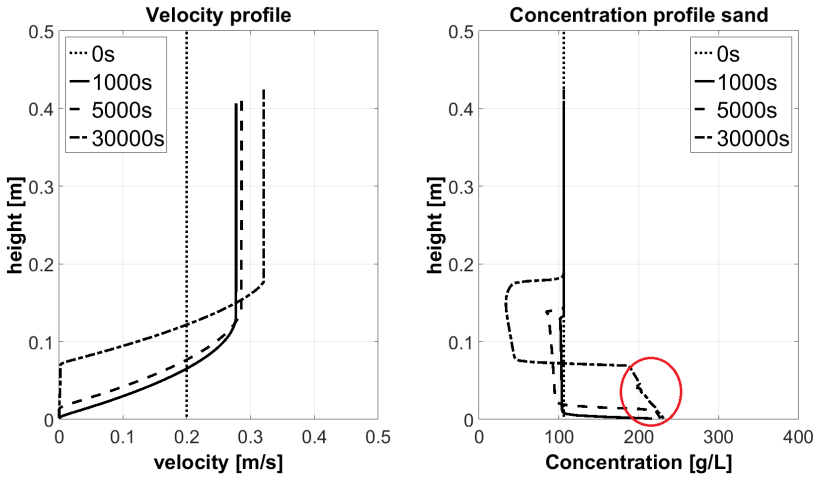

Figure 5.4: Velocity and concentration profiles for Simulation II, (SFR = 0.25, parameters are found in Table 4.1). Rheological model M3, (parameters are in Table 4.3), is used at different time instances for the central difference scheme. The wiggles in the bed layer are indicated by the red circle.

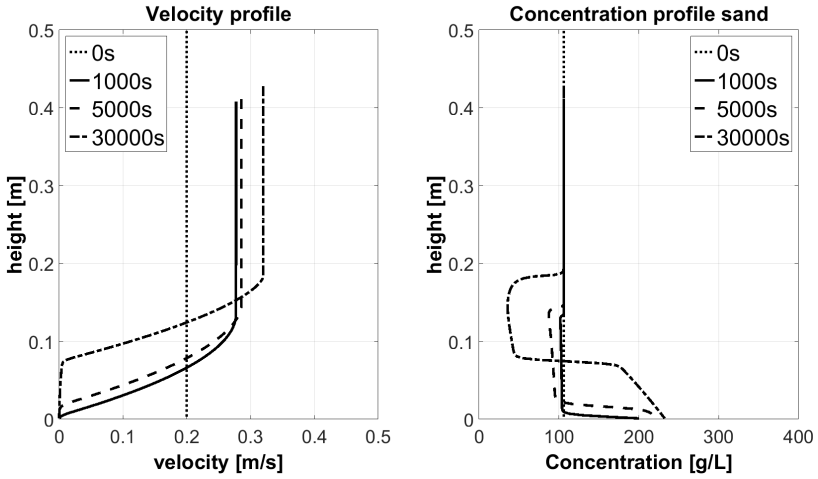

Figure 5.5: Velocity and concentration profiles for Simulation II, (SFR = 0.25, parameters are in Table 4.1). Rheological model M3, (parameters are in Table 4.3), is used at different time instances for the upwind scheme

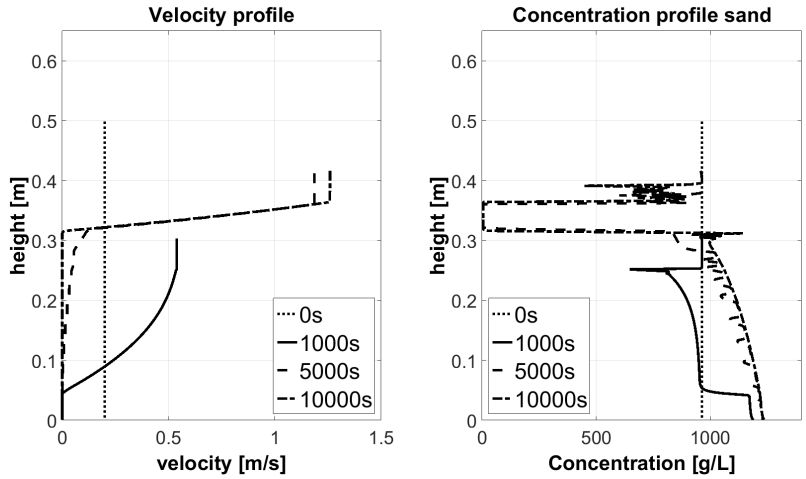

Figure 5.6: Velocity and concentration profiles for Simulation III, (SFR = 5, parameters are in Table 4.1). Rheological model M3 (parameters are in Table 4.3) is used at different time instances for the central difference scheme

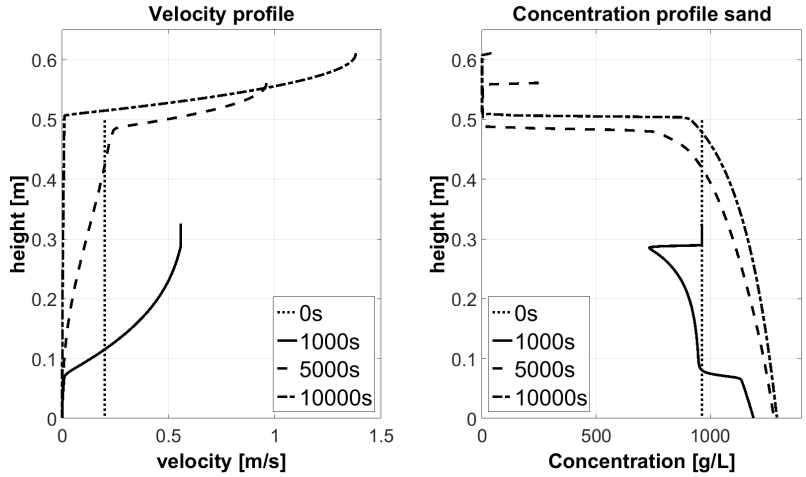

Figure 5.7: Velocity and concentration profiles for Simulation III, (SFR = 5, parameters are in Table 4.1). Rheological model M3 (parameters are in Table 4.3) is used at different time instances for the upwind scheme

5.3. Hydro-Mechanical Balance in 1DV

The non-Newtonian behaviour of a slurry gives a peculiar mechanical balance. The presence of a yield stress creates an opportunity for plug formation. As the shear stress of the fluid is lower than the yield stress, no settlement of particles will occur and a uniform plug layer is made above a shear layer where sand will settle and form a bed at the bottom. In the 1DV model this effect can be simulated and a clear plug can be distinguished. In reality however this plug above a shear layer that has lost all its sand can lead to instability. Simply because the plug layer becomes heavier than the shear layer, due to gravitational force the plug will tend to move downwards and affect the flow. This problem has to be transported to the 2DV/3D environment, preliminary results of 2DV model are provided in Chapter 6.

5.3.1. Decreasing Plug Layer

For non-Newtonian fluids the shear induced settling of particles only occurs when the shear stress surpasses the yield stress of the fluid, described in Section 2.4.1 and Eq. 2.22. In the 1DV model the particles are only subjected to shear settling. The static settlement of particles is some orders smaller and negligible for the used timescales. This means that theoretically the plug layer in the 1DV model should stay constant.

In the 1DV model this balance was not met. The plug thickness decreased with time. The plug layer was losing sand at the bottom of the plug. The reason behind this decreasing plug layer can be found in the applied numerical scheme. The numerical scheme was already mentioned in the 'wiggles' problem Section 5.2, and here it is again the main suspect. The upwind scheme that solved the 'wiggles' seemed to increase the decreasing plug problem, but it was also present with the initial central difference method. The following things are responsible for the decreasing plug:

1. The background in the decreasing plug layer lies in the computational scheme.
2. The yield stress is calculated by taking the information of the sand concentration from the cell beneath (upwind), or from a mediated value from the cell itself and beneath (central difference) see Section 5.2.
3. Point 2 has the consequence that at the bottom of the plug the yield stress is computed with lower sand concentrations from the shear layer than the original plug layer. The yield stress in the last cell of the plug is lower than it should be.
4. Point 3 causes the shear stress and yield stress converge faster (i.e. the intersection point of shear and yield stress is closer to top of the slurry).
5. The bottom of the plug starts losing sand as yield stress drops below shear stress and the thickness becomes unintentionally smaller than it theoretically should be.
6. The decreasing plug layer occurs for all rheological models.

5.3.2. Switch in Numerical Scheme

The computational scheme for the slurries yield stress and viscosity needs to be adapted in a way that this will not happen anymore. Basically a numerical scheme switch is implemented; The numerical scheme stays upwind but instead of taking information from the cell beneath, for the plug layer it will take information from the cell above.

The upwind scheme is adapted with an if-loop which states: IF the shear stress at a certain layer k is lower than the yield stress of the plug layer AND it is computed withing a margin of the original plug thickness. THEN the yield stress in that cell is not computed with sand concentration from the layer below but above it! ELSE the upwind scheme remains the same. So in principle a backward scheme applies for the plug layer. The same is done for the viscosity calculation. For the code see Appendix F.

The hydro-mechanical balance is much better approached with this adaption. Differences can be seen between Figures 5.8 & 5.9 for SFR = 0.25 and Figures 5.10 & 5.11 for SFR = 5. A summary of these simulations is given: general input parameters of the slurry are found in Table 4.1, rheological parameters in Table 4.3 and model M2 is used. The goal of these results is to demonstrate the effect of the code adaptions or the different numerical schemes. The simulations are made for the three different tailings described in the Section 4.1.2, changing only the sand and clay concentration. Only Simulations II and III are shown because simulation I has no sand, so no settlement and therefore no change in yield stress. The two simulations are shown at different time intervals to optimise the visualization of the decreasing plug.

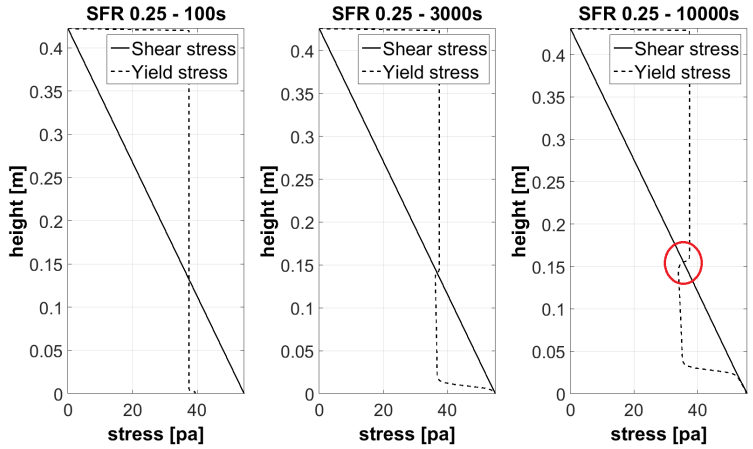

Figure 5.8: Mechanical balance of simulation II with old code, parameters from Table 4.1. Rheological model M2 is used with parameters from Table 4.3. The red circle indicates a the intersection point of yield and shear stress. This point is different compared to the initial situation at time 100 s.

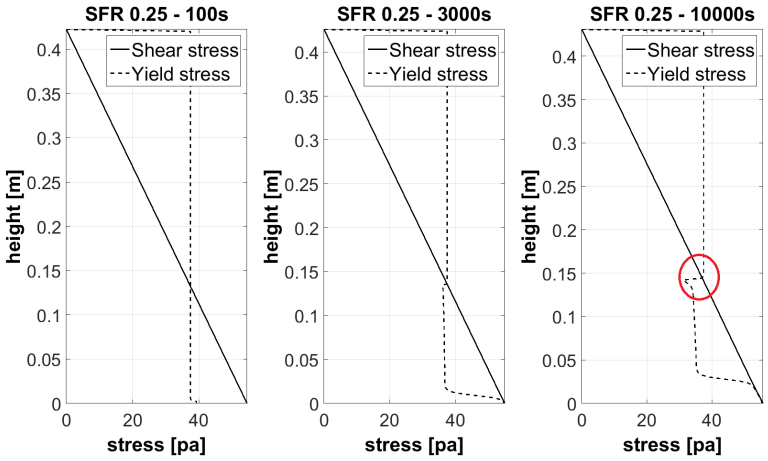

Figure 5.9: Mechanical balance of simulation II with new code, parameters from Table 4.1. Rheological model M2 is used with parameters from Table 4.3. The red circle indicates a the intersection point of yield and shear stress. This point is similar compared to the initial situation at time 100 s.

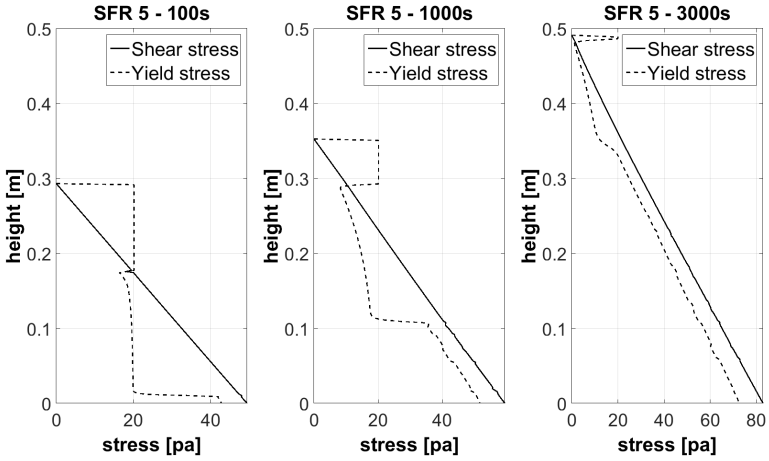

Figure 5.10: Mechanical balance of simulation III with old code, parameters from Table 4.1. Rheological model M2 is used with parameters from Table 4.3.

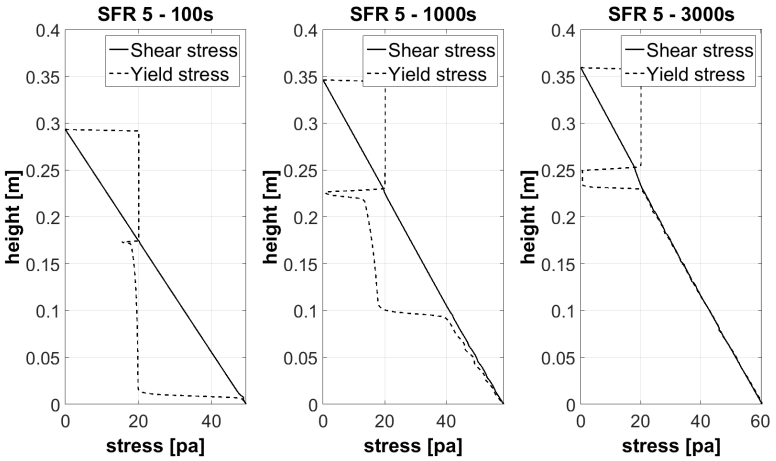

Figure 5.11: Mechanical balance of simulation III with new code, parameters from Table 4.1. Rheological model M2 is used with parameters from Table 4.3.

From these plots may be concluded that :

- The plug thickness is now constant. Simulation II old code starts with an initial plug layer of 28 cm and ends with plug layer of 26.5 cm: a decrease of 1.5 cm. Simulation II new code starts and ends with a layer of 28 cm. Simulation III old code starts with an initial plug layer of 11.5 cm and ends with 0.5 cm so the plug almost disappeared. Simulation III new code starts with 11.5 cm and ends with 11 cm.
- Still there is a minor deviation at bottom of plug, as can be seen in Simulation III where the plug size did not stay exactly the same. There is no straight line of yield stress from intersection of shear stress and yield stress upwards. This can be explained by the use of a modification for shear stress, Equation 4.3. The curve in the yield stress is influenced by the adaption of the flow curve and this indicates that there is no sharp angle in the flow curve.
- In simulation III with the new code there is a very sharp decline in yield stress just below the plug layer, this means that there is a small layer beneath the plug completely drained of sand particles. This is expected as the fluid did not contain a lot of clay. Simulation II has a lot more clay and the settling of sand particles takes a lot more time.
- At the bottom of the flow, the yield stress and shear stress converge. This means that the slurry is in a bed phase and the bed value will therefore have a particular yield stress that is equal and limited to the shear stress of the flow. This will determine the concentration of sand in the bed layer. This also means that sand concentration values in the bed layer will not reach the theoretical maximum granular volume concentration of 0.6.

5.4. Conclusions on Improvements

- The rheological model matches with the analytical solution for non-settling slurries.
- An upwind numerical scheme is used to calculate yield stress and viscosity to correct the ”wiggles”. This makes the solution monotone, but introduces a truncation error. The use of an upwind scheme can be justified in this case because only falling particles in the vertical direction are considered. The influence of cells that are underneath is much more important than the cells above. This creates a more realistic resistance and explains the chose for an upwind scheme.
- The 1DV model has been included with a numerical switch that keeps the plug from being depleted of sand particles.
- The adaptions of an upwind scheme and ”plug preservation” only applies to the 1DV model. In Delft3D-Slurry this is not coded because there are more effects in these environments and a constant flow of information comes from the upstream section. For the time being this justifies the application of the original central difference scheme in Delft3D-Slurry.

6

Results and Performance Delft3D-Slurry

In this chapter the Delft3d-Slurry results are documented. First a comparison with the 1DV model is made to validate a correct transition of the added equations for rheology and segregation. This is done first with a simulation with only clay and later with both clay and sand. Hereafter a sensitivity analysis is made to test the robustness of the model. Finally applications of oil sands are tested by the flow of strong over weak material and weak over strong material. A quantitative comparison with the data set is made.

6.1. Verification of Delft3D-Slurry with Clay Only

To check the transition of the 1DV code with the code implemented in Delft3D-Flow, a comparison between the two models is performed. In Delft3D-Slurry only two dimensions are used for now (vertical and longitudinal), that why this model is referred to as 2DV model. This comparison is made for a fluid simulation with carrier fluid only. A comparison with sand is not easy to make because the 2DV environment receives information from upstream and the 1DV does not. All other parameters like: slope, discharge, sediment properties and rheology are taken exactly the same as in the 1DV model.

The 2DV plot is discussed first, Figure 6.1, basically what can be seen in the plot is a fluid flowing down a slope. The fluid starts flowing in point (0,0) and the slope can be seen as the BAW. At the end of the slope the fluid reaches a pond, which is a body of the fluid with the same characteristic as the incoming fluid. This pond begins with a steeper slope before turning horizontal, this part can seen as the BBW. The horizontal axis represents the longitudinal distance in $[m]$ and the vertical axis height in $[m]$. Difference in height divided by difference in longitudinal directions give the slope angle θ, which in this case is 1 %. The colour scale represent the velocity and runs from zero at the bottom to 1.2 m/s at the top of the bar. The specific discharge is 1 m^2/s, the volume concentration of clay is 10 % and rheological model M2 is used. Numerical parameter are: run time 2 hours, time step is 1 s, 200 grid cells in longitudinal direction with grid space of 2 m, 1 grid cell in lateral direction of 10 m width and 40 grid cells in vertical direction which are equally distributed. In the middle of the sketched simulation, in this case at 200 m, a 1DV velocity profile is retrieved. This velocity profile is then compared with an original result from the 1DV model.

All parameter in the original 1DV model are set the same to match the simulations. The vertical axis represents height and the horizontal axis represents velocity. Both simulations are considered to be in steady state, or at equilibrium height. Figure 6.2 shows the comparison of the models. What can be distinguished is the equal flow height but a slightly different flow speed. The 2DV model returns a higher plug velocity than the 1DV. There can be multiple causes. It can be the result of the Chezy boundary or something else, grid and time step are taken more accurate but give no change in result. Overall profiles, including the plug thickness, are very similar though. Decided is to leave it as it is and further research is needed at bottom boundary before more conclusions can be made.

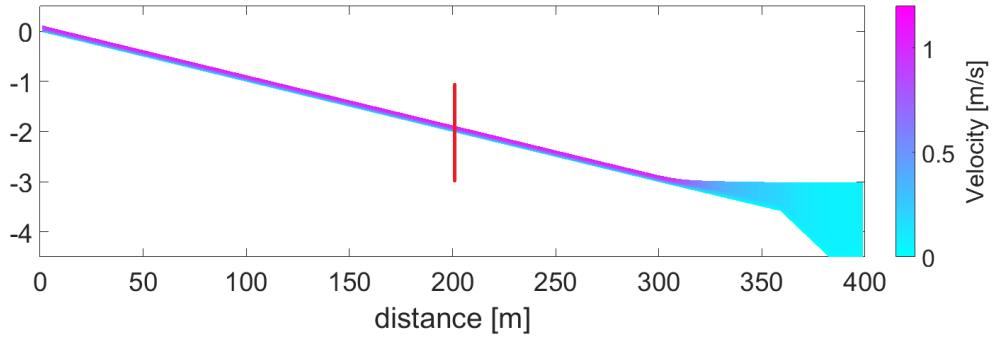

Figure 6.1: Horizontal cross section of beach slope with velocity profile. Taken after two hours. The red line in the middle of the profile indicates the location of the retrieved 1DV profile

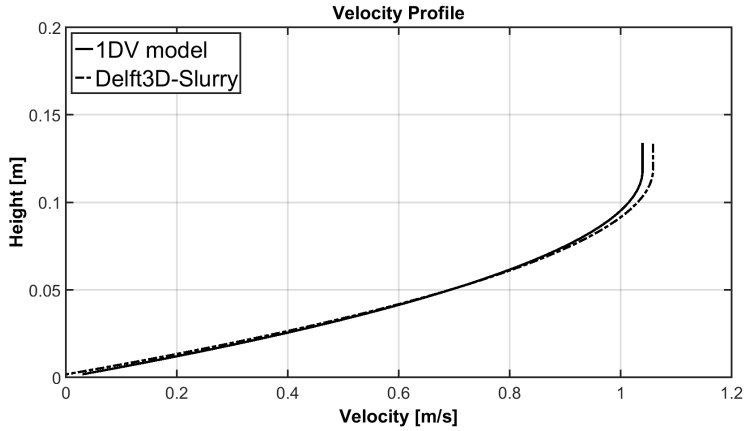

Figure 6.2: 1DV vs Delft3D-Slurry model results, comparison of velocity profile. Rheological Model 2 is used with parameters Set REF from Table 4.3.

6.2. Delft3D Sensitivity Analysis on Generic Slurries

In this section a sensitivity analysis is performed to test the capability, robustness and behaviour on different parameters of the model. The simulation with only carrier fluid from Figure 6.1 is chosen to be the Reference Run. The characteristics of this run are covered in Table 6.1. The Reynolds number (calculated with Eq. 2.9) is 105. yield stress is 2 Pa. Mean velocity is 0.74 m/s and slurry thickness H is 0.135 m. The computations of The Reynolds number of the Reference Run and the others runs can be found in Appendix A. The grid is composed of longitudinal cells M, lateral cells N and vertical cells k.

Table 6.1: Characteristics of the Reference Run from Figure 6.1 with only carrier fluid and 10 % by vol. clay. Rheological parameters provided in Tables 4.3 and 4.4

Reference Run							
sand $[g/l]$	0	q $[m^2/s]$	0.1	SFR $[-]$	0	grid cells M	200
clay $[g/l]$	260	Reynold Number	471	FOFW [%]	22.4	spacing M $[m]$	2
Rheology	Set REF	Yield Stress $[Pa]$	2	Run time	2 h	grid cells N	1
$c[\%]$	22	Velocity $[m/s]$	0.74	Time step	1 s	spacing N $[m]$	10
ρ $[kg/m^3]$	1160	Height $[m]$	0.136	Slope θ	1 °	grid cells k	40

The sensitivity analysis is constructed by changing only one parameter at a time for each run with respect to the Reference Run. This analysis is done to see the effect on the flow, sand settling and deposition. The parameters that are changed are clay concentration, rheological parameters set, sand concentration and sand particles diameter.

The whole set-up of the sensitivity analysis is shown in Figure 6.3. Clay concentration is varied to check the increase in strength and coupling to flow speed (represented in green). The rheological parameter sets are from Chapter 4, Tables 4.3 and 4.4 (represented in red). The different sets are for specific tailings, like mineral tailings, oil sands "TT" and oil sands "fMFT". The sand concentration is increased to check the increase in strength and depositional patterns (represented in blue). Different sand particle diameters are compared to check the effect on segregation (represented in purple). Finally a combination between clay content en rheology is made to check more extreme conditions.

The simulations with only fines have a run time of two hours, as they reach an steady flow state quickly. The simulations with sand included have a run time of five hours, as this will show a better influence of the segregation effects. The results are shown through velocity profile and, when sand is present, also by sand concentration profile and SFR.

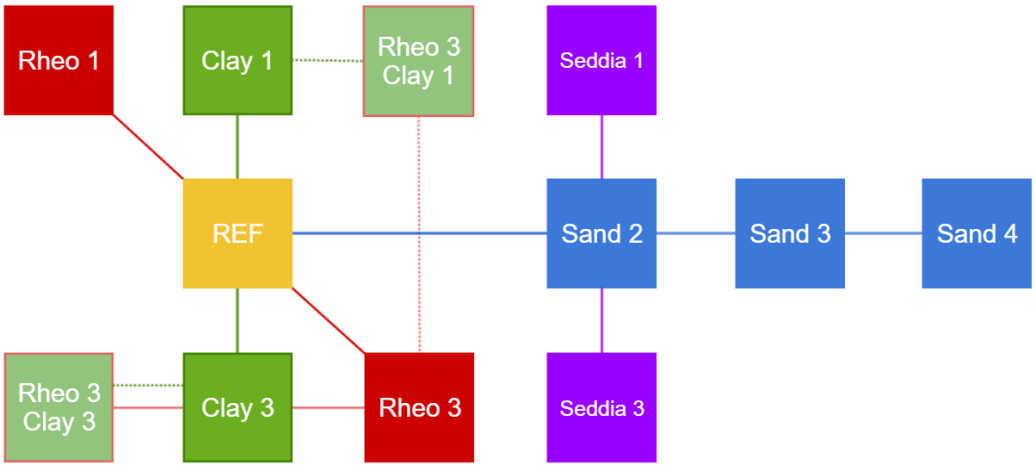

Figure 6.3: Set-up of the sensitivity analysis. All blocks and lines in the same colour represent the change in one parameter. Specifics can be read in Table 6.2

Table 6.2: Sensitivity parameters for each run, presented in Figure 6.3. Rheological input in Chapter 4, Tables 4.3 and 4.4

	Sand $[g/l]$	Clay $[g/l]$	Rheology	Sand d $[\mu m]$	Density $[kg/m^3]$	c [%]	SFR	FOFW [%]	Rheological model
REF	**0**	**260**	**Set REF**	-	1160	22.4	0	22.4	M2
Clay 1	0	**100**	Set REF	-	1062	9.4	0	9.4	M2
Clay 3	0	**415**	Set REF	-	1255	33.1	0	33.1	M2
Rheo 1	0	260	**Set 1**	-	1160	22.4	0	22.4	M2
Rheo 3	0	260	**Set 3**	-	1160	22.4	0	22.4	M2
Rheo3 Clay1	0	**100**	**Set 3**	-	1062	9.4	0	9.4	M2
Rheo3 Clay3	0	**415**	**Set 3**	-	1255	33.1	0	33.1	M2
Sand 2	**100**	260	Set REF	200	1222	29	0.38	23.2	M2
Sand 3	**450**	260	Set REF	200	1440	49	1.73	26.3	M2
Sand 4	**900**	260	Set REF	200	1720	67	3.46	31.7	M2
Seddia 1	**100**	260	Set REF	**100**	1222	29	0.38	23.2	M2
Seddia 3	**100**	260	Set REF	**400**	1222	29	0.38	23.2	M2

The rheological parameters are compared in a situation with only carrier fluid, there is no influence of β_y and β_v. The clay concentration is taken as a changing contant, however to accurately compare the effect of carrier fluid one should keep the FOFW ratio constant. The results are shown in 2DV: velocity profile and SFR. A different color profile is subjected to either velocity or SFR output so they are easy to hold apart. Cross sectional profiles are given in the middle of the slope. Those profiles are then compared for each changed parameter.

6.2.1. Clay

Clay is the first variable to be examined and to check its influence on slurry flow. Figure 6.4 give the 2DV profiles for runs Clay 1 and 3. The set-up of simulation is the same as the Reference Run, the only change is clay concentration. First thing to notice is that the Clay 1 run is not flowing. The reference run already has a high flow speed, lowering the clay concentration with the same rheological parameters has no flowing solution. The Yield stress of the fluid is in the order of 0.01 Pa. This will lead to a flow speed that is too large and no sustainable laminar flow will be possible. The corresponding Reynolds number is 5419. As discussed in Theory Section 2.3 the transition point for non-Newtonian fluids in open channels is located at Re $\sim$ 700. This confirms that the flow is not laminar but well into the turbulent region. This confirms the result that there is no solution for Clay 1. If the discharge would be lower a solution probably exists, since the flow velocity will be significantly lower. The two bumps that can be observed in the run are left overs from initial top condition and discharge of first seconds of discharge before the flow becomes unstable. The Clay 3 run does have a solution and flows with a speed of 0.31 m/s and a thickness of 0.33 m. The increase in fines increases the yield stress, 25 Pa, and therefore plug size. The Reynolds number is 9. Figure 6.5 shows the vertical velocity profile over each layer. The solid line is that from the reference run see section 6.1. The dotted line from the Clay 1 run is lacking as there is no flow. The dashed line shows the Clay 3 run.

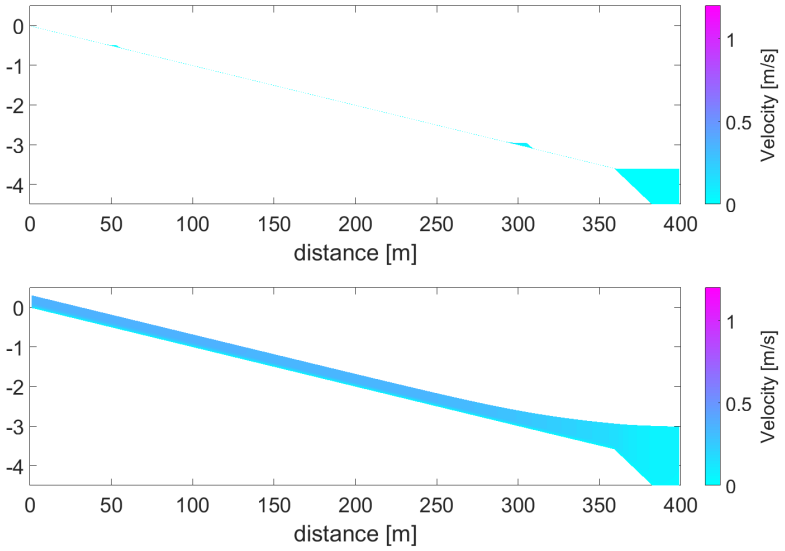

Figure 6.4: Horizontal cross section of the slope with velocity profiles. Taken after two hours. For the Clay 1 and 3 run with clay concentration of 100 and 415 [g/l] respectively. The clay 1 run has no flowing solution.

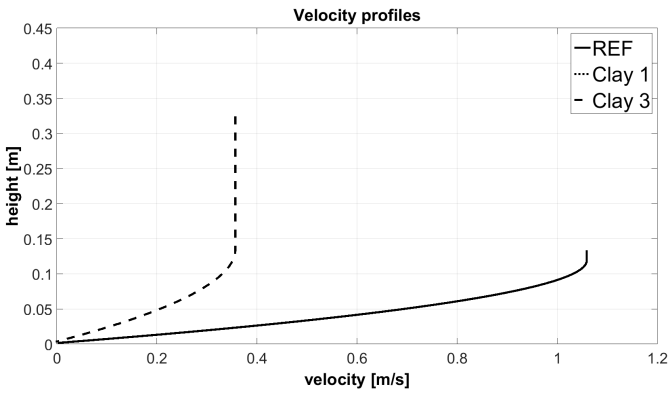

Figure 6.5: Comparison of velocity profiles taken at middle of the slope (so after 200 meter). The Reference Run is compared with the Clay 3 run, to see the effect of clay content. The Clay 1 run has no flowing solution so no velocity profile

6.2.2. Rheology

The Reference Run with rheological parameter Set REF has the lowest initial strength. The Rheo 1 run with rheological parameter set 1 has a higher yield stress for only carrier fluid than the Reference Run. The Rheo 3 run has rheological parameter set 3 and has the strongest yield stress for only carrier fluid of the three. Rheo 1 has a yield stress of 15 Pa and Rheo 3 of 30 Pa. This can be seen in plug size and thickness which are both larger for larger yield stress. Velocities for thicker flow are lower, 0.48 m/s for Rheo 1 and 0.25 m/s for Rheo 3. The Reynolds numbers of the runs are 17 for Rheo 1 and 6 for Rheo 3. Slurry thickness is 0.21 m for Rheo 1 and 0.39 m for Rheo 3. Both the results in clay and rheology show a similar pattern. Figure 6.7 shows an almost exponentially relation between the rheological sets and the thickness of the fluid, as the thickness increases for increasing rheological parameters. This relation is also expected for increasing clay concentrations. So probably the Clay 1 run will have a solution with Rheology Set 3 for instance.

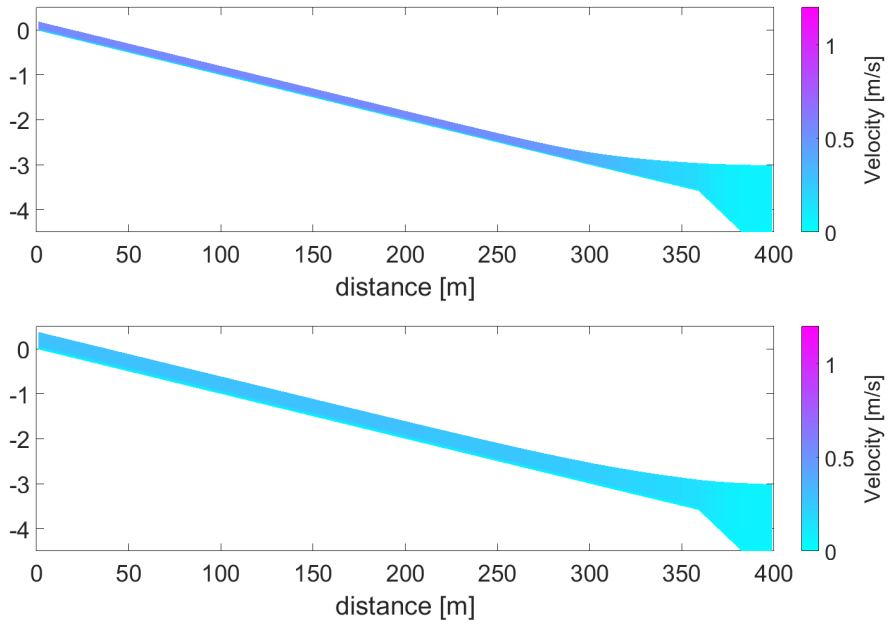

Figure 6.6: Horizontal cross section of the slope with velocity profiles. Taken after two hours. For the Rheo 1 and 3 run with rheological parameter Set 1 and 3 from Table 4.4 respectively.

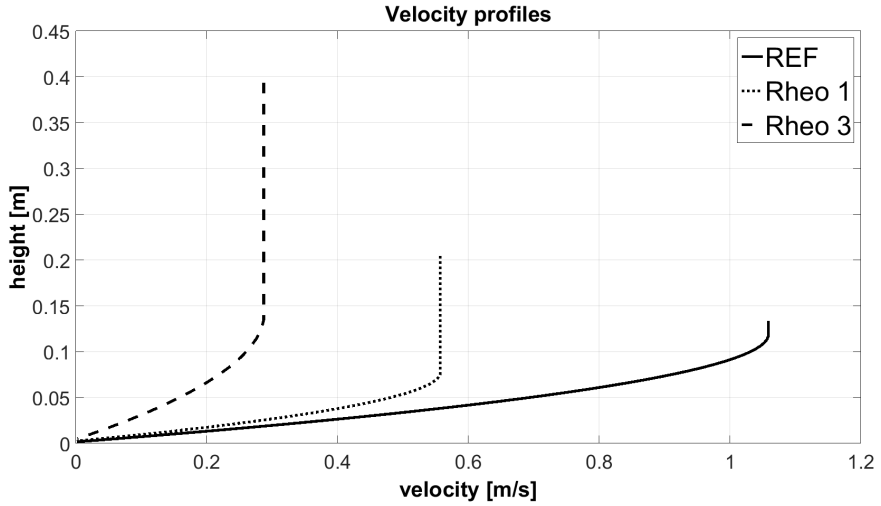

Figure 6.7: Comparison of velocity profiles taken at middle of the slope (so after 200 meter). Compared are the Reference Run with Rheo 1 and 3, to see effect of rheology.

6.2.3. Clay and Rheology Combined

Here the combination of rheological parameter set and clay content is reviewed. This is done to see what happens when the Clay 1 and the Clay 3 run are simulated with rheological parameter Set 3. Hereafter these runs are compared with the original Rheo 3 run. Figure 6.8 shows the 2DV velocity profiles for Rheological Set 3 and clay concentration 100 and 415 g/l. The low clay content does give a solution with Rheological Set 3 in contrast with the original Clay 1 run, so hypothesis from Section 6.2.2 is correct. The yield stress is 0.5 Pa for low clay and 260 Pa high clay content. This has a very clear effect on plug size and thickness. The mean velocity for the low clay content is 0.75 m/s with a flow thickness of 0.13 m. The mean velocity for high clay content is 0.05 m/s with a flow thickness of 1.76 m. Reynolds numbers are 346 and 0.1 respectively. Figure 6.8 has a better view at these numbers and shows the large differences between the runs.

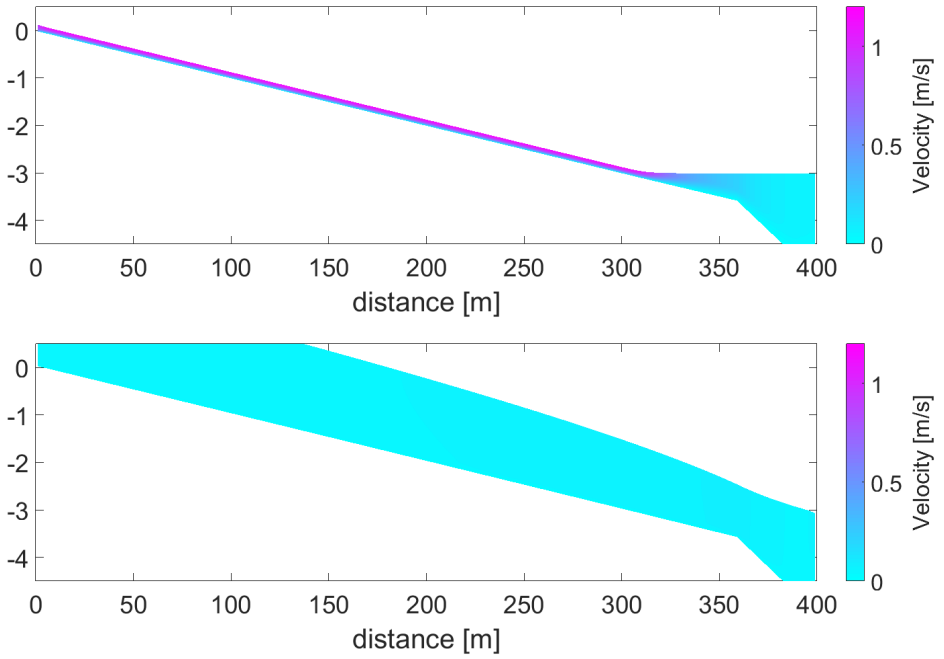

Figure 6.8: Horizontal cross section of slope with the velocity profiles. Taken after two hours, for rheological parameter Set 3 and clay concentrations 100 and 415 g/l respectively.

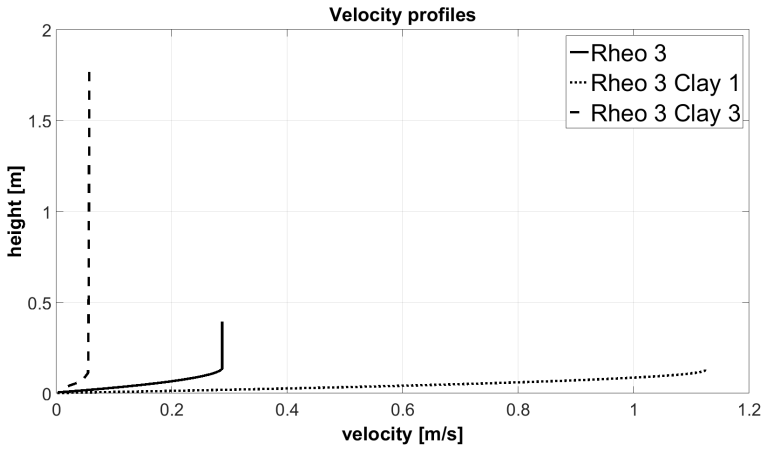

Figure 6.9: Comparison of velocity profiles taken at middle of the slope (so after 200 meter). Compared are the Rheo 3 run with a combination of rheological Set 3 and low and high clay concentrations. This is done to see the effect a stronger rheology on slurries

6.2.4. Sand

Here the results for runs with sand are provided. Figures 6.10 and 6.12 give the 2DV velocity and SFR profiles for: the Sand 2 run with 100 g/l sand, the Sand 3 run with 450 g/l and the Sand 4 run with 900 g/l.

The Sand 2 run is quite similar to the Reference Run as far as yield stress and velocity profile. The flow speed is 0.51 m/s with a thickness of 0.2 m. It has a yield stress of 3 Pa and a Reynolds number of 75. This small yield stress leads to a small plug size and therefore a relative large shear layer. The sand in the fluid is likely to segregate and form a bed layer, however since there is little sand present this will not be a significant layer. Only at the very bottom there will be a sand deposition with SFR's ranging from 1-2.5. The Sand 3 run has a flow speed of 0.32 m/s with a thickness of 0.3 m. The yield stress is 9 Pa and the Reynolds number is 25. This is an intermediate flow state with clear segregation. The bottom deposition has SFR ranging from 1.5 to 3.2. The Sand 4 run has a flow speed of 0.14 m/s with a thickness of 0.7 m. The yield stress is 70 Pa and the Reynolds number is 4. The slurry is moving slow with a very clear increase in yield stress and thickness. Plug thickness and shear layer have a 50/50 ratio, so at least half of the material stays suspended in plug, whereas the rest will segregate and form a bed. The bed SFR is not much higher than initial slurry SFR. SFR are stable and range from 3.5 in the plug, 3.25 in shear layer to 3.8 in the bed layer. At the bottom the sand particles have reached such concentrations that hindered settlement will affect the settling of the particles.

Figure 6.13 shows a clear presence of a plug over a shear layer, which is losing sand. At the bottom the sand particles are gathered and create a bed with higher SFR. The initial sand concentration determines the gradient of transition between bed and shear layer. This is very sharp for low initial concentrations (Sand 2 run) and less sharp for high initial concentrations (Sand 4 run).

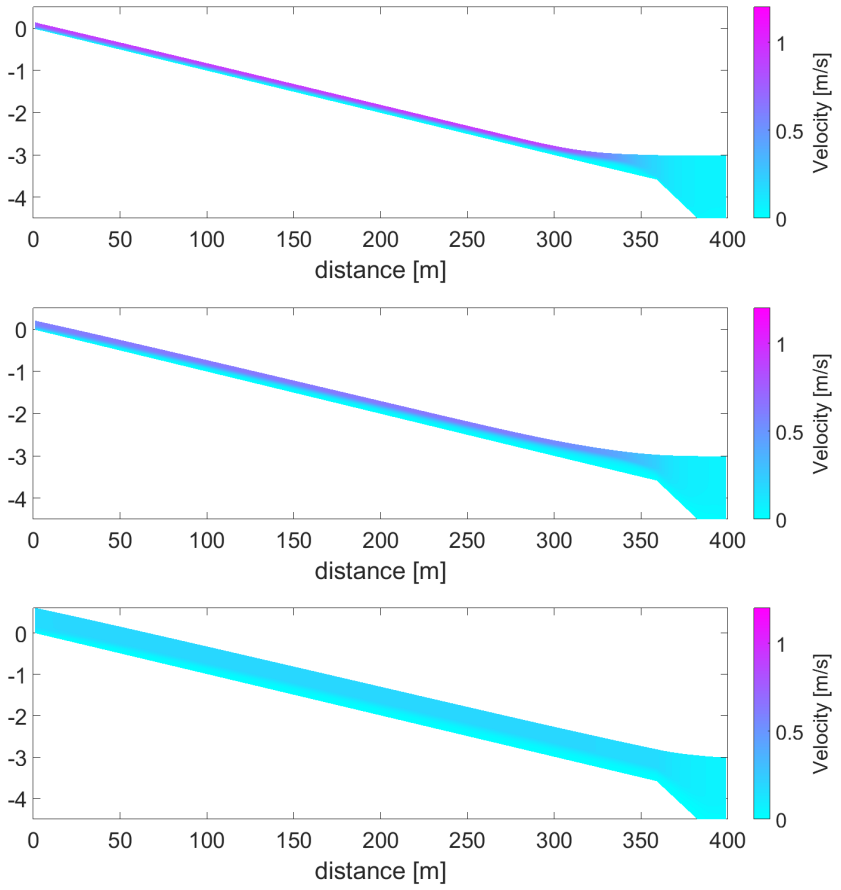

Figure 6.10: Horizontal cross section of slope with the velocity profiles. Taken after five hours. For the Sand 2, 3 and 4 run with sand concentrations of 100, 450 and 900 [g/l] respectively.

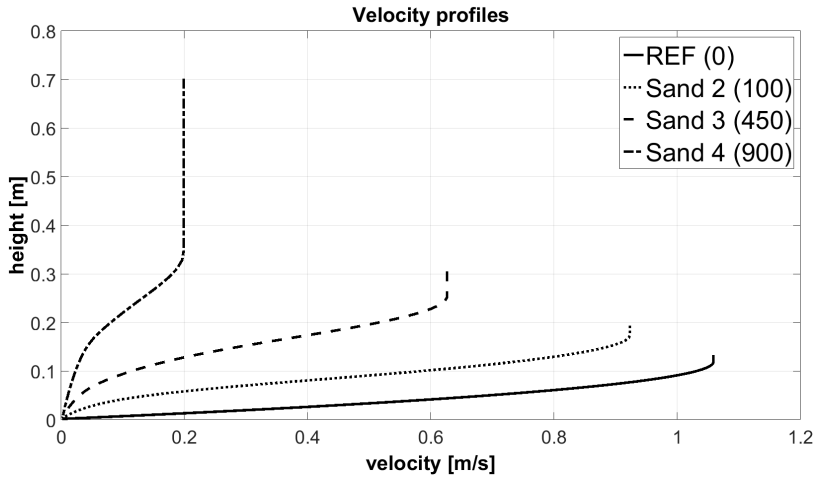

Figure 6.11: Comparison of velocity profiles taken at middle of the slope (so after 200 meter). Compared are the Reference Run with Sand 2, 3 and 4 run, to see the effect on velocity by changes in sand concentration.

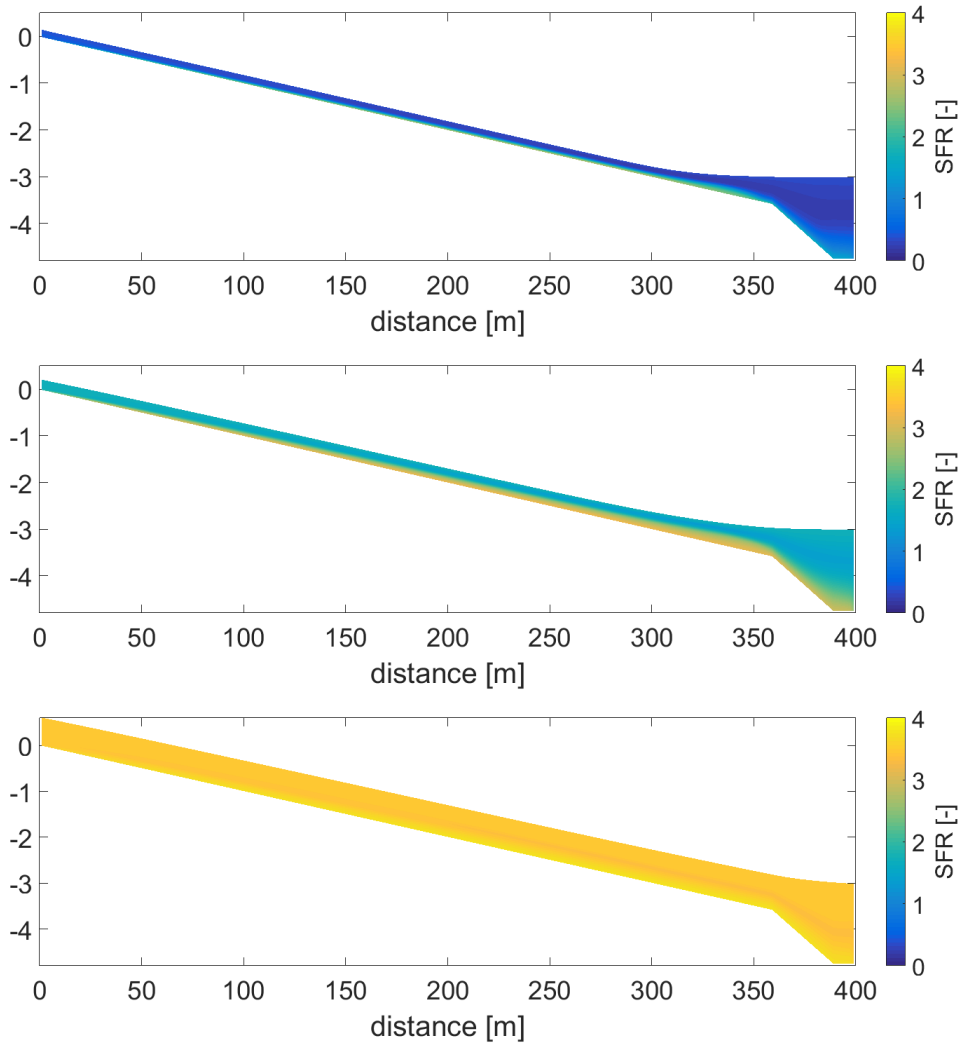

Figure 6.12: Horizontal cross section of slope with the SFR's. Taken after five hours. For the Sand 2, 3 and 4 run with sand concentrations of 100, 450 and 900 $[g/l]$ respectively.

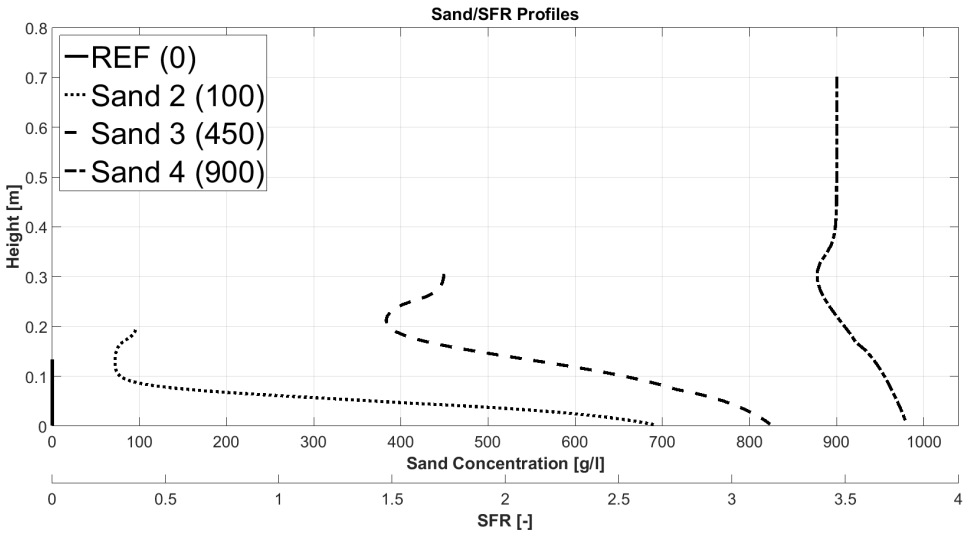

Figure 6.13: Comparison of sand and SFR profiles taken at middle of the slope (so after 200 meter). Compared are the Reference Run with Sand 2, 3 and 4 run, to see the effect on SFR by changes in sand concentration.

The porosity of sand in the bottom of the bed can give an indication of what the slurry composition looks like. It can be computed by total volume minus the sand volume. Sand 2 has porosity of 0.74, Sand 3 of 0.69 and Sand 4 of 0.63.

The 2DV profiles with SFR show something interesting, when looking at the place of sand deposition. The thickest bed region is at the end of the slope, near the pond. In Section 2.5.3 however, a typical beach profile is described by a decreasing thickness of the beach, so the thickest beach section exists at top of the slope. Also the flow speed at the bottom near pond is lower, so less segregation is expected there. The model can give this results because of four reasons:

- At the bottom of the slope the slurry thickness is larger and hydraulic gradient is less steep, this means less kinetic energy in the flow and a more suitable environment for solid particles to settle.
- The force that is created by the discharge is rather large and may therefore be pushing the entire bed towards the bottom of the slope where it stacks up due to resistance. The flow speeds that lies around 1.0 m/s can definitely play a big part in the depositional behaviour in such thin flow layers. There is need to see the propagation of flow in time and what will happen if discharge is lowered.
- It could also be a spatial effect, that is not occurring in a 3D environment. For instance a lobbed form of deposition, where the tailings spread widely somewhere down the slope, this may centre the deposition in 2DV situation at the bottom of the slope.
- Numerically the entire bed flows with a velocity that is inversely proportional to sand concentration. The model may need some adjustment between maximum sand packing and yield strength. In other words, the yield strength needs to be larger in the bed layer so that it will not flow towards the bottom of the slope.

The Sand 450 run is repeated with a lower discharge in Figure 6.14. This has the desired result, note the axis in the colour bar is different. The beach profile is now thicker at the top of the slope than at the bottom. However the amount of settled sand is less, because a lower flow speed leads to lower shear rates which in turn leads to lower fall velocity. It is difficult to draw a definite conclusion, but this run highlights the discharge dependency of the entire flow profile and deposition. The water depths of both simulations with different discharge are given in Figure 6.15. The increase in slurry depth for the Sand 450 can be seen here as well as the slightly decrease of slurry depth in the run with a lower discharge. This is an indication for the place of sand segregation.

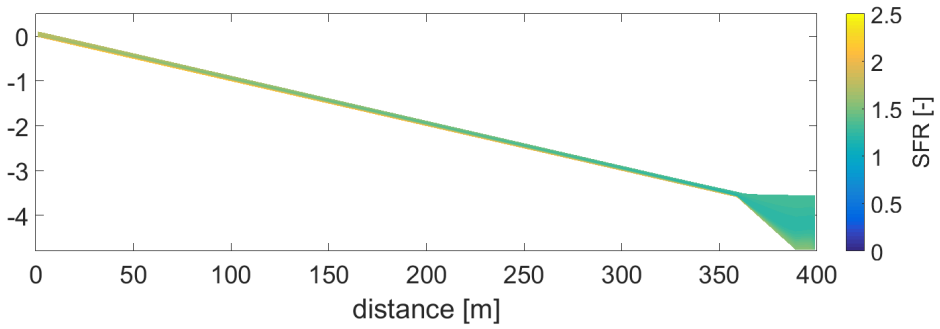

Figure 6.14: Horizontal cross section of the slope with the SFR profile of Sand 3 (450) run but with a lower discharge. Taken after five hours.

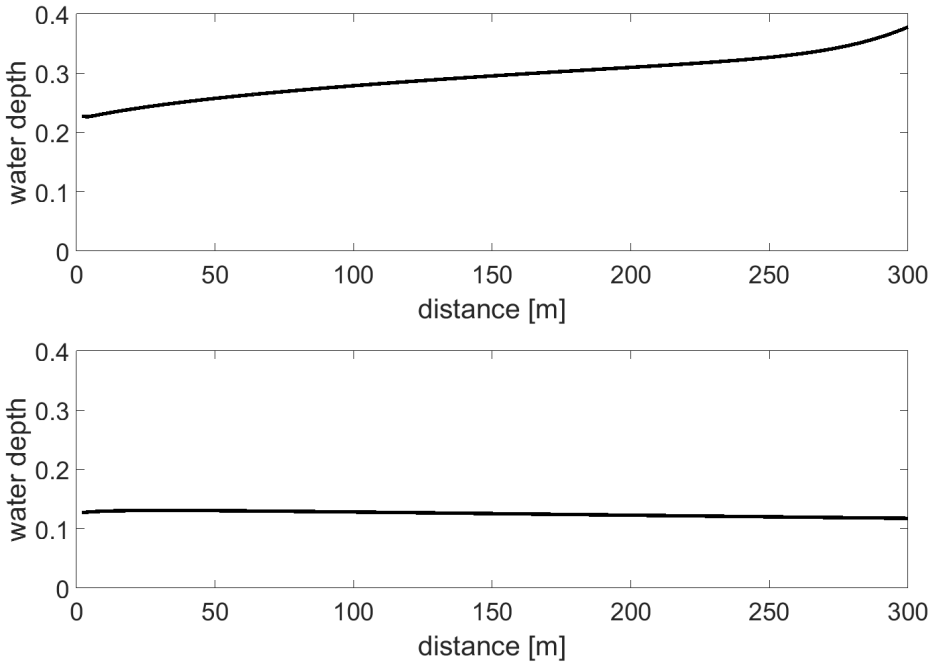

Figure 6.15: Water depths of the original Sand 3 run and the run with a lower discharge respectively.

6.2.5. Sediment Diameter

Figures 6.16 and 6.18 provide the 2DV velocity and SFR profiles for a changing sand particle diameter. These runs all have a sand concentration of 100 $[g/l]$, only the sand particle diameter is changed. The Seddia 2 run is already given and reviewed in the Sand 2 run. This run will be the reference for the other two runs with adapted sand particle diameter.

Lowering the sand diameter by a factor 2 (the Seddia 1 run) gives the same flow speed of the Seddia 2 run, of 0.62 m/s. The yield stress stays 3 Pa. The thickness is less, about 0.15 m and this is because there is almost no bed formation. The Reynolds number is 71, almost the same as the Sand 2 run. Increasing the sand diameter on the contrary has a drastic effect on the flow and segregation process. In the Seddia 3 run the mean flow speed is significantly lower due to the almost stationary thick bed layer: 0.23 m/s and the thickness is around 30 cm. The Reynolds number is 53 in this run. Figure 6.19 shows that with larger particle diameter the shear layer is almost entirely depleted of sand particles. A clear separation between the dense bed layer and fluid top layer can be seen in the last 2DV cross section.

These results are not unexpected, because the settlement formula (Eq 2.18) shows that the particle diameter has a quadratic influence on the fall velocity. For an accurate simulation a particle size distribution to determine the d_{50} is desirable. The runs again have a beach deposition that is thicker at the bottom of the slope but this has already been discussed in Section 6.2.4.

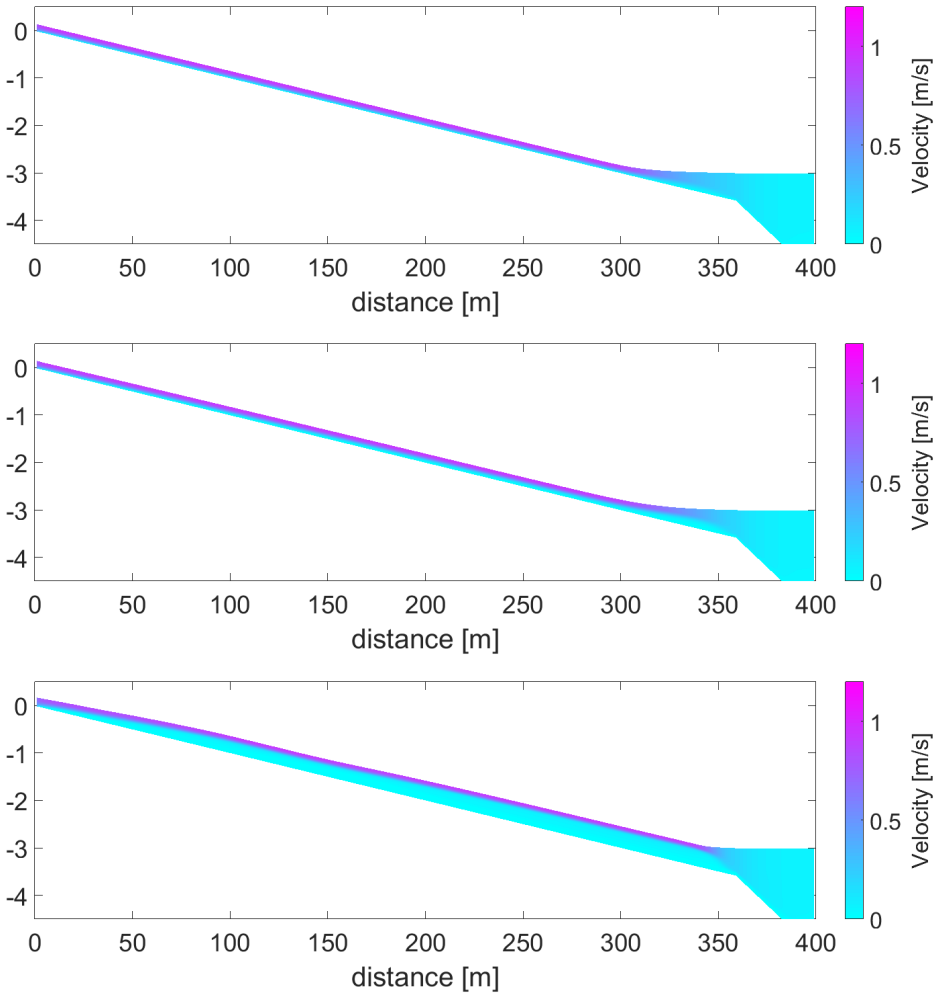

Figure 6.16: Horizontal cross section of slope with the velocity profiles. Taken after five hours. For Seddia run 1 and 3, with sand diameters 100, 200 and 400 $[\mu m]$ respectively.

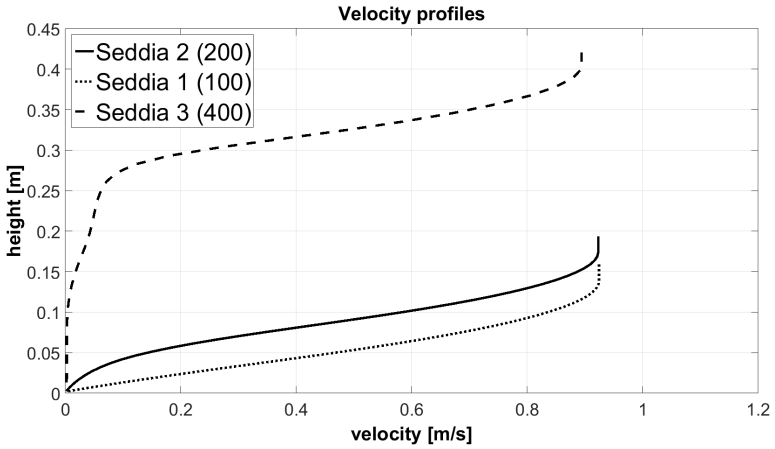

Figure 6.17: Comparison of velocity profiles taken at middle of the slope (so after 200 meter). Compared are the Sand 2 run with Seddia 1 and 3, to see the effect of changes in sand diameter.

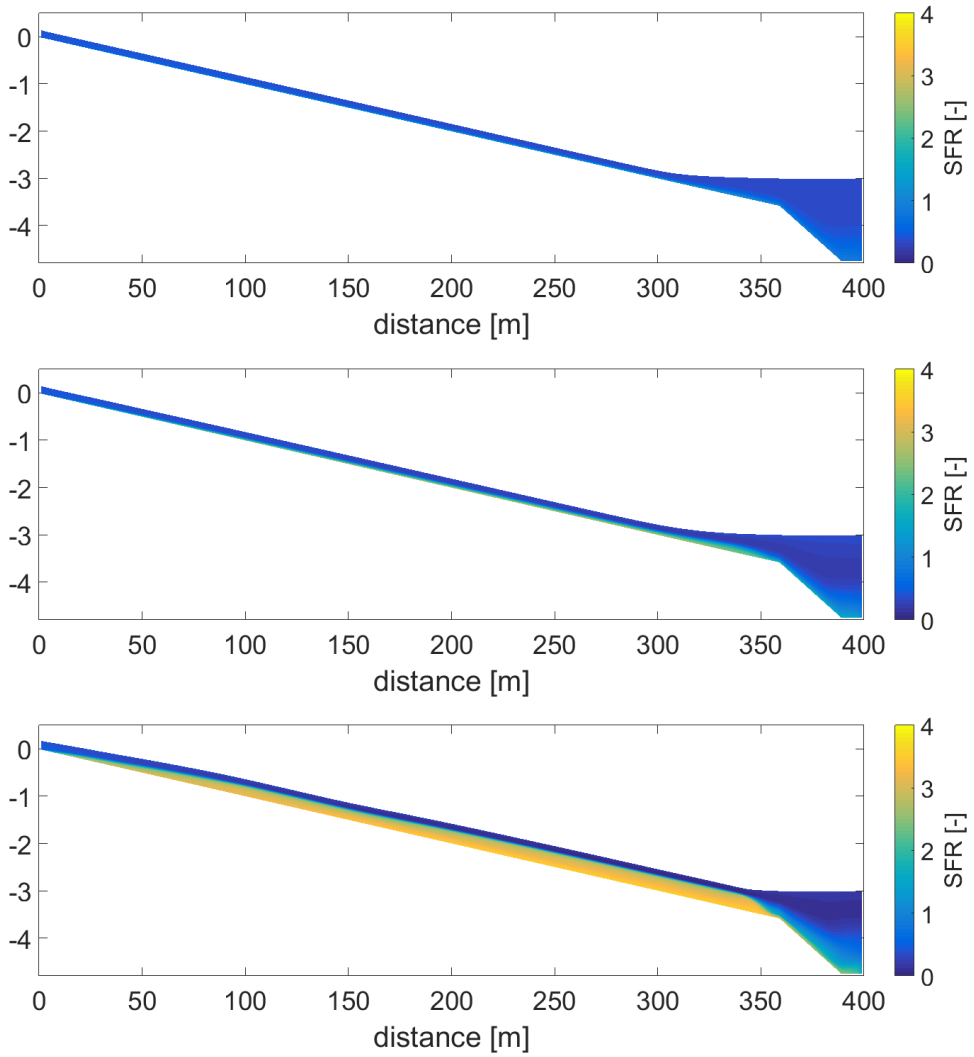

Figure 6.18: Horizontal cross section of slope with the Sand to fines ratios. Taken after five hours. For Seddia run 1 and 3, with sand diameters 100, 200 and 400 [μm] respectively.

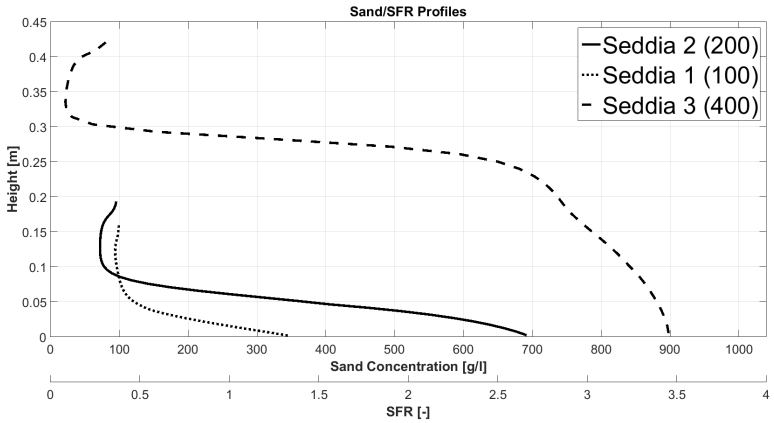

Figure 6.19: Comparison of sand and SFR profiles taken at middle of the slope (so after 200 meter). Compared are the Sand 2 run with Seddia 1 and 3, to see the effect of changes in sand diameter.

6.2.6. Propagation in Time

Until now the results that have been shown are either after 2 hours, for runs with carrier fluid only, and after 5 hours for runs including sand. In this section the propagation of the slurry in time will be provided to see the time dependency. 2DV profiles of the Sand 3 run (450 g/l sand) are selected as this run shows both rheological and segregation effects. Shown are the results after times: 0, 0h10m, 0h30m, 1h0m, 1h40m, 2h20m, 3h0m, 3h40m, 4h20m and 5 hours in Figures: 6.20 and 6.21. At the beginning of the simulation (Figure:6.20) the entire slope is dry with initial material in the pond, which has the same properties as the incoming slurry. After 10 minutes the slurry has already travelled half way down the slope. Interesting to see is the front of the slurry, a hydrostatic bore is formed that is thicker than the flow depth behind it. This behaviour is not yet understood by the author and can have multiple causes. It can be the numerical advection scheme that cannot keep up with discharge rate. It can be a rough bottom condition that affects the travelling front. It can be real behaviour, with the front experimenting high friction forces which it has to overcome. After 30 minutes the slurry has reached the pond and has reached a steady state. Sand can be seen segregating in the shear layer and forming a bed. Also in the next plots it can be seen that the bed layer near the pond is thickest but does not start at that location. The bed at the bottom is there after being pushed from the upper part of the slope. This means that flow and erosion of the sand layer need to be well investigated in future developments. After 3 hours the 2DV profile does not change anymore, see Figure 6.21. An equilibrium between deposition and erosion is developed.

The water level in the pond is a minor point of attention. As can be seen in the plots, the initial water level that is imposed as a boundary is elevated when the slurry has reached the pond. This then stays the same, about 40 cm above the boundary water level. A possible explanation is that discharge rate from the left boundary is simply larger than the right boundary can process. The larger water level gives the ability to process more volume of water and reach an equilibrium. This higher water level may have effect on the deposition behaviour at the bottom of the slope, because a thicker flow has a lower flow velocity and kinetic energy that give a more suitable environment for settlement of sand particles in that region.

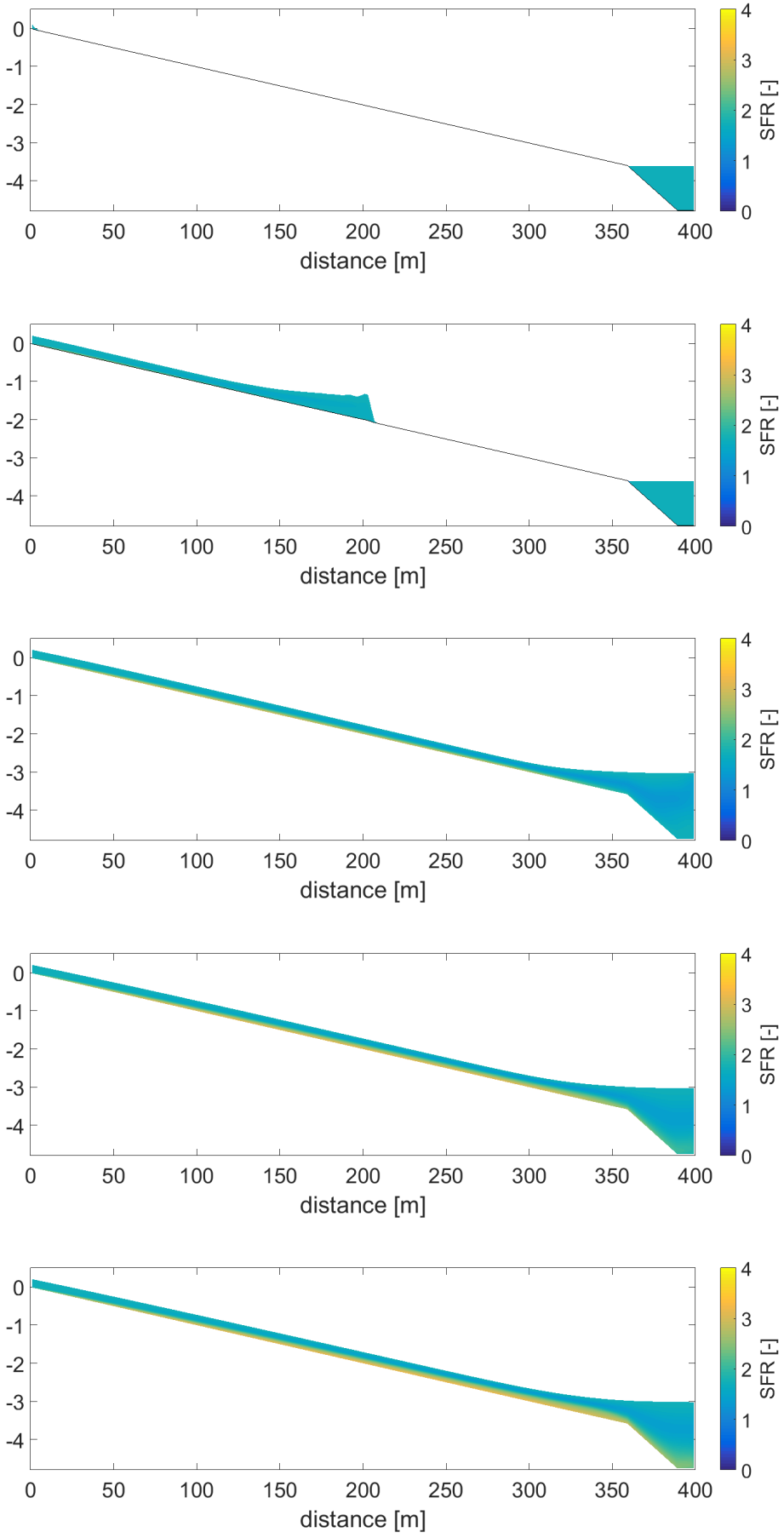

Figure 6.20: Horizontal cross section of slope with the SFR's. Run Sand 3 (450). Time steps are: 0, 10, 30, 60 and 100 $[minutes]$ respectively.

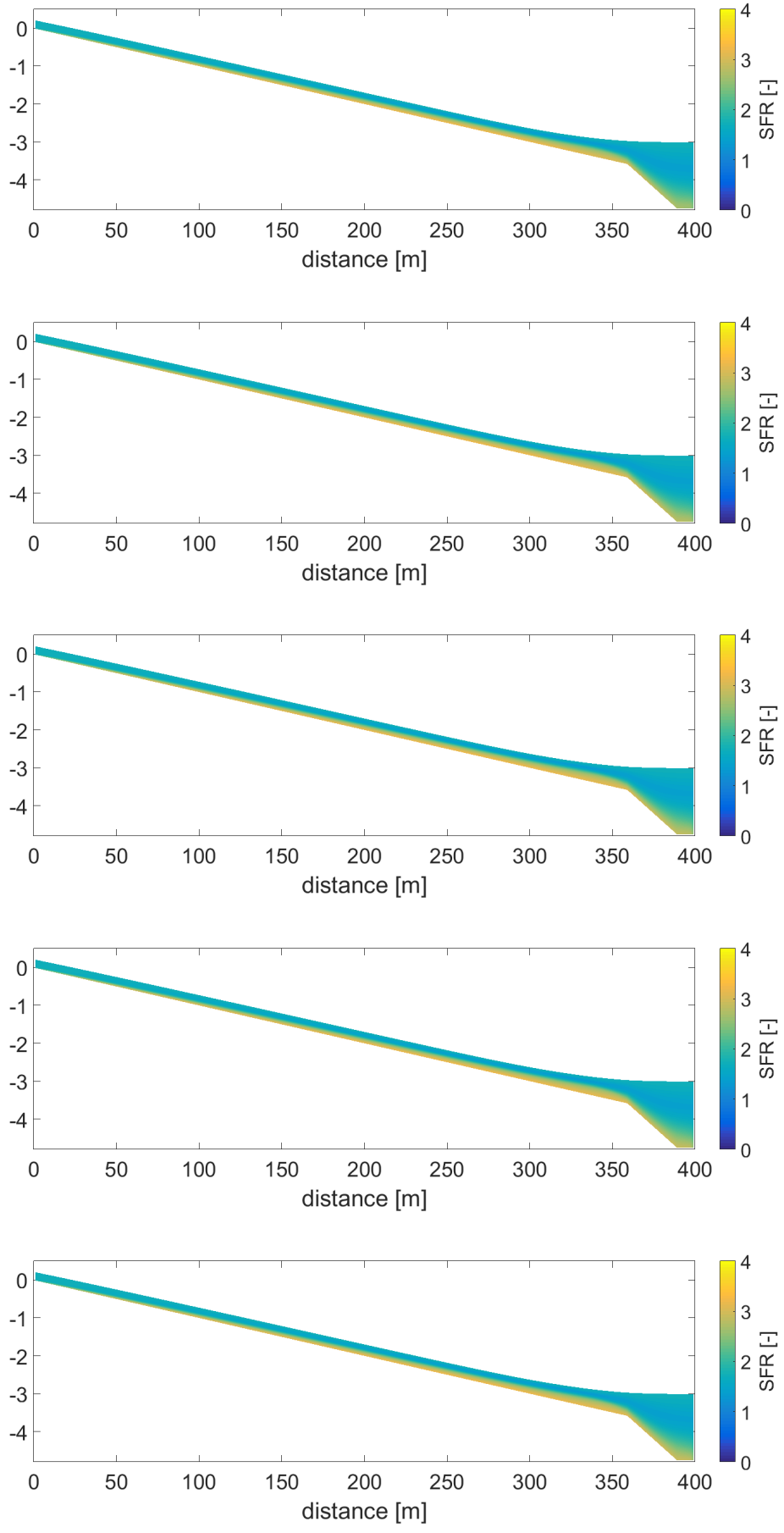

Figure 6.21: Horizontal cross section of slope with the SFR's. Run Sand 3 (450). Time steps are: 140, 180, 220, 260 and 300 [$minutes$] respectively.

6.2.7. Different Rheological Models

In Section 2.2.1, the three rheological models were described: M1, M2 and M3. All the results above are obtained with rheological model M2. One run from the sensitivity analysis will be used to compare the different rheological models. Specific properties between the 1DV and Delft3D-Slurry model are picked out and described. The selected run is the Sand 3 (450), because both rheological properties and segregation can be compared, with no extreme values. Figures 6.22 and 6.24 show the 2DV profiles for velocity and SFR with the same slope set-up for rheological models M1 and M3, taken after five hours.

From the Delft3D-Slurry results it can be concluded that rheological models M2 and M3 behave very similar. This is expected as it is the same in the 1DV environment. In Figures 6.23 and 6.25 the differences between the models can be seen for velocity and SFR/sand concentration. Differences between the rheological models are indicated in line style, differences between the 1DV and Delft3D-Slurry model are indicated by line colour. In the 1DV model there is a clear bed formation where the flow velocity is zero. This is in contrast to the 2DV model where the bed layer still has a small flow velocity and is not at standstill.

The 1DV model and Delft3D-Slurry profiles should not be matched but it is interesting to see the differences between the profiles. The two differ in some aspects:

- The 1DV model starts with a concentration that is effectively modelled down the slope but the profile is directly connected with the original condition. Delft3D-Slurry has a constant stream of information from the upper boundary.
- The upwind code and numerical switch for ”plug preservation” is not implemented in Delft3D-Slurry.

These are two reasons that cause differences which make the models incomparable for exact matches. The first point is also a reason for point two. Probably the set-up of the Delft3D-Slurry case also has its influence. The flow down the slope creates a sort of equilibrium by the balance of friction and driving forces, keeping the shear layer from segregating completely. This difference can also be attributed to the fact that the 1DV model has the numerical switch implemented to keep the plug layer constant described in Section 5.3.1.

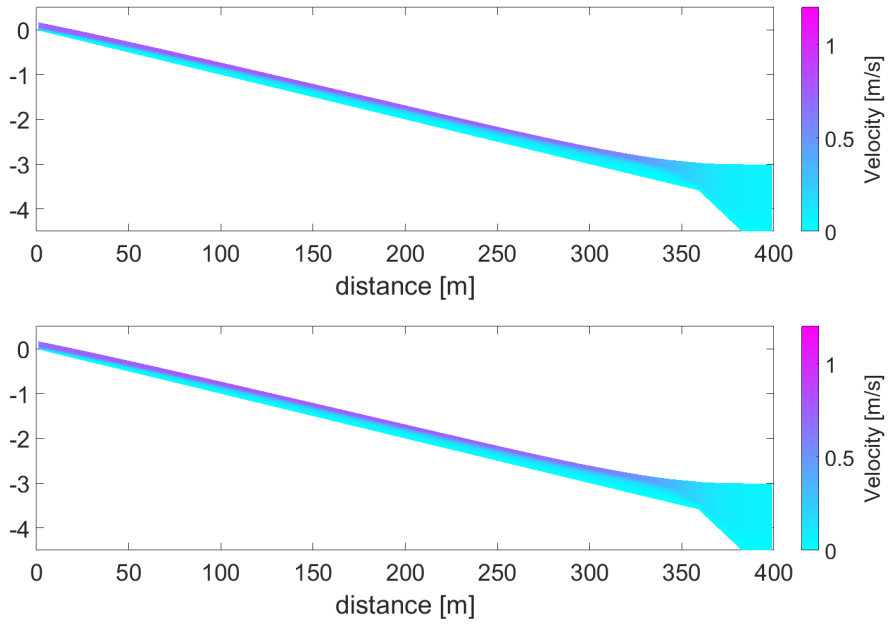

Figure 6.22: Horizontal cross section of slope with the velocity profiles. For run Sand 3 (450) and rheological models M1 and M3 respectively. Taken after five hours.

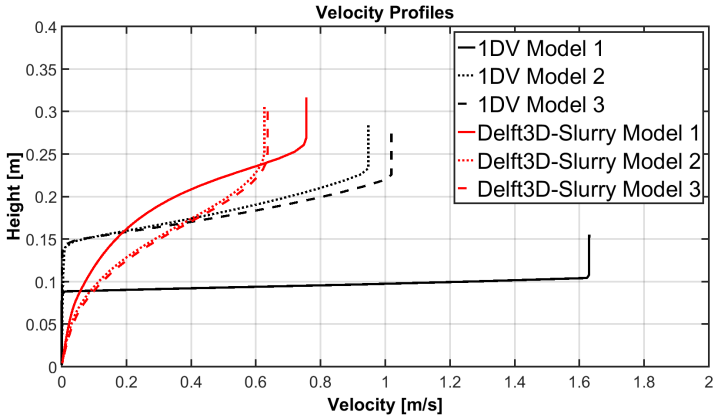

Figure 6.23: Comparison of velocity profiles between the 1DV model (black) and Delft3D-Slurry (red) taken at middle of the slope (so after 200 meter). For changes in rheological model (dashed lines).

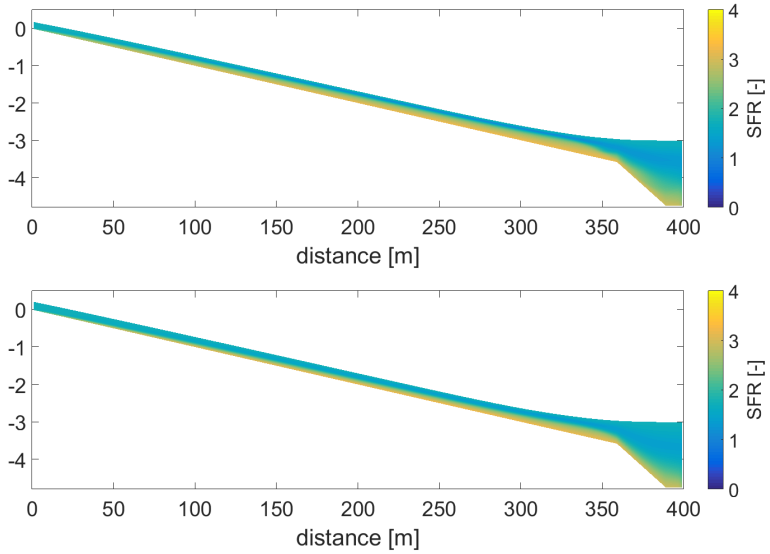

Figure 6.24: Horizontal cross section of slope with the SFR profiles. For run Sand 3 (450) and rheological models M1 and M3 respectively. Taken after five hours.

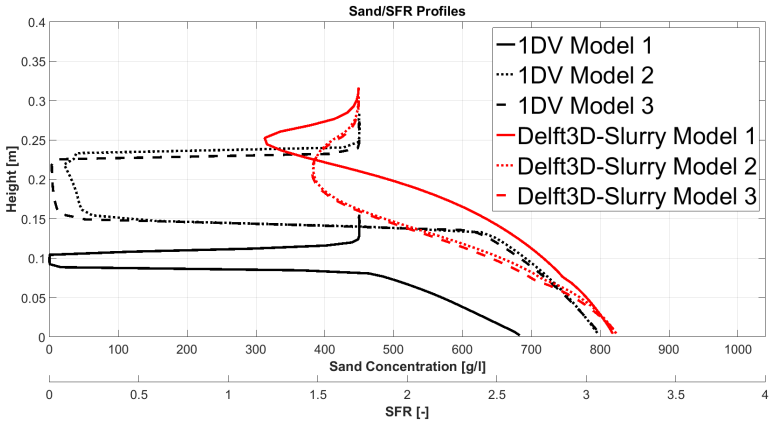

Figure 6.25: Comparison of SFR profiles between the 1DV model (black) and Delft3D-Slurry (red) taken at middle of the slope (so after 200 meter). For changes in rheological model (dashed lines).

In the Delft3D-Slurry model, the SFR/sand profile from rheological model M1 has a smaller shear layer and therefore a higher plug velocity. This creates a higher shear rate and more sand settling. Comparing the 1DV with the Delft3D-Slurry model, the two Bingham models do not have a linear shear layer in the Delft3D-Slurry model, whereas they have in the 1DV model. The segregation of the shear layer in the 1DV model is much larger than in the Delft3D-Slurry model. This can occur because there is a larger difference between bed velocity and plug velocity which gives a higher shear rate. The fall velocity of sand particles is higher in the 1DV model but yet again this formulation is coupled with the apparent viscosity of the fluid and this depends on shear rate.

The results between the two models clearly show differences in behaviour due to the different set-up. However the coupling between rheology and segregation seems to work in both models. The formation of a shear layer and a gelled bed is present in both the 1DV and Delft3D-Slurry model.

6.3. Delft3D-Slurry Applications to Oil Sands

This section will provide some possible applications of the Delft3D-Slurry model with respect to the oil sands. First a comparison is made with the data set from Chapter 3. The depositional behaviour of the model can be put into terms of fines capture, this number can then be compared with the actual data on fines capture. Hereafter some scenarios are simulated regarding operational aspects. In a tailings facility the discharge of slurry is preferably a continuous stream. However it can happen that the discharge rate is disturbed by a defect or enforced stop of activity. This means that sometimes only a water or fluid fine tailings are discharged. After a while the original tailings stream can be turned on again. The question of the industry is: What will happen when two tailings with different strength flow over each other ?

There can occur two situations.

1. Strong tailings discharged over initial weak tailings.
2. Weak tailings discharged over initial strong tailings.

There are multiple possibilities or hypotheses. The tailings can mix with each other or flow completely separated. The strong material can run over the initial material or underneath. Another option can be that the discharged slurry pushes the initial tailings away down the slope.

6.3.1. Computations of Fines Capture

A preliminary comparison of the deposition model is made with the data set from Chapter 3. The final goal of the comparison is to check whether a slurry with a higher SFR has a higher fines capture. This comparison can only be made when the bottom topography and other operational aspects than initial slurry concentration are very similar. This can either be flume tests or field test using the same deposition cell. Different options are: the flume tests from 2011, the Küpper field tests and the OSLO field tests. The flume tests are performed in a small flume, which is closed at time is zero and then filled with slurry allowing solid to settle before a plug is opened that releases a runoff of water and fines. Although a comparison of 2DV with a flume test is preferable, this depositional process is not straightforward. The flume is contained at the end, has wall effects and probably erosion when being depleted. This gives different kinetic energy levels of the flow that are not easy to validate with simulations. Than there are the observed field tests with only a BAW that come closest to the typical set-up. Focus therefore will be on field test from Küpper and OSLO, which are BAW tests.

To be able to compare the given data, the concentrations are derived from SFR and solid content. A rheological set of parameters compatible with oil sand is used. Rheological parameter Set 3 is chosen with parameters from Table 4.4, because it resembles thickened tailings the most. Rheological model M2 is used. The concentration parameters for küpper and OSLO are listed beneath in Table 6.3 also the result on fines capture from the data is given.

Table 6.3: Kupper and OSLO field tests, input information retrieved from the data set from Chapter 3

	sand $[g/l]$	clay $[g/l]$	water $[g/l]$	Density $[kg/m^3]$	SFR slurry	fines capture
Kupper 1	981	82	598	1660	12.2	42
Kupper 2	684	174	675	1533	4	21
Kupper 4	338	142	818	1298	2.4	20
OSLO 1	844	70	654	1568	12	71
OSLO 7,8,9	901	97	622	1620	9.3	65
OSLO 2,4	798	185	628	1610	4.3	41
OSLO 3,5,6	621	226	679	1526	2.7	29

From Table 6.3 some conclusions can be made. Some tests are close to the cohesive boundary, Kupper 1 and OSLO 7,8 and 9 have fines content underneath the 10 % solids (ranging from 7.5 top 10 %). The rheological models are made on the assumption that the fluid is in a cohesive regime, this must be explicit. Observed data are probably in the turbulent regime, but this is not well described in the report. But this does have large influence on the actual fines capture. More detailed information besides concentrations is needed en found for Küpper tests. These are the tests that will be compared with the data. The OSLO test are not detailed enough.

In the phd thesis from [Kupper, 1991] the field tests are described in detail. The beach length is approximately 300 m and also a height profile is given. Kupper 1 has a difference in height of 9 meters so a 3 % slope, Kupper 2 and 4 have 6 meters of difference in height so a 2 % slope. General overview, top views and geometry profiles from the Küpper tests can be found in Appendix C. The discharge is 0.3 m^3/s over the entire width, which leads to a specific discharge of 0.003 m^2/s. Two-dimensional velocity and SFR profiles are given in Figures 6.26 and 6.27. From the 1DV SFR profile taken at the middle of the beach (Figure 6.28), the average beach SFR can be estimated. From this estimation, an indication for fines capture can be calculated by the ratio of SFR_{slurry} over SFR_{beach} and considering a 100 % sand capture. The fines capture percentages are compared with the data set.

The 2DV profiles from the Küpper tests are not very thick to begin with. This is due to the small discharge rate. This leads to a low flow velocity but the flow is subjected to segregation. It is interesting to see the lower part of the slurry being completely depleted of solids in Figure 6.27, kupper 4 that is. Kupper 2 does not even reach the pond in 5 hours and also has significant difference in SFR when bottom and top of the slope are compared. Kupper 1 has started with strong material in the pond, Kupper 2 and 4 with weak material. In Kupper 1 the top part of the pond is filled with FFT that have been the left over from segregated tailings. They do not mix, but stay on top of the material. In the

Kupper 2 test it is visible that in the top part of the slope a thicker area exist. This keeps forming from time to time and has a sort wave like character. It builds up due resistance and then breaks and flows down the slope with rather high flow velocities. This can occur when the simulation has a relatively low viscosity.

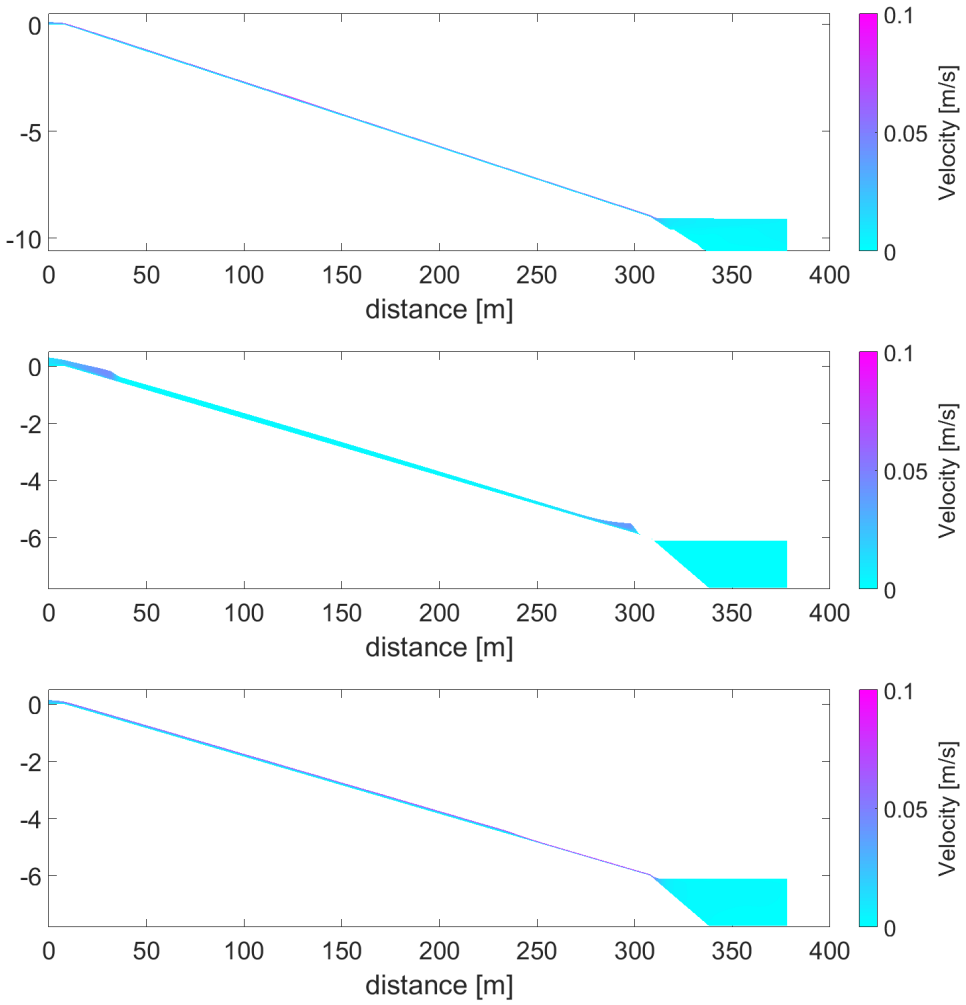

Figure 6.26: Horizontal cross section of slope with velocity profiles. For Kupper tests 1, 2 and 4 respectively.

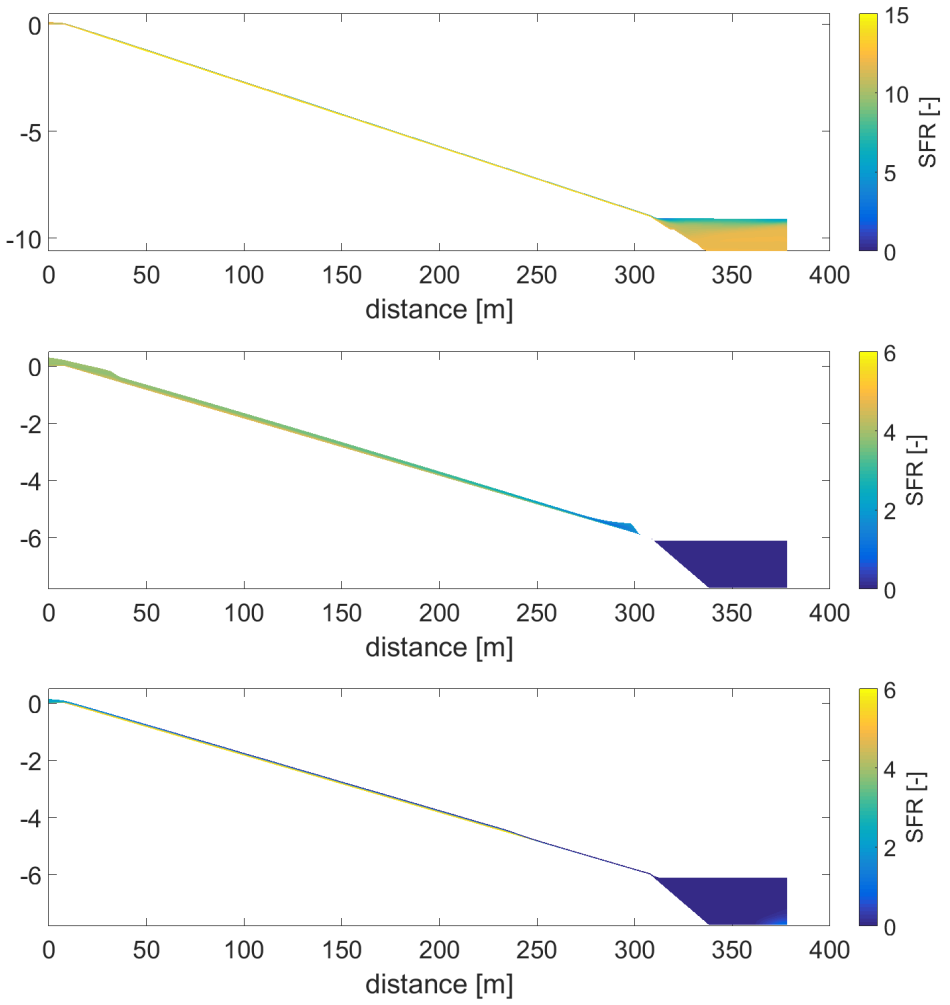

Figure 6.27: Horizontal cross section of slope with SFR profiles. For Kupper tests 1, 2 and 4 respectively.

To determine the SFR of the beach in the Küpper runs figure 6.28 is analysed.

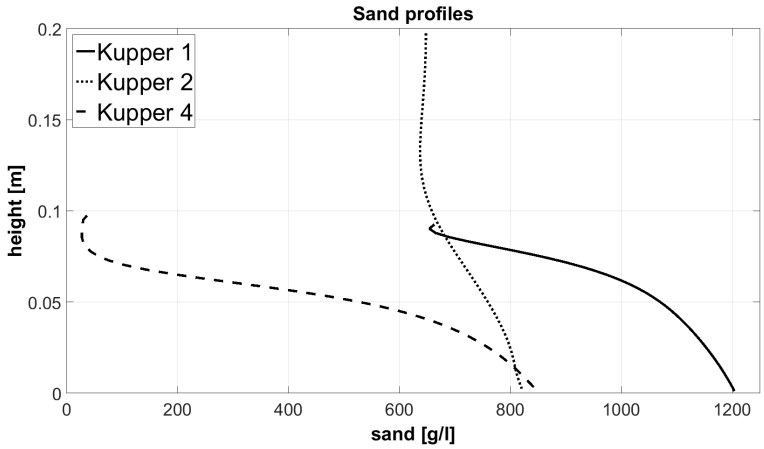

Figure 6.28: Comparison of sand profiles for the three different küpper tests. Used to determine SFR of beach.

Kupper 1 has a beach SFR of 1120/82 = 13.66 which leads to a fines capture of 89 %.
Kupper 2 has a beach SFR of 780/174 = 4.5 which leads to a fines capture of 89 %.
Kupper 4 has a beach SFR of 780/142 = 5.5 which leads to a fines capture of 44 %.

Resulted fines capture is larger than the data set. If looked at the trend line, the only interesting thing to see is that Kupper 1 and Kupper 4 differ by factor 2. Kupper 2 is out of range by a lot.

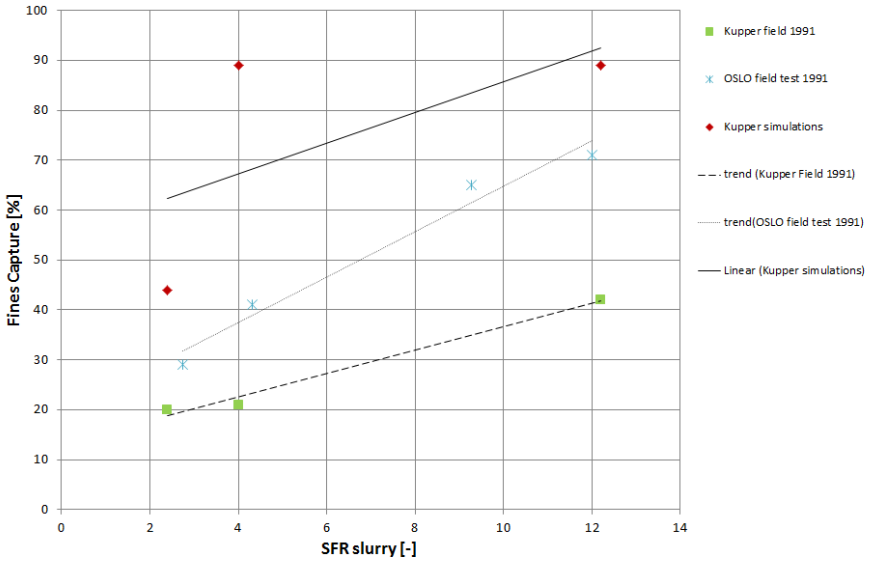

Figure 6.29: Fines capture vs SFR slurry. Plot from data now with simulations included küpper tests.

6.3.2. Strong Tailings over Weak Tailings

The two options from the list in the begin of this Section 6.3 are simulated in Figures 6.30 to 6.33. Both options show 2DV profiles for velocity and SFR. Note that the colour bar axes for velocity differ in magnitude to increase legibility. The time instances that are shown are at time: 0, 1h, 2h30m, 4h, 5h, this was chosen to focus on the initial and end situation.

The Rheological parameter set that is used is Set 1, from Table 4.4. Rheological model M2 is used. This Set 1 was chosen based on a relative strong influence of sand particles (Figure 4.7). This sand influence was needed because although there are two different tailings present, Delft3D-Slurry can only attribute one rheology per simulation. By adapting the sand content the different tailings can forced a certain behaviour although it can be unrealistic (like the strong tailings from Section 6.3.3). However these simulations are quantitative and only performed to show behavioural effect of multiple tailings on each other.

The first situation is Strong over Weak tailings. The situation is plotted in Figure 6.30 and Figure 6.31 representing velocity and SFR profiles respectively. The initial weak slurry is evenly distributed over the slope and has a height of 10 cm. The initial sand content is 53 $[g/l]$ and clay content is 260 $[g/l]$. This gives an initial yield stress 15 $[Pa]$ for the weak slurry. The stronger discharged slurry has 1 specific discharge rate of 0.01 $[m^2/s]$, sand content is 653 $[g/l]$ and clay content is 260 $[g/l]$. This gives a yield stress of 165 $[Pa]$ for the stronger slurry. What can be seen is that the weak initial layer is at standstill, so it is below equilibrium height. When the stronger slurry is being discharged the initial weak material is being pushed away. The front of the slurry does show some mixing behaviour but in front of the discharged stronger slurry, clearly some bumps with the initial weak concentration can be distinguished. The stronger slurry is not flowing over the weaker initial layer, this is expected as the stronger slurry is heavier. The average flow velocity is only 0.015 $[m/s]$. After 5 hours the simulations has ended and it is interesting to see what has happened to the front of the stronger slurry. Until now we have seen rather vertical fronts on dry beds. Now however, the stronger slurry is in contact with an initial material and the entire front has spread over a wide hundred meters.

6.3.3. Weak Tailings over Strong Tailings

Here the second situation, Weak over Strong tailings, is described. The situation is plotted in Figure 6.32 and Figure 6.33 representing velocity and SFR profiles respectively. The strong initial slurry reaches approximately half way down the slope and has a height of 40 cm. The initial sand content

is 1060 $[g/l]$ and clay content is 260 $[g/l]$. This gives a yield stress of 4000 $[Pa]$ for the strong initial slurry. This is very high and unrealistic but necessary to force the slurry at a standstill on the slope. The specific discharge rate of the weak slurry again is 0.01 $[m^2/s]$, the sand content is 53 $[g/l]$ and clay content is 260 $[g/l]$. This gives a yield stress of 15 $[Pa]$ for the weaker slurry. What can be seen is that the strong initial slurry layer is not completely at standstill, it is slightly moving to find an equilibrium. When the weaker slurry is being discharged it builds up a relative thick layer. At the top of the strong initial layer and bottom of weak slurry there is some mixing between the slurries. This causes the entire slurry to slow down. Once the weak tailings are past the initial material the flow layer is thinner. The initial material with high SFR and the mixed layer on top are not moving, the weaker slurry is flowing over the initial material. The average velocity of the weaker slurry on top of the strong beach is 0.08 [m/s], but the flow velocity is more dynamic and not as constant as the strong over weak tailings simulation.

Between the different tailings there is some mixing visible for both Strong over Weak and Weak over Strong tailings. The flow regime is laminar, which does not allow vertical mixing. This process may be a form of numerical stretching of cell layers but is not fully understood yet. Summarised characteristic of the slurries can be found in Table 6.4

Table 6.4: Characteristics of the different cases of oil sands running over each other

Case	**Tailings**	**Sand content** $[g/l]$	**Clay content** $[g/l]$	**Yield stress** $[Pa]$
SoW	Weak	53	260	15
SoW	Strong	653	260	165
WoS	Weak	53	260	15
WoS	Strong	1060	260	4000

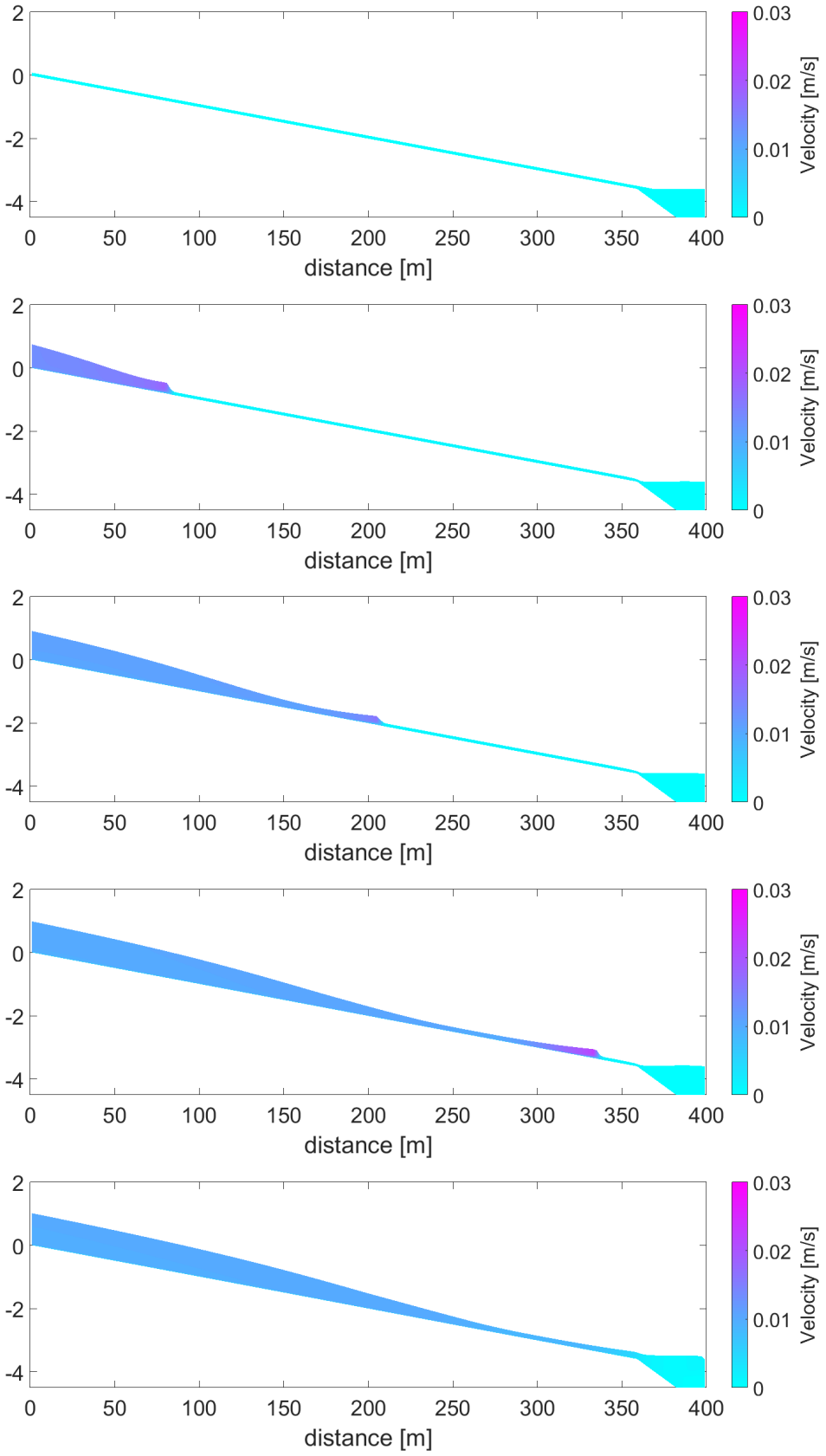

Figure 6.30: Horizontal cross section of slope with the velocities. Strong over weak tailings. Time steps are: 0, 60, 150, 240 and 300 $[minutes]$ respectively.

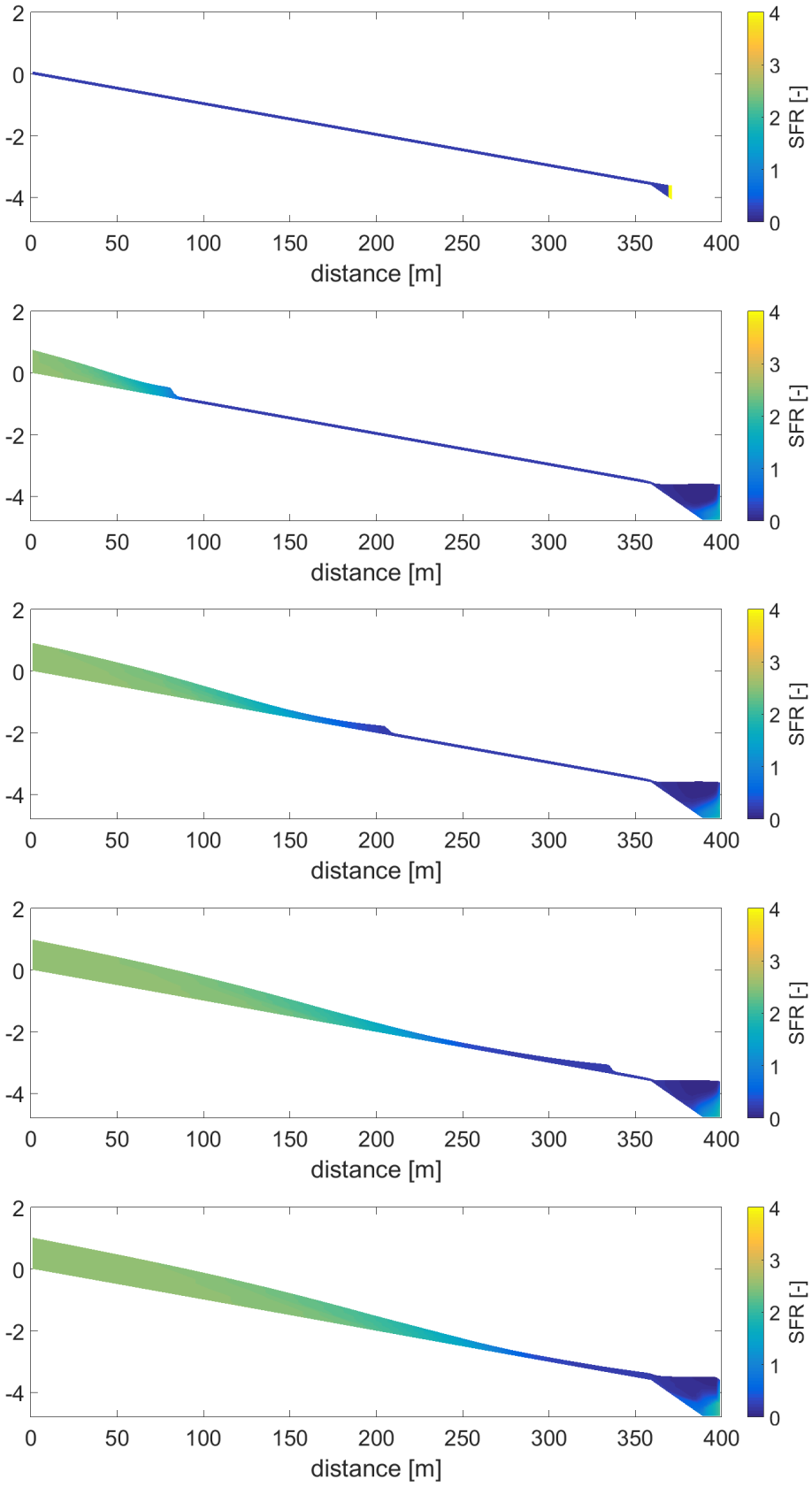

Figure 6.31: Horizontal cross section of slope with the SFR's. Strong over weak tailings. Time steps are: 0, 60, 150, 240 and 300 [$minutes$] respectively.

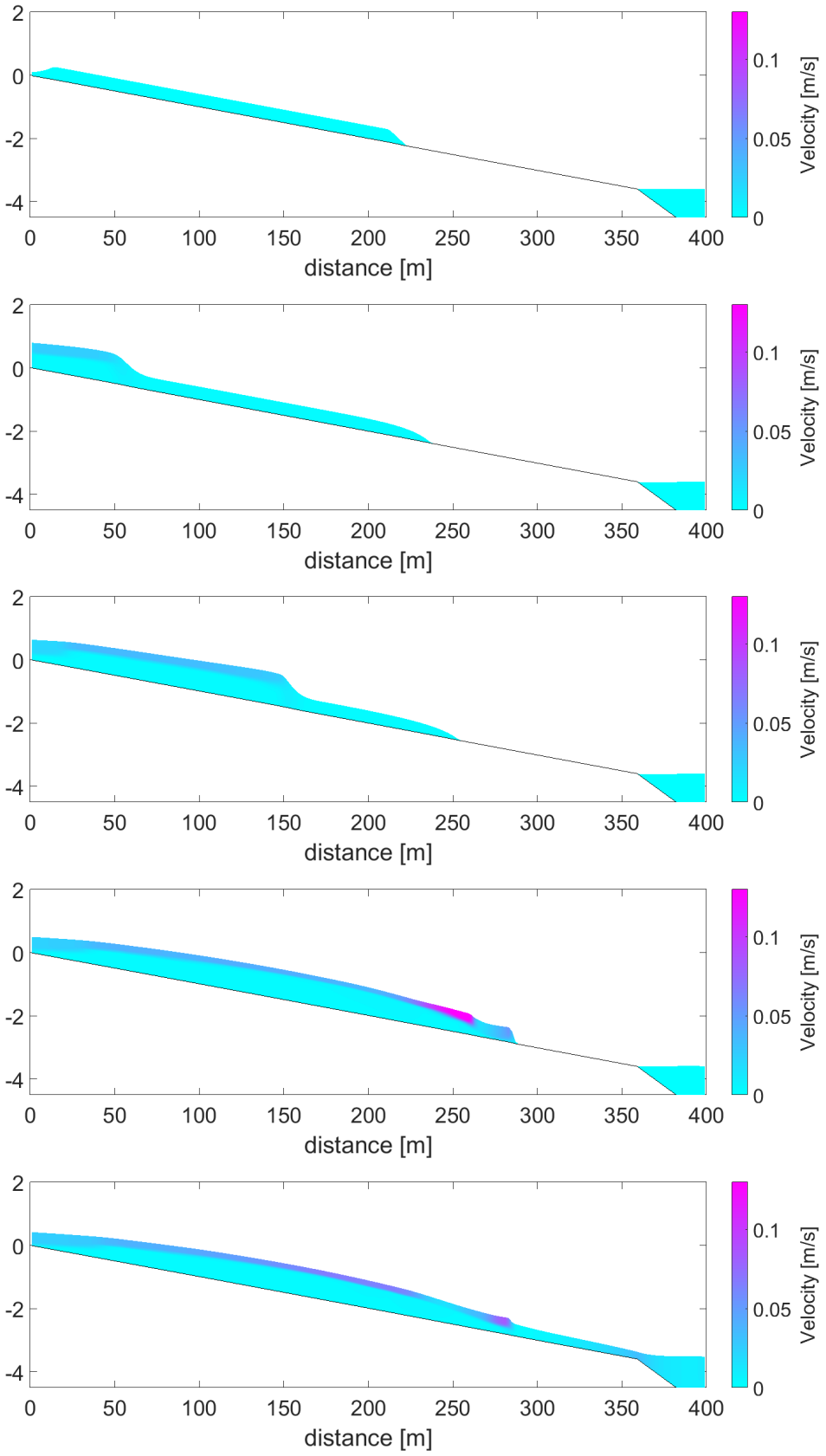

Figure 6.32: Horizontal cross section of slope with the velocities. Weak over strong tailings. Time steps are: 0, 60, 150, 240 and 300 $[minutes]$ respectively.

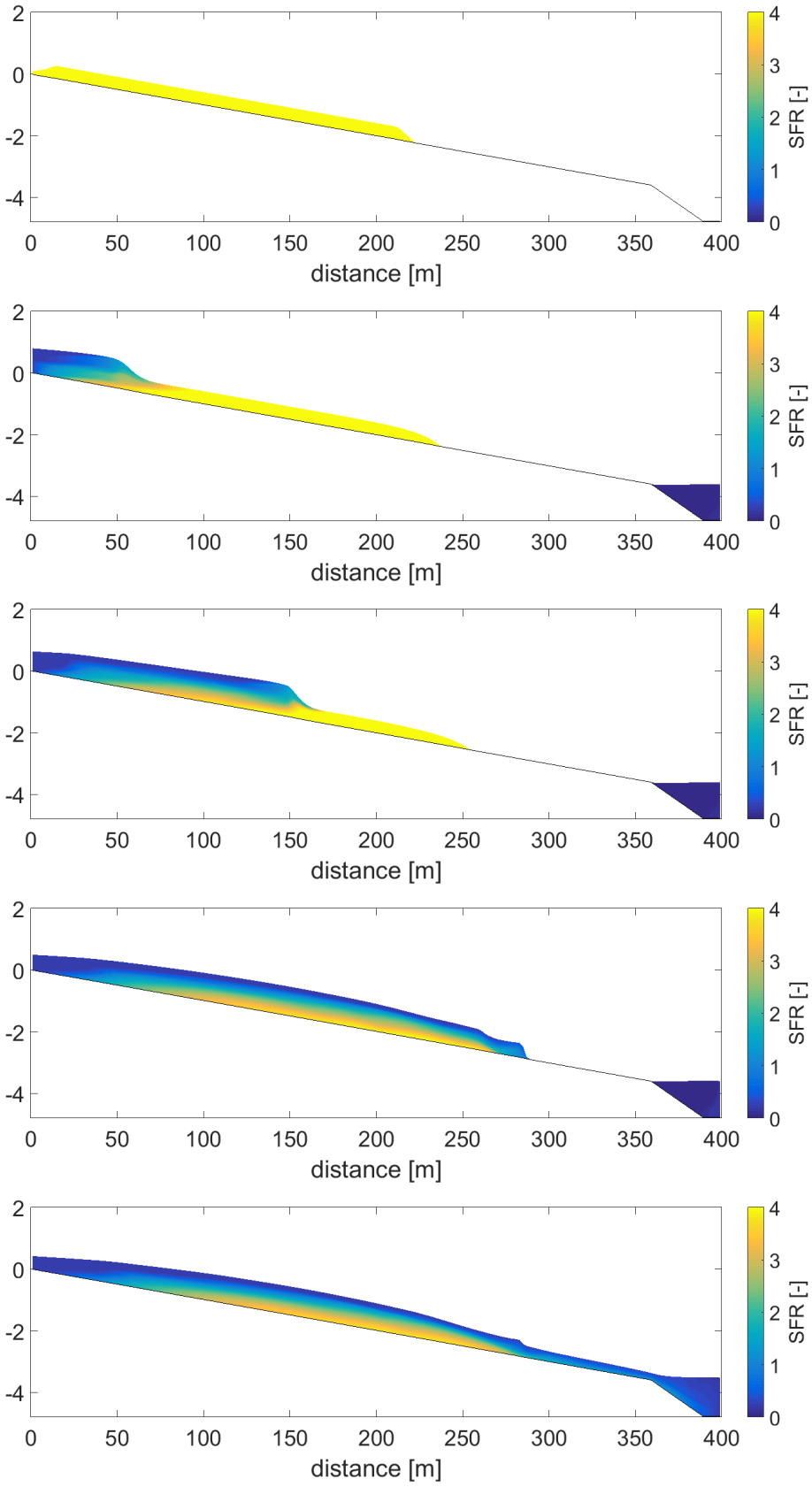

Figure 6.33: Horizontal cross section of slope with the SFR's. Weak over strong tailings. Time steps are: 0, 60, 150, 240 and 300 [$minutes$] respectively.

6.3.4. Strong tailings that do not reach the pond

What happens when a material is very strong ? In most of the simulations the slurries do reach the pond quite quickly, due to high discharge rate and low strength. After reaching the pond, the slurries start to form an equilibrium where deposition on the beach and into the pond are equal. This leads to a non-changing velocity profile. In reality and in field tests the slurries travel slower and the front of the slurry gradually connects to the bottom instead of having a vertical front. Figure 6.34 provides a simulation with lower specific discharge rate of 0.01 m^2/s and a higher yield stress. This is performed to show the travelling front of the slurry. The yield stress is 150 Pa and this is achieved by increasing the sand concentration. This is done to see what happens with the entire slurry and especially its front, when it flows down the slope and does not reach the pond in five hours. The strong material forms a square root function front. Also there is no segregation due to the high yield and low flow speeds. As a matter of fact it can be seen as a NST simulation.

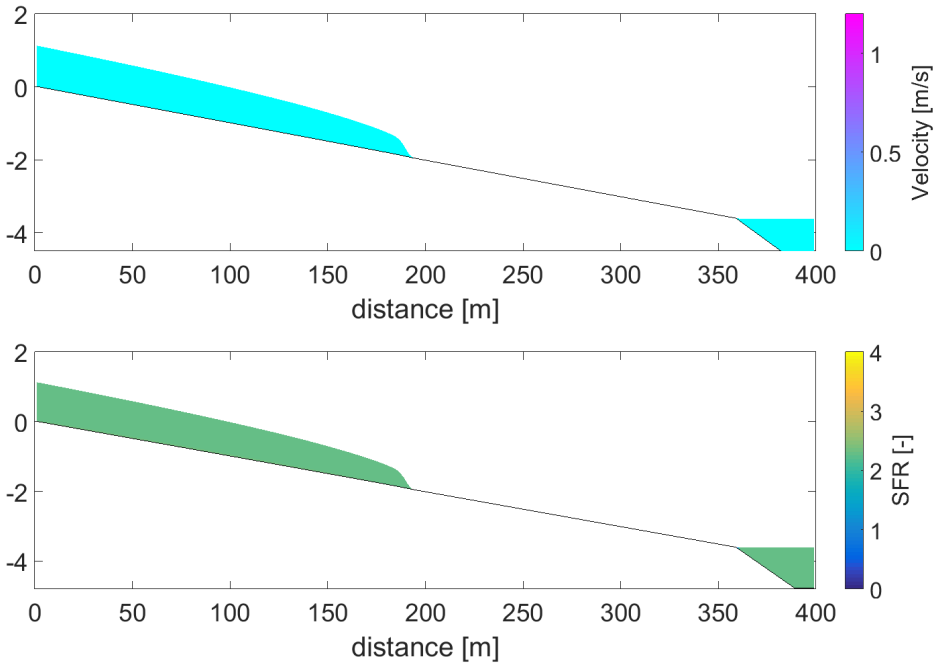

Figure 6.34: Horizontal cross section of slope with velocity and SFR profiles. For a high yield slurry. Taken after 5 hours.

6.4. Conclusions on Results

- The velocity profiles between the 1DV and Delft3D-Slurry model for simulations with only fines are very similar.
- Velocity and sand profiles between the one-dimensional and two-dimensional model for simulations with fines and sand are different. The Delft3D-Slurry model receives constant information from upstream whereas the 1DV model only computes profiles from an initial profile. Results are also different because the 1DV model has been coded with of plug preservation and Delft3D-Slurry does not. The bed layer in 1DV is at near standstill and in 2DV still clearly moving, because the mechanism behind bed friction is different.
- It is unknown how much smoothing is provided by longitudinal advection. A test against an analytical solution from [Childs, 2013] for the verification of advection scheme at low concentrations or a test against the flume test from [Spelay, 2007] and numerical model from [Treinen et al., 2010] & [Treinen and Jacobs, 2015] is advised.
- If the strength of the mixture increases, also the plug thickness increases. Stronger and more viscous materials have lower flow speeds and therefore a larger flow thickness.
- The laminar flow assumption does not work for material with almost no yield or with properties very similar to water.

- Increasing the clay content shows similar behaviour as increasing the rheological parameters.
- The deposition of sand creates a sliding bed on a 1 % slope, this together with the deposit being pushed away by the discharge causes the thickest bed deposition to appear at the bottom of the slope.
- Sand particle diameter has a big influence on fall velocity and therefore bed formation.
- Gelled bed concentrations for Delft3D-Slurry are well calculated compared to the 1DV model, apart from rheological model 1, but M1 has a much thinner flow height to make a accurate comparison.
- Not many conclusions can be drawn on the verification of the data set. The model over predicts the calculation of fines capture by a lot. At this point there are not enough details in the COSIA data set from Chapter 3 and not enough experience with the model to worry about this result.
- Strong material over weaker material and Weak material over strong material show mixing between the interface level of the different tailings. The flow is laminar and this should not provide a physical mixing mechanism. This process is not yet understood but can be the numerical stretching of the vertical grid cells.
- The front of the slurry does show square root function behaviour when strong and viscous enough. For lower strength slurries a vertical front or a ”bore”-like flow is observed until the pond is reached. This behaviour is still unclear for the author.

7

Discussion

There are still many points of attention for the model. Some will be pointed out in this discussion. The depositional behaviour: for now only a 2DV channel with laminar flow has been simulated, mainly to check non-Newtonian behaviour and the shear induced settling process. In reality tailings flow is likely to be deposited as sheet flow, where flow will spread over a large area and create a lob like deposition. When the resistance force reaches a certain point, the flow will adapt its path and create a new lob. Flow speeds over these lobs are relatively low and can be considered laminar. However over time channel formation can take place, due to the changed topography that creates low zones. In a channel the same amount of material flows through a much smaller area. This means that flow speeds and energy are increased and that the flow can enter turbulent or transition regime. Turbulence is likely to hinder the settlement mechanism. This explains that channels can run for long times (multiple hours) without changing direction. The 2DV situation simulates a 10 meter wide channel, so turbulence can play a role in combination with a large discharge. This should be researched in the next phase.

The upwind code in combination with the numerical switch the 1DV model seem to solve the disturbances and the depletion of the plug layer. In the 1DV model only processes in the vertical direction are considered and only fluxes downwards due to gravitational force are modelled in laminar conditions at the moment. This justifies the use of the upwind approach for the 1DV model. In Delft3D-Slurry the computational scheme is not changed to an upwind scheme since there are more processes involved, also future development of the model will probably include re-suspension processes or fluxes in upward direction. No critical disturbances in the Delft3D-Slurry model are found in the results (Section 6.2). For the time being the original central difference scheme is used. Detailed research into these changes in calculation schemes in Delft3D-Slurry are not yet performed though and need some review in further development.

In simulations including sand particles and bed formation a critical note must be placed with calculation of characteristics of the flow. When the slurry is segregated, the bed, shear and plug layer of the flow behave different and no single Reynolds number or yield stress can be appointed to the slurry. A formed bed may be left out of the equation when calculating the Reynolds number, and rather a annulus velocity and height of sheared layer needs to be used instead of a mean velocity and total slurry height.

The lower boundary is a water level boundary. A fixed water level is prescribed and the pond boundary lets fluid pass through with a reflection coefficient that is set so it behaves very permeable. The prescribed specific discharge in the sensitivity analysis of 0.1 m^2/s can be larger than the lower boundary can process. The presence of a carrier fluid with fines instead of only water may affect the prescribed water level to deviate. Observed can be this rise in water level of pond until incoming and outgoing fluid reach equilibrium. This can be seen and read in the propagating in time result (Section 6.2.6). There are no direct solutions for this pond behaviour. The bottom of the slope is affected by this and the deposit in that area. It does show a larger settlement for beaches below water even though that area was designed as a beach above water.

The bed layer is slipping down the slope. Either the defined slope is steeper than naturally would occur or a force created by the discharge is pushing harder than resistance formed by the bed. This can also be seen in the propagation in time result (Section 6.2.6 and Figure 6.15), but also in other simulations with sand. If the function of yield stress compared to bed concentration is analysed it is interesting to see at which value of sand concentration the yield stress is large enough to form a bed at standstill and if this value is realistic. The influence of the sand can be adapted in the rheological parameters β_y.

The front of the slurry is a point of attention. Depending on the yield stress of the slurry the front will have vertical ”hydrostatic bore” or a square root function; ultimately the equilibrium thickness will be reached when moving away from the front. When the slurry is relatively weak and has high flow velocities a vertical ”bore-like” is observed. This front can lead to instabilities and numerical complications when the front collapses or reaches the pond, creating large waves in the pond. In experiments the front often has a square root function with increasing height until it reaches equilibrium height. If the viscosity and strength is large enough this behaviour can be observed (see Section 6.3.4).

The results from the 1DV model and the Delft3D-Slurry model in 2DV cannot be compared directly, due to differences in set-up and information stream. However it does gives an indication of the correct transported rheology and shear induced settling equations from the simple 1DV model to Delft3D-Flow. The non-Newtonian behaviour can be distinguished clearly as well as the segregating process with gelled bed concentrations similar for both the 1DV and Delft3D-Slurry model when rheological models M2 and M3 are considered.

The comparison with the COSIA data set does not provide a satisfactory result. The supplied data is not sufficient or detailed enough to draw concrete conclusions due to missing rheological measurements mainly. Also it is not ideal to test Delft3D-Slurry with the present definition of fines capture. The model has the assumption that fines stay homogeneously suspended in the mixture and there is no mechanism of coarse particles actively trapping fines in between their pores. Verification of velocity profile, flow height and concentration profile with known rheology is critical for further development.

The rheology needs more attention nonetheless. Stated before was the enhancement of the plastic viscosity in almost all runs by factor 100, compared to the few available viscosity data on mineral and oil sand tailings. This enhancement is performed by changing the rheological coefficient for the calculation of the viscosity. A larger plastic viscosity maintained a laminar flow and showed a clear shear layer. However this viscosity enhancement also affects the fall velocity of sand particles. It is possible to increase the particle diameter of the sand particles to keep a realistic view on sand segregation. The ratio of the apparent viscosity of the original and enhanced slurry needs to be determined, this ratio will be identical to the factor for increased particle diameter. This ratio differs for every slurry with a changed yield stress, so it is not that easy to come up with a coefficient.

When different materials flow over each other, some mixing behaviour can be observed. Laminar flow is characterized by no vertical mixing. Probably a numerical effect is occurring here where the vertical grid cells are stretched out and the concentration constituents on the interface are averaged between the different materials.

8

Conclusions and Recommendations

8.1. Conclusions

The main conclusion from this thesis are:

- Different types of oil sand tailings exist and pressure from governments have pushed slurries to become thicker, thus reaching higher sand contents. Tailings are classified depending on their solid content, FOFW and fines percentage. Some are called Whole Tailings (WT), Fluid Fine Tailings (FFT), Thickened Tailings (TT), Mature Fine Tailings (MFT) and Non-Segregating Tailings (NST). MFT cause problems due to long settlement times of the fines.
- The laminar-turbulent transition of non-Newtonian fluids often occurs at lower Reynolds numbers than for Newtonian fluids. However no well-known transition criteria for non-Newtonian open channel flow exist. Expected transition number may lie in the range of $Re \sim 700$, so tailings can enter turbulence at lower flow speed than Newtonian fluids.
- Up to date there is no accurate or widely used numerical model available that is able to simulate high density non-Newtonian flow with included formulations for rheology and segregation. The development of such a model may lead to: solving problems faced by the industry, reducing environmental issues and a better understanding of overall slurry flow.
- Slurries with a higher SFR have more sand available to capture fines and therefore a higher fines capture, but also relative less fines to begin with. The most important parameter on fines capture is not in slurry material but in initial topography and the kinetic energy of the flow.
- The rheological parameters still have a plastic viscosity that is enhanced with a factor 100 compared to the original retrieved parameters from experiments. This is done to be able to create a larger shear layer as well as to stay inside the laminar regime.
- Velocity profiles between the 1DV and Delft3D-Slurry model for simulations with only fines or carrier fluid only are very similar. So it can be concluded that the equations for rheology and shear settling are transferred correctly.
- Velocity and sand profiles between the 1DV and Delft3D-Slurry model for simulations with fines and sand are different. The Delft3D-Slurry model receives constant information from upstream whereas the 1DV model only computes profiles from an initial profile. Results are also different because the 1DV model has been coded with ”plug preservation” and Delft3D-Slurry has not. The bed layer in 1DV is at near standstill and in the 2DV situation clearly moving. This difference is probably because the mechanism behind bed friction is different.
- The deposition of sand creates a sliding bed on a 1 % slope, this together with the deposit being pushed away by the discharge causes the thickest bed deposition to appear at the bottom of the slope. Also the hydraulic gradient in the bottom part of the slope is smaller, this creates an area with less kinetic energy so more suitable for sand settlement.

- Not many conclusions can be drawn on the verification of the data set. The model over predicts the calculation of fines capture by a lot. At this point there are not enough details in the data set and not enough experience with the model to worry about this result.

8.2. Evaluation

The objective of this study was to continue the work on the development of a numerical dynamic depositional model. This model should be able to simulate a broad range of different tailings down a slope. Furthermore the model should be verified against laboratory or field data.

- The 1DV model was used to test the processes for rheology and segregation in the vertical direction. After this was tested the transition to Delft3D-Flow could take place.
- Rheological properties determine tailing properties a lot. Three different sets of empirical rheological parameters are composed to compare different sort of tailings, (Mineral tailings and Oil sand tailings).
- The COSIA data set for oil sand tailings did not provide rheological properties for the slurries (yield stress and viscosity measurements). This resulted that a decent verification could not be realised.

8.3. Recommendations

- The laminar-turbulent regime for non-Newtonian flow in open channels needs to be defined appropriately and needs to compatible with Delft3D, the k-epsilon model or a new implemented turbulence model.
- A proper formulation for the interaction of slurry with the a solid bottom boundary has to be incorporated.
- A more consistent determination of rheological parameters is needed. Multiple rheological measurements are needed to achieve these parameters like, fractal dimension, sand influence and other constants. Hereafter, in combination with measured flow and concentration profiles, further and better validation of the model can take place.
- The Delft3D-Slurry model is not yet accurate enough for testing against the field data from the COSIA data set. Experimental flume data with accurate measurements on velocity, concentration and rheology should be the next step forward. For instance data from flume tests described in [Spelay, 2007]. Flume tests are also closer to a 2DV environment than entire field tests that are subjected to 3D effects.
- The Delft3D-Slurry model should be tested in a 2DV environment against an analytical solution for non-Newtonian sand depositing in a power-law fluid. For instance the work from [Childs, 2013] and/or [Sisson et al., 2012].
- The typical set-up needs to be improved if the beach below water and its effects on fines capture is to be examined. The current set-up has a beach below water too close to the end boundary, which will have its influence.
- The code adaption for plug preservation has not been implemented in Delft3D-Slurry. This can be an option to implement, the question is whether this mechanism is working the same in 2DV/3D as in 1DV.
- Verify working with a plastic viscosity that is a 100 times larger than normal. This increase in plastic viscosity leads to an increase in apparent viscosity and a decrease in the settling velocity. The particle diameter can be increased to sustain a realistic sand settling velocity.
- The Delft3D-slurry model has only been tested in a 2DV environment; in the longitudinal direction. Tests in the lateral direction and in 3D should be performed. A channel that runs diagonal through the computational grid can be a first set-up in 3D.

- Until now the fines fraction only consisted of clay particles that are suspended in the carrier fluid. In reality there is a presence of silts, this can be estimated as a 50/50 silt/clay distribution. These silt particles will have its influence on the rheology of the mixture and should be incorporated once validated.
- The effect of thixotropy, or time-dependent rheological parameters, should be investigated. This will have its effect on tailings flow and the sand deposit.
- investigating the physics behind ”gap closing” and ”shear bending”. These processes are not mentioned in the report but need some attention.

Bibliography

AMEC, Environmental & Infrastructure (2013). Beach fines capture study. Technical report, Cosia.

Bagnold, R. A. (1954). Experiments on a gravity-free dispersion of large solid spheres in a newtonian fluid under shear. *The royal society, Mathematical and Physical Sciences*, 225(A):49–63.

BGC Engineering Inc (2010). Oil sands tailings technology review. Technical report, Oil Sands Research and Information Network, University of Alberta, School of Energy and the Environment., Edmonton, Alberta.

Charlebois, L. E. (2012). On the flow and beaching behaviour of sub-aerially deposited, polymer-flocculated oil sands tailings: A conceptual and energy-based model. Master's thesis, The university of British Colombia.

Chhabra, R. P. (1993). *Bubbles, drops and particles in non-Newtonian fluids*. CRC Press.

Childs, L. H. (2013). *Low Reynolds Number Flows Of Generalized non-Newtonian Fluids*. PhD thesis, School of mathematics, University of Bristol.

Coussot, P. (1994). Steady, laminar, flow of concentrated mud suspensions in open channel. *Journal of Hydraulic Research*, 32(4):535–559.

Dankers, P. J. T. and Winterwerp, J. C. (2007). Hindered settling of mud flocs: Theory and validation. *Continental shelf research*, 27:1893–1907.

De Kee, D., Chhabra, R. P., Powley, M. B., and Roy, S. (1990). Flow of viscoplastic fluids on an inclined plane: evaluation of yield stress. *chemical engineering communications*, 96(1):229–239.

Deltares (2016). *Delft3D-Flow User Manual, Hydro-Morphodynamics*. Deltares, 3.15 edition.

Diep, J., Weiss, M., Revington, A., Molys, B., and Mittal, K. (2014). In-line mixing of mature fine tailings and polymers. In *Paste 2014,* 17^{th} *international seminar on paste and thickened tailings*, pages 111–126, Vancouver, Canada.

Fitton, T. G. and Slatter, P. T. (2013). A tailings beach slope model featuring plug flow. In *Paste 2013,* 16^{th} *international seminar on paste and thickened tailings*, pages 493–506, Belo Horizonte, Brazil.

Fitton, T. G., Williams, M. P. A., Seddon, K. D., Bhattacharya, A. G., and Chryss, A. G. (2007). Simulation of thickened tailings stacks. In *Paste 2007,* 10^{th} *international seminar on paste and thickened tailings*, Perth, Austrailia.

Gresho, P. M. and Lee, R. L. (1981). Don't suppress the wiggles, they're telling you something! *Computers and fluids*, 9:223–253.

Haldenwang, R. (2003). *Flow of non-Newtonian Fluids In Open Channels*. PhD thesis, Cape Technikon.

Hanssen, J. L. J. (2016). Towards improving predictions of non-newtonian settling slurries with delft3d: theoretical development and validation in 1dv. Master's thesis, Delft University of Technology.

Jacobs, W., Le Hir, P., Van Kesteren, W. G. M., and Cann, P. (2011). Erosion threshold of sand-mud mixtures. *Continental shelf research*, 31:S14–S25.

Kranenburg, C. (1994). The fractal structure of cohesive sediment aggregates. *Estuarine, Coastal and Shelf science*, 39:451–460.

Kupper, A. M. A. G. (1991). *Design of Hydraulic Fill*. PhD thesis, University of Alberta.

Mitsoulis, E. and Zisis, T. (2001). Flow of bingham plastics in a lid-driven square cavity. *non-Newtonian Fluid Mech.*, 101:173–180.

Morris, P. H. (2004). Mine waste beach profile and flow resistance equations. *International Journal of Surface Mining, Reclamation and Environment*, 18(4):253,272.

Papanastasiou, T. C. (1987). Flow of materials with yield. *Journal of rheology*, 31(5):385–404.

Pennekamp, J. G. S., Talmon, A. M., and van Kesteren, W. G. M. (2010). Determination of non-segregating tailings conditions. In 19^{th} *World Dredging Congress*, pages 848–858.

Pirouz, B., Kavianpour, M. R., and Williams, M. P. A. (2005). Thickened tailings beach deposition, field observations and full-scale flume testing. In *Paste 2005,* 8^{th} *international seminar on paste and thickened tailings*, pages 53–72, Santiago, Chile.

Pirouz, B., Seddon, K., Pavissich, C., Williams, P., and Echevarria, J. (2013). Flow through tilt flume testing for beach slope evaluation at chuquicamata mine codelco mexico. In *Paste 2013,* 16^{th} *international seminar on paste and thickened tailings*, pages 457–472, Belo Horizonte, Brazil.

Sanders, R. S., Schaan, J., Gillies, R. G., McKibben, M. J., Sun, R., and Shook, C. A. (2002). Solid transport in laminar, open channel flow of non-newtonian slurries. *Hydrotransport*, 15:597–611.

Sisson, R., Lacoste-Bouchet, P., Vera, M., Costello, M., Hedblom, E., Sheets, B., Nesler, D., Solseng, P., Fandrey, A., van Kesteren, W., Talmon, A., and Sittoni, L. (2012). An analytical model for tailings deposition developed from pilot scale testing. In 3^{rd} *International oil sand tailing conference 2012*, pages 53–63, Edmonton, Alberta, Canada.

Sittoni, L., Hanssen, J. L. J., van Es, H. van Kester, J. A. T. M., Uittenbogaard, R. E., Winterwerp, J. C., and van Rhee, C. (2016). Optimizing tailings deposition to maximize fines capture: Latest advance in predictive modeling tools. In *Proceedings IOSTC2016*.

Sittoni, L., Talmon, A. M., van Kester, J. A. T. M., and Uittenbogaard, R. E. (2015). Latest numerical developments for the prediction of beaching flow and segregating behavior of thick non-newtonian mixtures. In *Proceedings* 17_{th} *International conference on transport and sedimentation of solid particles*. Wroclaw University and Delft University of Technology.

Slatter, P. T. (2013). Analysis and flow behaviour prediction of paste material in sheet flow. In *Paste 2013,* 16^{th} *international seminar on paste and thickened tailings*, pages 473–480, Belo Horizonte, Brazil.

Sobkowicz, J., Hyndman, A., Dawson, R., and Watts, B. (2014). Guidlines for performance managment of oil sands fluid fine tailings deposits to meet closure commitments. Technical report, Canada's Oil Sands Innovation Alliance.

Soleimani, S., Simms, P., Wilson, W., Dunmola, A., and Freeman, G. (2013). Optimizing deposition of polymer-amended mature fine tailings. In *Geo Montreal 2013, 66th Canadian Geotechnical Conference*.

Spelay, R. B. (2007). *Solids Transport in Laminar, Open Channel Flow of non-Newtonian Slurries*. PhD thesis, University of Saskatchewan.

Spelay, R. B., Sumner, R. J., Sanders, R. S., and Gillies, R. G. (2006). Laminar open channel flow of kaolin clay slurries containing sand. In 13^{th} *International Conference on Transport And Sedimentation Of Solid Particles*, pages 300–313.

Swenson, J. B., Sheets, B., Kolstad, D., and van Kesteren, W. (2014). Semi-analytical modeling of thickened tailings flows. In *Proceedings of the* 4^{th} *International oil sand tailings conference*, Lake Louis Canada.

Talmon, A. M. (2016). Lecture notes oe4625, segregating non-newtonian slurries. TU Delft University of Technology.

Talmon, A. M., Hanssen, J. L. J., Winterwerp, J. C., Sittoni, L., and van Rhee, C. (2016). Implementation of tailings rheology in a predictive open-channel beaching model. In *Paste 2016,* 19^{th} *international seminar on paste and thickened tailings*, Santiago, Chile.

Talmon, A. M. and Huisman, M. (2005). Fall velocity of particles in shear flow of drilling fluids. *Tunnelling and underground space technology*, 20:193–201.

Talmon, A. M. and Mastbergen, D. (2004). Solids transport by drilling fuilds concentrated betonite-sand slurries. In 12^{th} *International Conference on Transport and sedimentation of solid particles*, pages 641–649.

Talmon, A. M., van Kesteren, W. G. M., Mastbergen, D. R., Pennekamp, J. G. S., and Sheets, B. (2014). Calculation methodology for segregation of solids n non-newtonian carrier fluids. In *Paste 2014,* 17^{th} *international seminar on paste and thickened tailings*, pages 139–154.

Thomas, A. D. (1999). The influence on coarse particles on the rheology of fine particle slurries. In *Rheology in mineral industry II*, Kahuku, Oahu, Hawaii. United Engineering Foundation.

Thomas, A. D. and Fitton, T. G. (2011). Analysis of tailings beach slopes based on slurry pipeline experience. In *Paste 2011,* 14^{th} *international seminar on paste and thickened tailings*, pages 295–306, Perth, Australia.

Treinen, J. M., Cooke, R., and Salinas, C. (2010). Energy induced rheology reduction of flocculated slurries. In 18^{th} *International Conference on Hydrotransport*, pages 487–503, Rio de Janeiro, Brazil.

Treinen, J. M. and Jacobs, J. (2015). Cfd approach using granular kinetic theory to predict particle settling and migration in viscoplastics fluids. In *Proceedings* 17_{th} *International conference on transport and sedimentation of solid particles*, Delft, The Netherlands. Wroclaw University and Delft University of Technology.

Van De Ree, T. (2015). Deposition of high density tailings on beaches. Master's thesis, Delft, University of Technology.

van Kesteren, W. G. M., van de Ree, T., Talmon, A. M., de Lucas Pardo, M., Luger, D., and Sittoni, L. (2015). A large-scale expermimental study of high density slurries deposition on beaches. In *Proceedings* 17_{th} *International conference on transport and sedimentation of solid particles*, pages 147–154, Delft,. Wroclaw University and Delft University of Technology.

van Ledden, M., van Kesteren, W. G. M., and Winterwerp, J. C. (2004). A conceptual framework for the erosion behaviour of sand-mud mixtures. *Continental shelf research*, 24:1–11.

Vreugdenhill, C. B. (1989). *Computational Hydraulics*. Springer-Verlag.

Williams, M. P. A. (2001). Tailings beach slope forecasting a review. In *Proceedings of High Density and paste Tailings 2001 seminar*, Pilanesberg, South Africa. University of the Witwatersrand.

Winterwerp, J. C. and van Kesteren, W. G. M. (2004). *Introduction to the physics of cohesive sediment in the marine environment*, volume Developments in Sedimentology 56. Elsevier B.V, Amsterdam, 1st edition.

List of Figures

List of Tables

A

Hydrodynamics

A.1. Laminar Flow

Non-Newtonian open channel flow formulation comes from [Kozicki and Tiu, 1967]. The simplest form to describe non-Newtonian flow state is by adaption of Newtonian formulas from pipe flow. [Holland 1973 and Wilson 1986]. The Reynolds number depends on the viscosity, if apparent viscosity is substituted it can be used to approximate non-Newtonian laminar flow, [Slatter, 1996].

$$Re_{newt} = \frac{\rho V 4 R_h}{\mu_a} \tag{A.1}$$

With:

$$\mu_a = \frac{\tau}{\dot{\gamma}} \tag{A.2}$$

When the transition point for laminar regime stays the same the Reynolds number Re does not change. If ρ and R_h also stay the same, which is not a strange assumption, from these equations it then follows that the velocity required to reach the transition criteria increases when the apparent viscosity increases. The apparent viscosity depends on rheological parameters of slurry, mixtures with stronger rheological properties have a higher apparent viscosity. This indicates that non-Newtonian fluids, which have higher apparent viscosity need to flow faster before reaching the turbulent transition point, described by a certain Reynolds number.

The basic velocity profile of laminar open channel flow is characterized by starting from zero velocity at the bottom wall and then has parabolic increase towards the surface. For non-Newtonian fluids the velocity profile is different, described by [Coussot, 1994]. The velocity profile starts uniform in the top part of the channel, the so called ”plug layer”, until the yield stress is reached by the shear stress. After this the velocity goes to zero at the bottom wall. It looks like figure A.1.

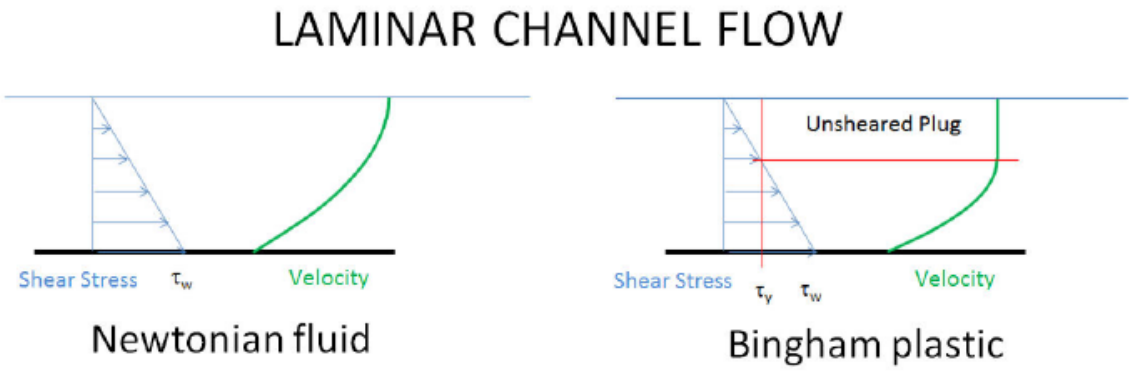

Figure A.1: Laminar velocity profiles for open channel flow, Source [Slatter, 2013]

[Slatter, 2013] improved the Reynolds number formulation derived from a Newtonian adaption, by including rheology. Resulting in Eq. A.3 which describes the Reynolds number for an infinite wide channel. It is especially good for powerlaw but also Hershel-Bulkley and Bingham type fluids. Depending on the fluid type, the τ_y and flow index n will change. A powerlaw model has no yield strength and Bingham plastics have a flow index of $n = 1$.

$$Re_4 = \frac{8\rho V^2}{\tau_y + \mu_a(\frac{3V}{H})^n} \tag{A.3}$$

The correlation for the Moody diagram stay the same as for Newtonian fluids. Therefore the convenient explicit linear relation for the laminar regime also applies for this $Re4$ number.

$$f = 16/Re \tag{A.4}$$

A.2. Laminar Turbulent Transition

In literature only pipe flow work from Hanks criteria is adapted to open channel by [Zhang & Ren, 1982]. Well known transition Reynolds number is ~2100, for pipe flow and open channel. [Haldenwang, 2003] performed experimental work and noticed that the transition for non-Newtonian high viscous fluids, turbulence started at a lower Reynolds number than for Newtonian low viscous fluids. This transition point also was much smoother, as in it extended over a broader range of Reynolds numbers. Haldenwang also found that different fluids had same rheological characteristics at specific shear rates. He created a function that estimates onset to transition and full turbulence regimes based on a relation with the apparent viscosity and Froude number.

$$Fr = \frac{V}{\sqrt{gh}} \tag{A.5}$$

$$Re_{transition} = \frac{200}{(\mu_{a(100s^{-1})})^{0.21}}Fr + \frac{71}{(\mu_{a(100s^{-1})})^{0.75}} \tag{A.6}$$

$$Re_{full\ turbulence} = \frac{105}{(\mu_{a(500s^{-1})})^{0.52}}Fr + \frac{108}{(\mu_{a(500s^{-1})})^{0.65}} \tag{A.7}$$

A.3. Turbulent

Literature work from [Naik 1983 and Wilson 1991] is based on pipe flow. No decent turbulent model exist for non-Newtonian open channel flow. On the same data sets as before [Haldenwang, 2003] fitted a new model based on [Slatter 1994] where turbulence is described in terms of particle roughness. The average velocity and friction factor are:

$$V_{turb} = \sqrt{ghsin\theta}(2.5ln\frac{2R_h}{k} - 76.86\mu_{a(500s^{-1})} - 9.45) \tag{A.8}$$

$$f = \frac{0.66(2ghsin\theta)}{(V_{turb})^2} \tag{A.9}$$

A.4. Turbulence model in 1DV and Delft3D-Slurry

In the 1DV model and Delft3D-Slurry model a laminar flow state is assumed in this report. Current turbulence models may have problems, because they have to deal with thin layers with very sharp gradients in shear rate which are observed in the 1DV model. There is a damping function in Delft3D for Reynolds number that is used for mixtures with high fines concentrations. However material like the slurries that are used in this report this damping function is not accurate enough. More research towards the numerical implementation of turbulent non-Newtonian fluids is needed.

In this section the computations of Reynolds numbers for laminar non-Newtonian open channel flow are documented. This is done for the sensitivity analysis of the 2DV model. Values from the simulations are used in Eq. A.3. Results are in Table A.1. The hydraulic radius is computed by Eq. A.10, where H is total flow height and the width in the model is 10 m.

$$R_H = \frac{H \cdot W}{(2H + W)} \tag{A.10}$$

Table A.1: Computations of Reynolds number in laminar non-Newtonian open channel flow.

	$\rho[kg/m^3]$	$V[m/s]$	$\tau_y[Pa]$	$\mu_a[Pas]$	H	$R_H[m]$	$Re_4[-]$
REF	1160	0.74	2	0.76	0.136	0.13	105
Clay 1 (100)	1062	2.2	0.015	0.05	0.06	0.06	5419
Clay 3 (415)	1255	0.31	25	3.15	0.32	0.31	9
Rheo 1 (Set 1)	1160	0.48	15	0.6	0.21	0.2	17
Rheo 3 (Set 3)	1160	0.25	30	3.9	0.39	0.36	6
Rheo 3 Clay 1	1062	0.75	0.5	0.75	0.13	0.13	346
Rheo 3 Clay 3	1255	0.05	260	9.1	1.76	1.3	0.1
Sand 2 (100)	1222	0.51	3	1	0.2	0.19	75
Sand 3 (450)	1440	0.32	9	2.25	0.3	0.28	25
Sand 4 (900)	1720	0.14	70	10	0.7	0.61	4
Seddia 1 (100)	1222	0.62	3	1	0.15	0.15	71
Seddia 3 (400)	1222	0.23	3	1	0.42	0.39	53

B

Documented Beach Profiles

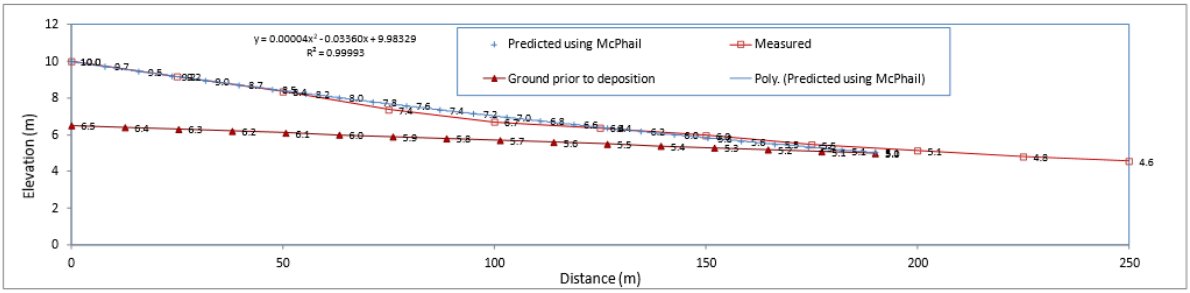

Figure B.1: Measured and predicted beach profile with rheological parameters τ_y = 18 [Pa], K = 3 and n=0.67. Measured at a TRO, Source [Charlebois, 2012]

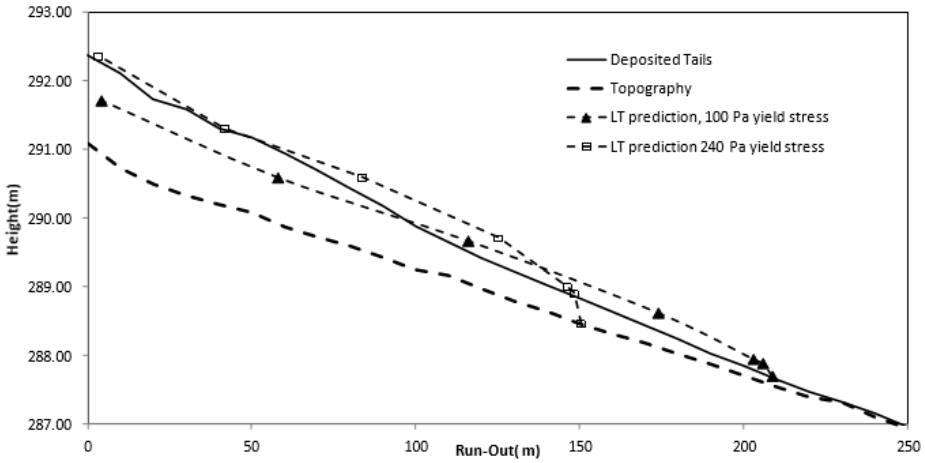

Figure B.2: Measured and predicted beach profile at the Muskeg River Mine, Source [Soleimani et al., 2013]

C

Küpper Field Tests

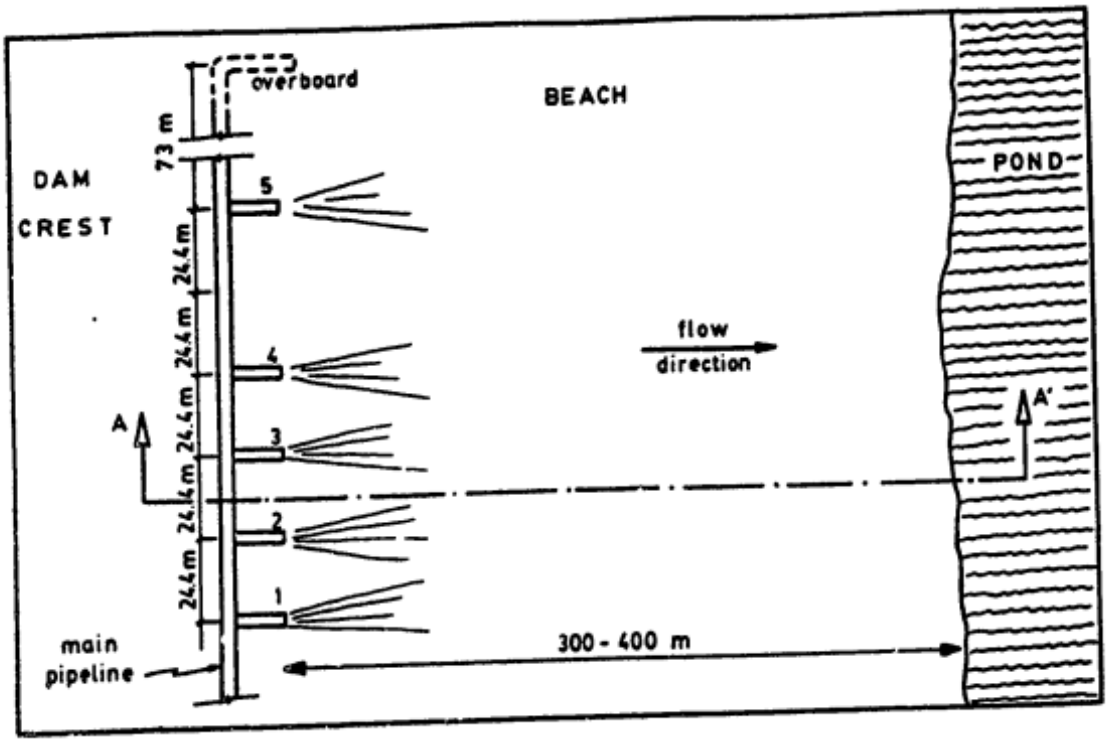

Figure C.1: Layout of the Küpper field tests.

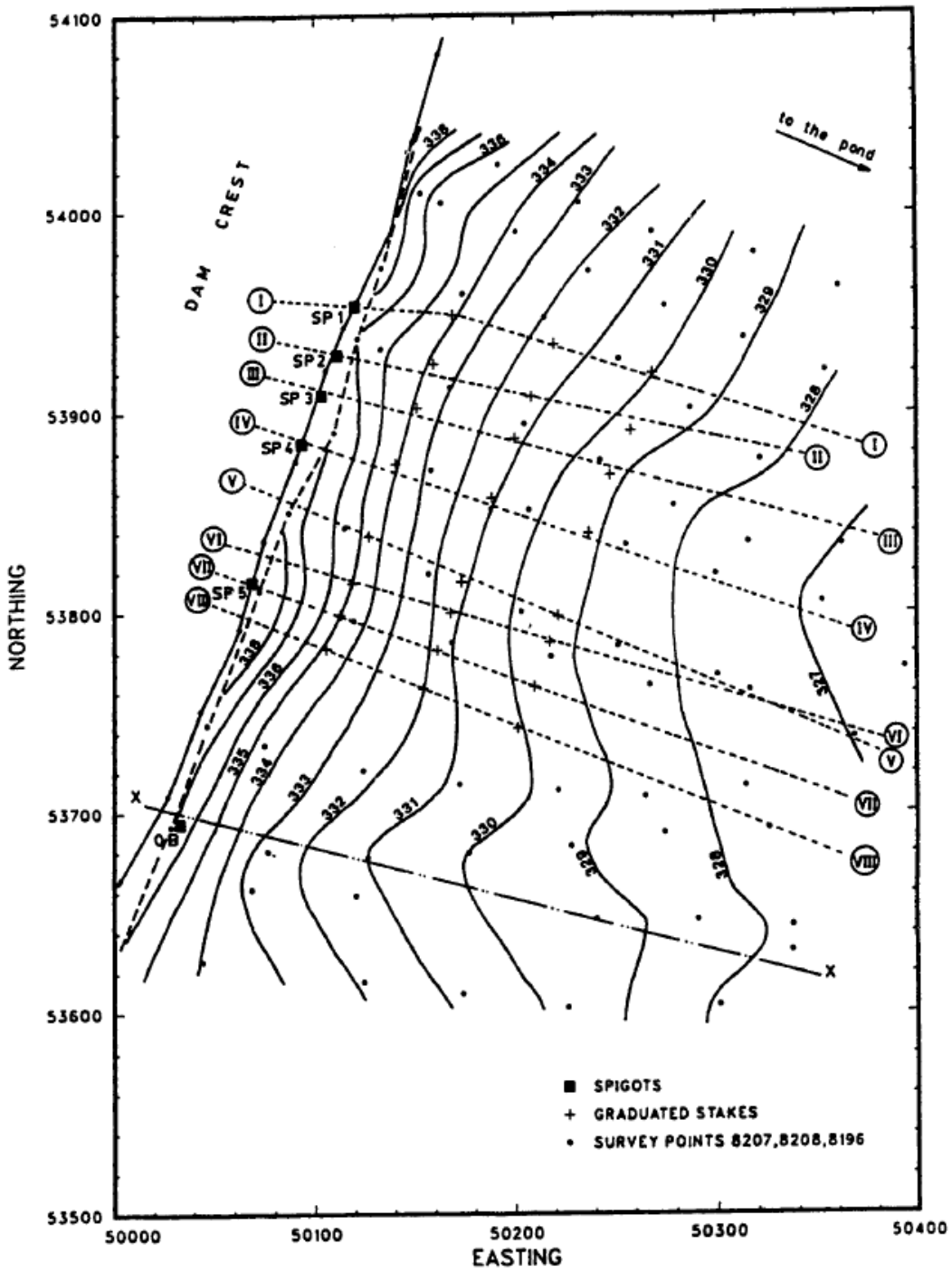

Figure C.2: Depth contours prior to Kupper test 1.

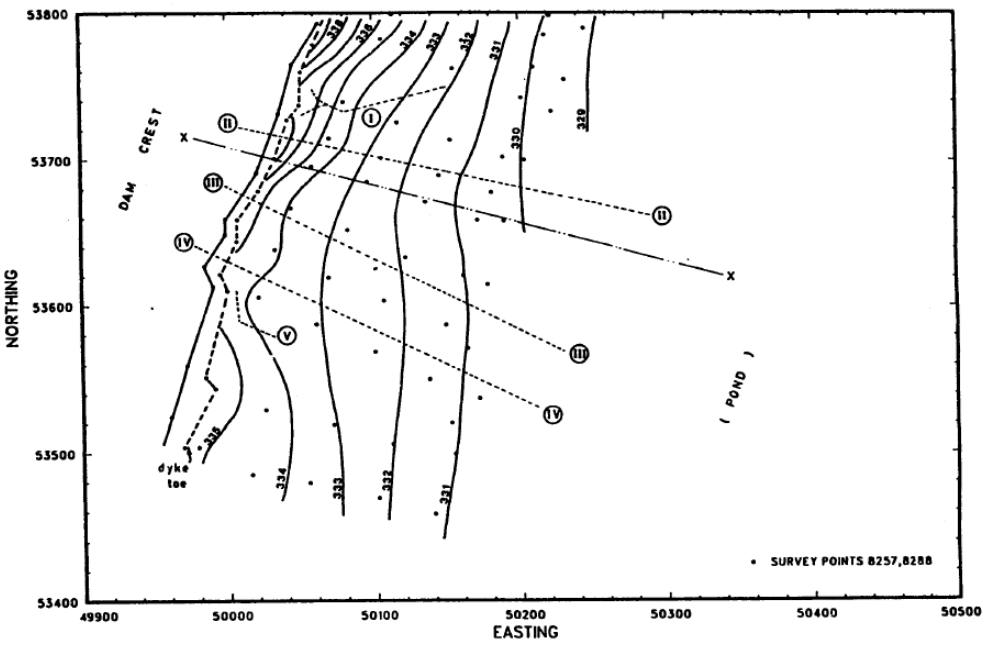

Fig. 5.28 - Contour map of the beach before Test nº 2

Figure C.3: Depth contours prior to Kupper test 2.

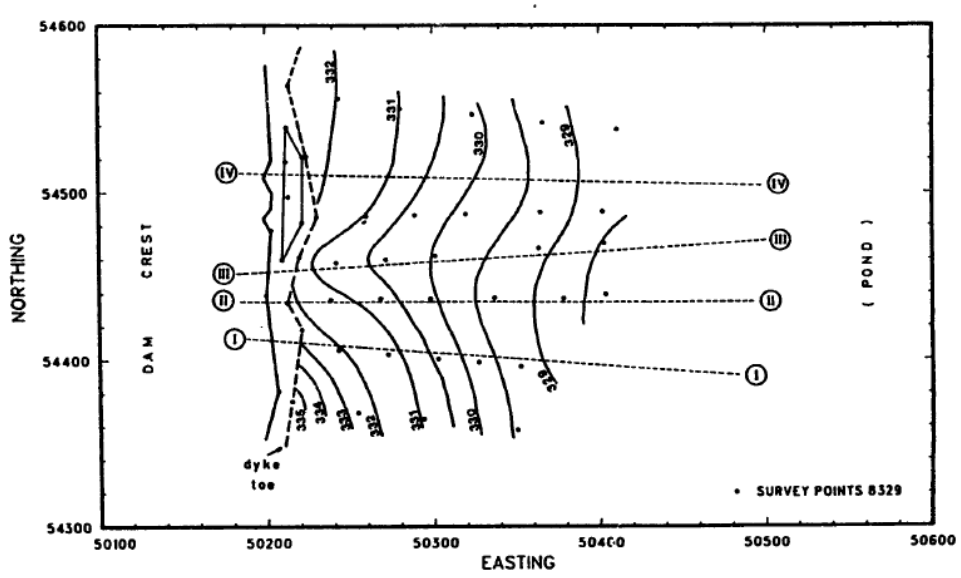

Figure C.4: Depth contours prior to Kupper test 4.

D

Governing Equations Delft3D-Flow

Delft3D-Flow is a model that computes and simulates shallow water flows, which is valid when the horizontal scale is much larger than the vertical scale. This is the case for coastal flows, river flows and off course these tailing flows. The fluid motion is described by the:

- continuity equation
- Momentum equations

The momentum equations are the classic Navier Stokes equations which are adapted by Reynolds decomposition and time averaging the velocity component. Achieving the RANS, or Reynolds Averaged Navier Stokes. Furthermore the following assumptions are made considering the flows as shallow water:

1. Incompressibility, particles do not deform and density is pressure independent.
2. Hydrostatic pressure assumption, neglected vertical velocity accelerations. The vertical momentum equation is reduced to a hydrostatic balance given by gravity and density.

This creates the ability to create momentum equations for x and y direction and use a pressure term for vertical direction z. This allow u and v to be calculated with these momentum equations and together with the continuity equation, no loss of mass in the system, w can be determined.

$$\frac{\partial u}{\partial x} + \frac{\partial v}{\partial y} + \frac{\partial w}{\partial z} = 0 \tag{D.1}$$

The momentum equations: *u*, *v* and *w* are the averaged velocities in respectively x, y and z direction. *f* is the Coriolis parameter that considers the force of the rotation of the earth. *p* is the pressure and v_h & v_t are eddy viscosity coefficient for both horizontal and vertical direction. *g* is the gravitational acceleration and ρ & ρ_0 are density and average density of the fluid.

$$x: \frac{\partial u}{\partial t} + u\frac{\partial u}{\partial x} + v\frac{\partial u}{\partial y} + w\frac{\partial u}{\partial z} - fv + \frac{1}{\rho_0}\frac{\partial p}{\partial x} - 2v_h\frac{\partial^2 u}{\partial x^2} - \frac{\partial}{\partial z}\left(v_t\frac{\partial u}{\partial z}\right) = 0 \tag{D.2}$$

$$y: \frac{\partial v}{\partial t} + u\frac{\partial v}{\partial x} + v\frac{\partial v}{\partial y} + w\frac{\partial v}{\partial z} + fu + \frac{1}{\rho_0}\frac{\partial p}{\partial y} - 2v_h\frac{\partial^2 v}{\partial y^2} - \frac{\partial}{\partial z}\left(v_t\frac{\partial v}{\partial z}\right) = 0 \tag{D.3}$$

$$z: \frac{\partial \rho}{\partial z} = -\rho g \tag{D.4}$$

The first four terms describe the inertial forces, time-dependent and convective. The fifth term is the Coriolis force, the sixth is the pressure difference and the last two are acceleration due advection and viscous stresses due turbulence. These equations solve the velocity, pressure and density for the concerning fluid. The combination of sand and fines with water creates mixtures which are modeled as single phase fluids containing coarse material, i.e The momentum and continuity equations are solved

for the entire mixture. Also called drift flux modelling. Besides these main equation there are transport equations in the model that handle the transport of sand particles or other dissolved matter, salinity and temperature. The eddy viscosity and diffusivity are either set constant, which results in a laminar flow or they are determined by a turbulence model. This will calculate the Reynolds stresses and give a general description of turbulence based on two transport equation see: [Deltares, 2016].

D.1. Governing Equations of the 1DV Model

In the 1DV model the general equations above need to be adapted or simplified, an overview will be given. The 1DV model was originally used for testing the equations used in Delft3D-Flow in a simple environment and is developed by Deltares by R. Uittenbogaard. Also the new equations for rheology and segregation could be tested and tuned in this 1DV model. Only the processes in the vertical z direction are important now. both x and y direction can be neglected using following assumptions: $u(x,y,z,t) -> u(z,t)$, $v \equiv 0$ and $\frac{\partial}{\partial x} = 0$; $\frac{\partial}{\partial y} = 0$. To incorporate the effect of a non-Newtonian fluid a viscous term is added to the vertical turbulent viscosity. These assumptions make the continuity and Navier-Stokes equations look like Equations D.5 and D.6

$$Continuity: \frac{\partial u}{\partial x} + \frac{\partial w}{\partial z} = 0 \tag{D.5}$$

$$momentum: \frac{\partial u}{\partial t} + \frac{1}{\rho_0}\frac{\partial p}{\partial x} - \frac{\partial}{\partial z}[(v + v_t)\frac{\partial u}{\partial z}] = 0 \tag{D.6}$$

The last equations needed are the transport equations,these are modelled as advection-diffusion equations. In the 1DV model only sediment transport is considered. The flow is put to laminar, no turbulence model, so diffusion is not accounted for except molecular diffusion. Also it is assumed that other variables like temperature and salinity are constant. The transport equation reads:

$$\frac{\partial c_l}{\partial t} + \frac{\partial}{\partial z}[w_s(c_l)c_l] - \frac{\partial}{\partial z}[(D_S + \Gamma_T)\frac{\partial c_l}{\partial z}] = 0 \tag{D.7}$$

where c_l is the concentration of a certain solid fraction, w_s is the settling velocity, D_S is the molecular sediment diffusion and Γ_T is the turbulent diffusion which is assumed zero.

D.1.1. Forcing of the 1DV Model

The situation is an inclined ground slope and a specific discharge as input. The forcing consist of gravity and slope angle:

$$\frac{\partial p}{dx} = \rho g sin(\theta) \tag{D.8}$$

The flow depth H and mean velocity V depend on the given specific discharge. Also an initial depth is an input to compute initial mean velocity after which the velocity profile changes with time step t due to changes in viscosity among others. Then this new mean velocity is used to correct the flow depth. This process looks a follows.

$$V = \frac{q_0}{H_0} \tag{D.9}$$

$$q^t = H^t V^t \tag{D.10}$$

$$H^{t+1} = \frac{q_0}{q^t} H^t \tag{D.11}$$

D.1.2. Numerical Grid

The vertical cross section has a numerical domain consisting of a certain amount of layers denoted as k. At each layer all different quantities as velocity, pressure, viscosity, etc. are computed. Both Delft3D-Flow as the 1DV version use a staggered grid, which means that some quantities (velocity and concentration) are computed in the cells centre (k) and others (viscosity, turbulence, fluxes and settling velocity) at the cells interface ($k \pm 1/2$), for a schematic insight see Figure 5.3. This staggered grid is used because it provides better numeric stability. Grid spacing is a function of total water depth and can either be evenly distributed, or it can have an exponential distribution, where grid size increases towards

the surface. The evenly distributed grid is used for the main flow hydromechanics and the exponential grid can be used to focus on a specific area, in this instance near the bed where fine sediments like silt are settling and all the important processes are happening. Conversion to exponential or sigma layers is done with following Eq D.12.

$$\frac{\partial}{\partial z} = \frac{1}{H}\frac{\partial}{\partial \sigma} \tag{D.12}$$

In this thesis only the evenly distributed grid is used. Although there is settling of sand, there is no need for focus near the bed layer. Because of the large quantity of solids that are used in slurries, thick beds can be formed which are near standstill. Therefore no specific focus near the bed region is needed. The shear layer is most important, but this layer can be anywhere in the slurry column.

E

Rheological parameters oil sands

In this appendix the rheological parameters are determined for **rheological model M2**. The rheological parameters are based on a confidential case study: oil sand Case A, mentioned in Section 4.2.5. This Case A consists of documented shear stress and viscosity data that have been fitted with simple Bingham models for different SFR vs FOFW, Figures E.1 and E.2. Focus is on rheological model M2, which has Bingham behaviour and it is the main rheological model for the simulations that used in the results of this thesis. The rheological Equations for model M2 are repeated below.

$$\tau_y = exp(\beta_y \lambda) A_y \left(\frac{\rho_w}{A_{clay} \rho_{solids}} \frac{1 - \phi_{solids}}{\phi_{cl}} \right)^{B_y} \tag{E.1}$$

$$\mu = exp(\beta_v \lambda) \left[\mu_w + A_\mu \left(\frac{\rho_w}{A_{clay} \rho_{solids}} \frac{1 - \phi_{solids}}{\phi_{cl}} \right)^{B_\mu} \right] \tag{E.2}$$

In which λ is the linear sand concentration described in the report (Bagnold). λ does not need to be determined for this case, it only depends on sand concentration ϕ_{sand} and maximum sand concentration $\phi_{sand,max}$, This $\phi_{sand,max}$ can be larger than 0.6, it is assumed the same for now. β is the friction coefficient of sand influence and is to be determined for both yield stress and viscosity. The solids effect, $exp(\beta\lambda)$ in the equations above, is a relation between influence of sand λ and the yield stress of the slurry over the yield stress of the carrier fluid or the viscosity of the slurry over the viscosity of the carrier fluid. It represents an exponential equation that describes the distance between different SFR lines in the figures below: Figures E.1 and E.2. A_y and A_μ are coefficients for yield and viscosity that are to determined last. B_y and B_μ are the power coefficients that are determined by the slope of the relation between shear stress and water content.

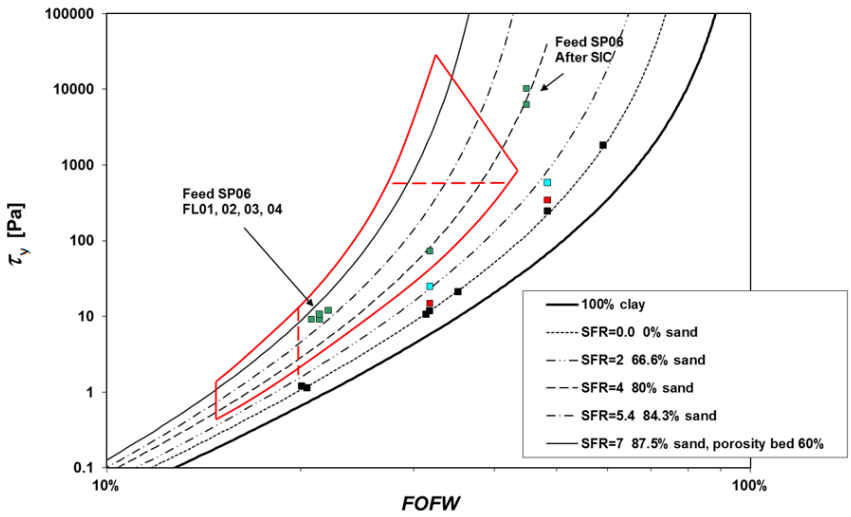

Figure E.1: Yield stress vs FOFW (oil sand Case A) Bingham behaviour.

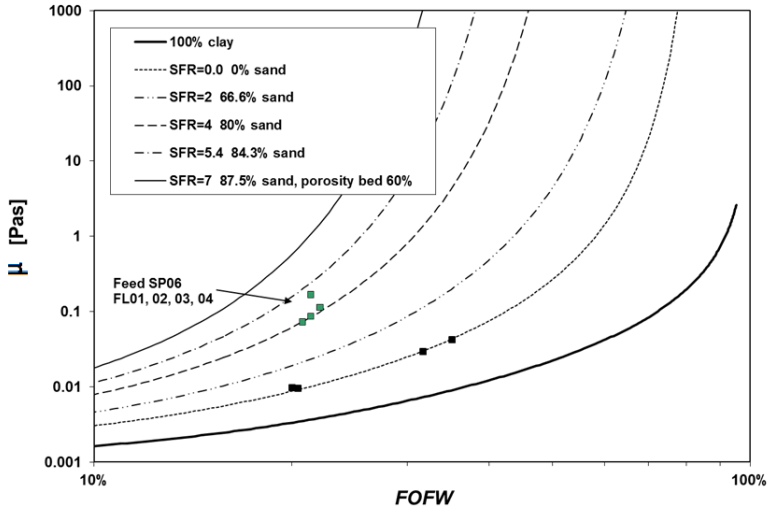

Figure E.2: Viscosity vs FOFW (oil sand Case A) Bingham behaviour.

These figures describe the relation of yield stress and viscosity with FOFW and are for Bingham oil sands. To retrieve the rheological parameters, FOFW needs to be rewritten in terms of water content. This is done by combining the following equations.

$$FOFW = \frac{Weight\ fines}{Weight\ fines + water} \tag{E.3}$$

$$Water\ content\ to\ clay = \frac{Weight\ water}{Weight\ fines} * 100 \tag{E.4}$$

Rewriting Equation E.3 in term of water content gives:

$$Water\ content = Weight\ fines\left(\frac{1}{FOFW} - 1\right) \tag{E.5}$$

Substituting Eq E.5 in Eq E.4 gives:

$$Water\ content\ to\ clay = \frac{1 - FOFW}{FOFW} * 100 \tag{E.6}$$

Recreating the figures above, by plotting yield stress and viscosity against water content to the clay gives the ability to determine the rheological parameters.

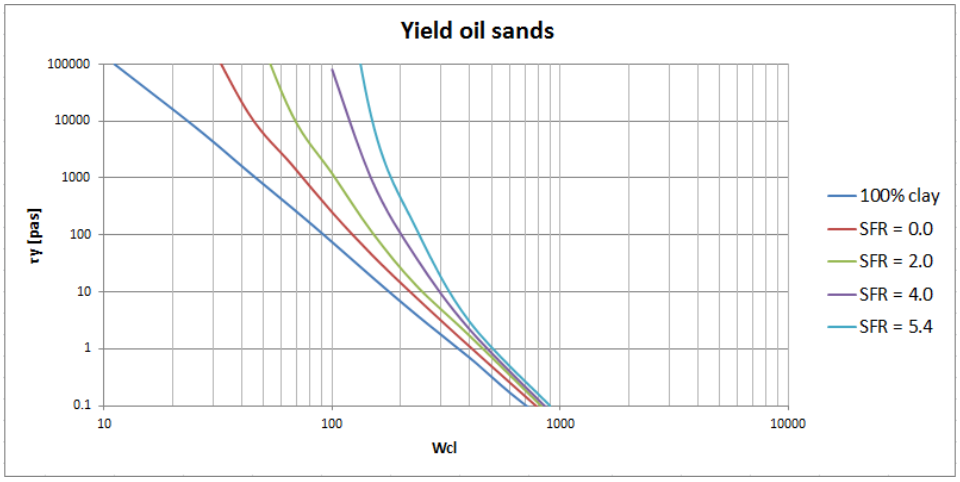

Figure E.3: Yield stress vs water content to the clay (oil sands Case A) Bingham behaviour.

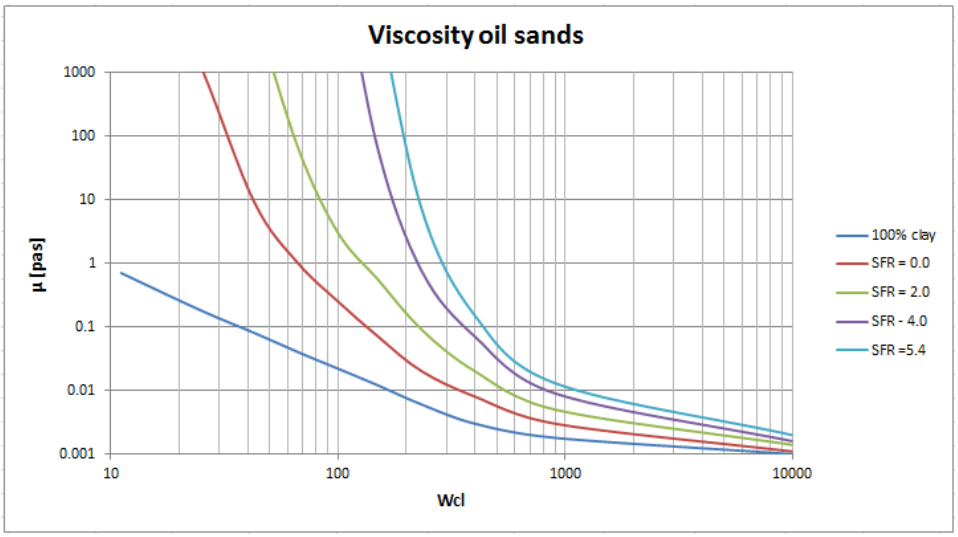

Figure E.4: Viscosity vs water content to the clay (oil sands Case A) Bingham behaviour.

The slope of the 100 % carrier fluid is number for the power coefficient. This means B_y **equals -3.2 and** B_μ **equals -1.6** for a w_{cf} range of 10-400.

The determination of frictional parameters is performed next. If looked at yield strength and viscosity for one specific FOFW ratio or water content the influence of sand can be determined. So lets take a FOFW ratio of 20 %. First the yield stress and viscosity of carrier fluid is determined and after that for different SFR. The ratio of the yield stress and viscosity of the mixture over the yield stress and viscosity of the carrier fluid is plotted against λ.

Table E.1: Friction coefficient oil sands input

tycf	visccf	SFR	Ty	Visc	λ	Ty/tycf	Visc/visccf
0.8	0.003	Only fines	0.8	0.003	0	1	1
0.8	0.003	0.0	1	0.007	0.43	1.25	2.3
0.8	0.003	2.0	1.5	0.014	1.87	1.88	4.7
0.8	0.003	4.0	3	0.05	4.59	3.75	16.7
0.8	0.003	5.4	6	0.18	9.80	7.5	60

When these number are put into graphs with yield and viscosity on log scale and λ on normal scale an exponential fit can be made.

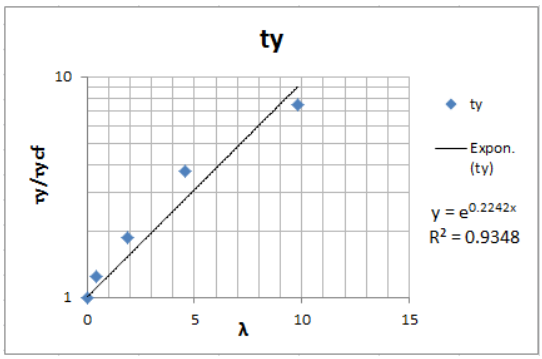

(a) Yield strength vs λ for the determination of friction parameter β, which is the exponent in the y equation

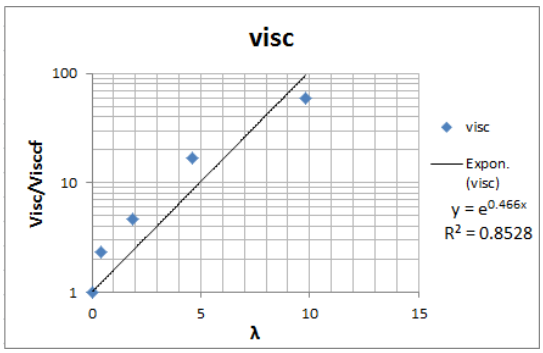

(b) Viscosity vs λ for the determination of friction parameter β, which is the exponent in the y equation

The friction parameter β **for yield stress equals 0.22 and for viscosity equals 0.47**. The only thing that remains are the coefficients A_y *and* A_μ, these can be determined by picking any point in Figures E.1 and E.2. For example the carrier fluid with a FOFW ratio of 20% has a yield of 0.8 so this makes the A_y **equals 1400**. Doing the same for the viscosity gives A_μ **equals 1.0**.

Note that the low viscosity for oil sands as determined for Case A can cause problems with the model as there is no turbulence model working yet and only laminar flow is considered. For the Rheological Sets 1 and 3 an enhanced viscosity coefficient is used.

The retrieved parameters from above are given in Table E.2 and compared in rheograms with the fitted data from Case A in Figures E.6.

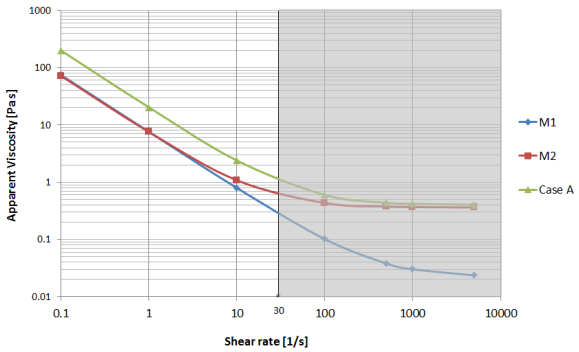

(a) Rheogram for the apparent viscosity of the parameter set from Table E.2 for oil sand "Case A". The shear rate range that is applicable is the white area, higher shear rates are indicated by the grey area

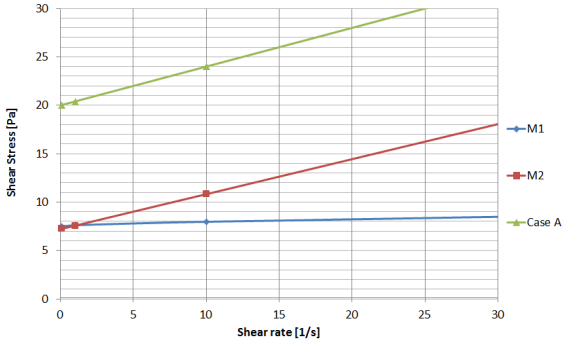

(b) Rheogram for the shear stress of the parameter set from Table E.2 for oil sand "Case A"

Figure E.6: Rheograms for apparent viscosity and shear stress from Table E.2 for Case A.

E.1. Rheological Parameter Sets

Oil sand tailings are not all the same, as described in Chapter 2 there are many different oil sand tailings. The retrieved number from this appendix and oil sands Case A are tuned and slightly adapted to form two different rheological parameter sets that will represent two different sort of tailings. This is done in Section 4.2.6. One set represents MFT treated with polymers and the other TT. The parameters for Model 1 are determined at a shear rate of $[1/s]$.

Table E.2: Rheological input parameters oil sands

Oil sands Case A				Set 1 "fMFT"				Set 3 "TT"			
M1		M2		M1		M2		M1		M2	
ϕ_{max}	0.6	ϕ_{max}	0.6	ϕ_{max}	0.6	ϕ_{max}	0.6	ϕ_{max}	0.6	ϕ_{max}	0.6
A_y	1640	A_y	1400	A_y	11000	A_y	17250	A_y	51000	A_y	2E+05
n_f	2.3	B_y	-3.2	n_f	2.3	B_y	-3.2	n_f	2.38	B_y	-4.0
β_y	0.22	β_y	0.22	βy	0.58	β_y	0.58	β_y	0.2	β_y	0.2
A_μ	6.5	A_μ	1	A_μ	150	A_μ	20	A_μ	965	A_μ	130
a	2.6	B_μ	-1.6	a	2.6	B_μ	-1.6	a	2.6	B_μ	-1.6
β_v	0.47	β_v	0.47	β_v	0.54	β_v	0.54	β_v	0.36	β_v	0.36
m	5E+03	m	5E+03	m	5E+03	m	5E+03	m	5E+03	m	5E+03

To show the differences between the original rheological parameter Set REF and the new oil sand rheological parameters Set 1 and Set 3, the influence of clay and sand content to yield stress will be analysed. This is done for rheological model M2. The oil sands Case A is not shown because the low viscosity made it unable to model, same goes for the original parameter set from A.D. Thomas before the viscosity was enhanced.

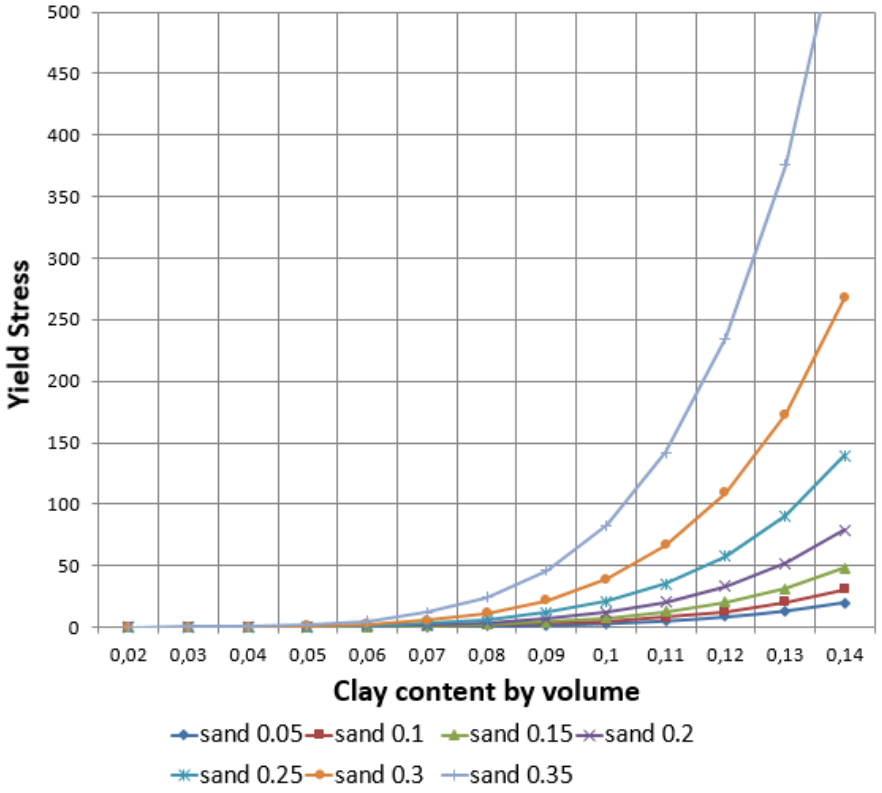

Figure E.7: Influence of clay content on yield stress for multiple sand contents. For original rheological parameters Set REF and Rheological Model 2

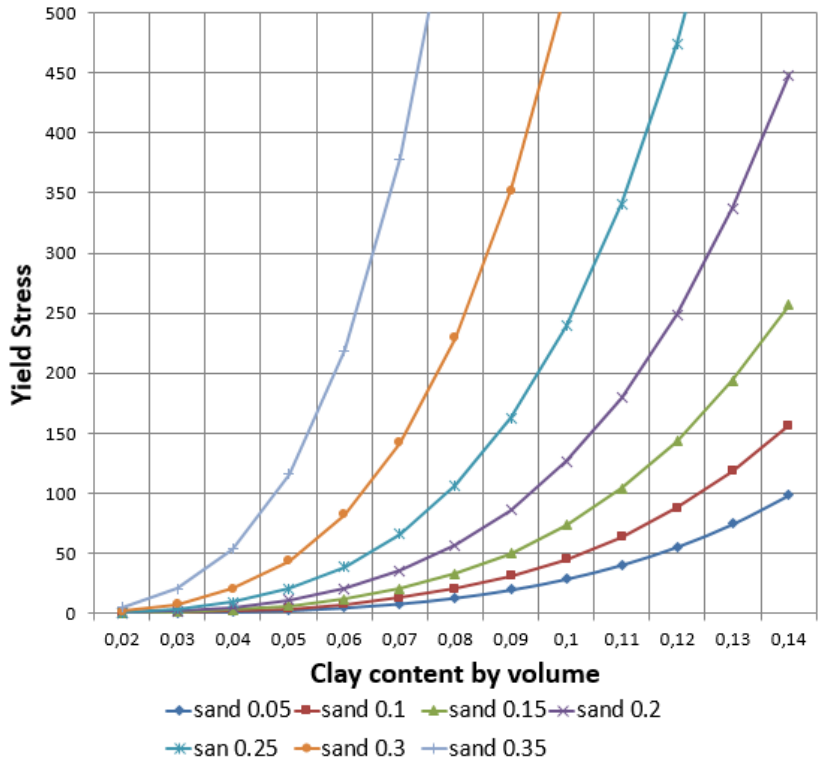

Figure E.8: Influence of clay content on yield stress for multiple sand contents. For fMFT tailings and rheological Model 2.

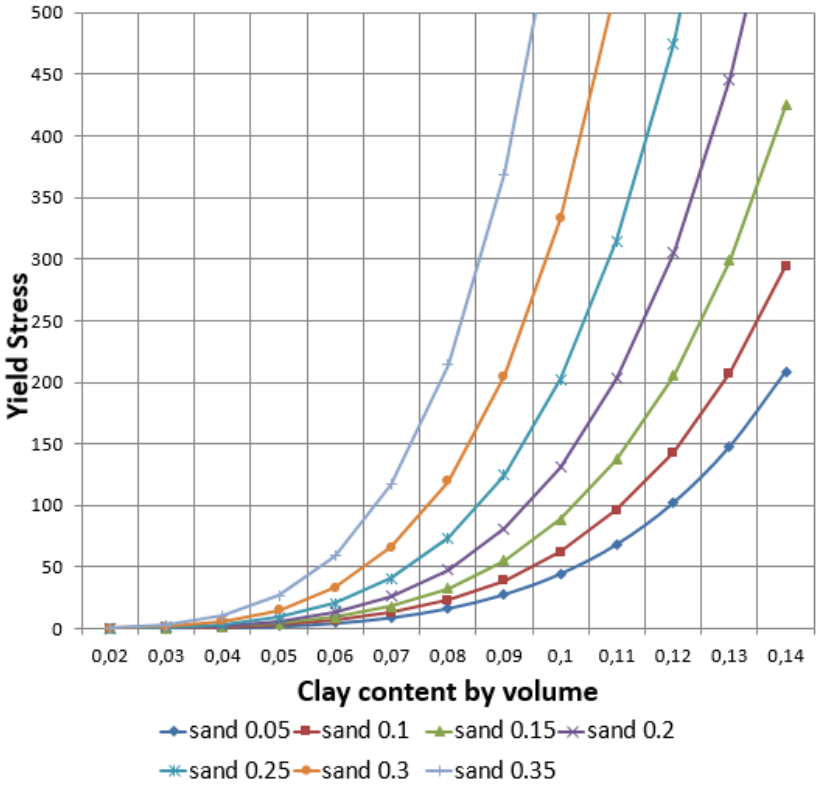

Figure E.9: Influence of clay content on yield stress for multiple sand contents. For TT and rheological Model 2.

F

Upwind and Plug Code for the 1DV Model

F.1. 1DV Model

F.1.1. Fall velocity Sand, Same for all Rheological Models

```
subroutine fallve(dudz)
c***********************************************************************
c
c D e l t a r e s S o f t w a r e C e n t e r
c
c Module: Subroutine FALLVE
c Function: Relation between sediment concentration
c and vertical fall velocity. Model for
c hindered settling.
c Fall velocity at layer interfaces.
c
c Method used:
c Date: 11-01-2016
c Programmer: R.E. Uittenbogaard, Jill Hanssen, H.E. van Es
c
c***********************************************************************
include 'pardef.inc'
include 'dimens.inc'
include 'physco.inc'
include 'turcoe.inc'
include 'conarr.inc'
include 'hydarr.inc'
include 'sedarr.inc'
include 'turarr.inc'
c
dimension dudz (0:kmaxd), dudzcr(0:kmaxd) ,
+ phisoi (1:kmaxd), wssa (1:kmaxd,lsand),
+ wssi (1:kmaxd,lsilt)
c
pi = 4.0*atan(1.0)
c
c fall velocity dependent on carrier fluid type and sediment type
c
c*******************************************************************
c ** Noting with water as carrier fluid is considered here, that part is skipped
```

```
c**************************************************
c Carrier fluid clay or clay +silt
c phisol(k) = total solid concentration calc in unesco
c
c ** retco is power parameter for hindered settlement **
c ** sasim is maximum sand concentration **
c ** shrco is the emperical alfa parameter for segregation **
c ** tyieldplug is a value initial yield stress of the plug layer, this needs to be defined **
retco = 2.0
sasim = 0.6
shrco = 1.
tyieldplug = 1.
c Here the bottom shear is established, to come to a plug ratio for plug conservation. This is done so
the if statement onlt works at the bottom of the plug and not in the bed layer where shear and yield
stress converge.
do k = 1 ,kmax
    if (k .eq. kmax) then
        taubot = MAX(1.,rxz(kmax))
    endif
enddo
c
c
c********** fall velocity single grain in viscous fluid - clay**********
c********** The fall velocity for all non-cohesive particles are calculated in each cell, c**********
silt is not part of the carrier fluid
if (carflu.eq.'cfclay') then
    do k = 1 ,kmax
        kk = max(1,k)
        ku = min(k+1,kmax)
        ki = max(1,k-1)
        ts = thick(kk)+thick(ku)
c
        rhocfi=(thick(kk)*rhocf(ku)+thick(ku)*
        * rhocf(kk))/ts
c
        wssa(k,lsand) = shrco*(rhosol(lsand)-rhocfi)*ag*
        * seddia(lsand)**2/(18*cfvic(k)*rhocfi)
c
        wssi(k,lsilt) = shrco*(rhosol(lsilt)-rhocfi)*ag*
        * seddia(lsilt)**2/(18*cfvic(k)*rhocfi)
c
c********** Here the if IF statement described in Chapter 5 comes into play. First the yield stress in
the plug is established by taking the yield stress in one of top cells. Furthermore the length of the plug
as an amount of layers k. This is done by taking the ratio of yield stress and bottom stress, including
a small safety factor to be certain of solution. Then it states that if layer k is in the plug range and the
shear stress is less than yield stress there is no fall velocity. So no sand settles out of the plug and the
thickness is preserved
c
        if (k .eq. 3) then
            tyieldplug = tyield(ki)
        endif
        safety = 1.0500000
        plugl = (tyieldplug*safety)/taubot
        if (k.LE.plugl*kmax .AND. rxz(k).LT.tyield(ki)) then
            wssa(k,lsand) = 0
            wssi(k,lsilt) = 0
```

```
        endif
c********** Hindered settling **********
c
        retsa = max(0.0,(1-phisa(ku)/sasim))
        retsi = max(0.0,(1-phisi(ku)/sasim))
        buoyan = max(0.0,(1-phisol(ku)))
c
        ws(k,lsand)= wssa(k,lsand)*buoyan*retsa**retco
        ws(k,lsilt)= wssi(k,lsilt)*buoyan*retsi**retco
c Settling velocity (- sign):
        ws(k,lsand) =-ws(k,lsand)
        ws(k,lsilt) =-ws(k,lsilt)
    enddo
c
c ***************************************************************
c********** fall velocity single grain in viscous fluid - clay+silt **********
The fall velocity for all non-cohesive particles are calculated in each cell, silt is not part of the carrier fluid. The idea is the same as for only clay as a carrier fluid, only silt has no fall velocity. ****
elseif (carflu.eq.'cfclsi') then
    do k = 1 ,kmax
        kk = max(1,kmax)
        ku = min(k+1,kmax)
        ts = thick(kk)+thick(ku)
c
        rhocfi=(thick(kk)*rhocf(ku)+thick(ku)*
        * rhocf(kk))/ts
        wssa(k,lsand) = shrco*(rhosol(lsand)-rhocfi)*ag*
        * seddia(lsand)**2/(18*cfvic(k)*rhocfi)
c
        if (k .eq. 3) then
            tyieldplug = tyield(ki)
        endif
        safety = 1.050000
        plugl = (tyieldplug*safety)/taubot
        if (k.LE.plugl*kmax .AND. rxz(k).LT.tyield(ki)) then
            wssa(k,lsand) = 0
        endif
c
c********** Hindered settling (1954): **********
c
        ku = min(k+1,kmax)
        retsa = max(0.0,(1-phisa(ku)/sasim))
        buoyan = max(0.0,(1-phisol(ku)))
        ws(k,lsand)= wssa(k,lsand)*buoyan*retsa**retco
c
c Settling velocity (- sign):
        ws(k,lsand) =-ws(k,lsand)
c
    enddo
endif
c
return
end
```

F.1.2. Slurry Yield Stress and Viscosity, Rheological Model 1

```
subroutine mudvic (zeta ,dp ,u1 ,dudz ,rho )
c***********************************************************************
c
c D e l t a r e s S o f t w a r e C e n t e r
c
c Module: Subroutine MUDVIC - HWCK
c Function: Determine equivalent viscosity (VICMUD) derived from
c rheological model for water-clay-silt-sand flow.
c
c Method used:
c
c date : 07-01-2016
c Programmer : R.E. Uittenbogaard
c***********************************************************************
include 'pardef.inc'
include 'dimens.inc'
include 'physco.inc'
include 'timefr.inc'
include 'turcoe.inc'
include 'hydarr.inc'
include 'sedarr.inc'
include 'turarr.inc'
include 'wrkarr.inc'
c
dimension u1 (*),dudz (0:kmaxd),rho (*),
+ phiss (1:kmaxd), solfrc(1:kmaxd), cl2 (1:kmaxd),
+ conlin(1:kmaxd), ssinfy(1:kmaxd), ssinfv(1:kmaxd),
+ actyie(1:kmaxd), actvic(1:kmaxd),
+ xmuwat(0:kmaxd), xmusol(0:kmaxd)
c
c ********** input parameters ********************
c
phissm = 0.6
ayield = 729884.
frcdim = 2.6426
bety = 0.2752
watmu = viscou*rhom
Avic = 931.86
powa = 3.65
betv = 0.2752
shrco = 5.E3
c
c***************** N E W - S L U R R Y ********************
c **************Vol. Frac SLURRY **************
c *** Computation of the volume fraction for all solid particles.
do k = 1,kmax
    phiss(k) = phisa(k) + phisi(k)
    if (phiss(k).eq.0.0) then
        phiss(k) = 10.e-99
    else
        phiss(k) = phisa(k) + phisi(k)
    endif
c
    solfrc(k) = phicl(k)/(1.-phiss(k))
c
```

```
c********* Linear concentration sand+silt
c******* (Bagnold) Equation, lambda Eq 2.10
c
    cl1 = 1./3.
    cl2(k) = ((phissm/phiss(k))**cl1)-1.
    conlin(k) = 1./cl2(k)
    ssinfy(k) = exp(bety*conlin(k))
c ****** Plug length calc, retrieving shear stress at bottom ******
    if (k .eq. kmax) then
        taubot = MAX(1.,rxz(kmax))
    endif
enddo
c
c ************* YIELD STRESS SLURRY ****************
c***** Computation of the yield stress with upwind scheme and numerical switch for plug preservation
Eq 2.3
c
tyieldplug = 1.
powyie = 2./(3.-frcdim)
do k=1,kmax
    kk = max(1,k)
    ku = min(k+1,kmax)
    ki = max(1,k-1)
    if (k .eq. 3) then
        tyieldplug = tyield(ki)
    endif
    safety = 1.0500000
    plugl = (tyieldplug*safety)/taubot
    if (k.LE.plugl*kmax .AND. rxz(k).LT.tyield(ki)) then
        tyield(k) = ayield*ssinfy(ki)*solfrc(ki)**powyie
    else
        tyield(k) = ayield*ssinfy(ku)*solfrc(ku)**powyie
    endif
enddo
c
c ******* VISCOSITY PARAMETERS SLURRY ********
c
powvic = 2.*(powa+1.)/3.
do k = 1,kmax
    ssinfv(k) = exp(betv*conlin(k))
enddo
c
c ******* Equivalent viscosity derived from shear stress for mixture:
c********* 0< Powshr < 1
powshr = ((powa+1.)*(3.-frcdim))/3.
rhoa = 0.0
do k = 1,kmax
    rhoa = rhoa+rho(k)*thick(k)
enddo
c***** Computation of the viscosity, with the upwind scheme and plug preservation. Eq 2.4 *****
do k=1,kmax
    kk = max(1,k)
    ku = min(k+1,kmax)
    ki = max(1,k-1)
c
    shear = abs(dudz(k))
```

```
    if (shear.eq.0.0) then
        vicmud(k) = 1.E4
    else
        shear = abs(dudz(k))
c
        if (k.LE.plugl*kmax .AND. rxz(k).LT.tyield(ki)) then
            xmuwat(k) = ssinfv(ki)*watmu*shear
            xmusol(k) = ssinfv(ki)*avic*(solfrc(ki)**powvic)*
            * (shear**(1-powshr))
        else
            xmuwat(k) = ssinfv(ku)*watmu*shear
            xmusol(k) = ssinfv(ku)*avic*(solfrc(ku)**powvic)*
            * (shear**(1-powshr))
        endif
        xmu (k) = xmuwat(k) + xmusol(k)
        taubh (k) = tyield(k)*(1-exp(-shrco*shear))+xmu(k)
        vicmud(k) = taubh(k)/shear
        vicmud(k) = vicmud(k)/rhoa
    endif
enddo
c
return
end
```

F.1.3. Slurry Yield Stress and Viscosity, Rheological Model 2

```
subroutine mudvic (zeta ,dp ,u1 ,dudz ,rho )
c***********************************************************************
c
c D e l t a r e s S o f t w a r e C e n t e r
c
c Module: Subroutine MUDVIC
c Function: Determine equivalent viscosity (VICMUD) derived from
c rheological model for water-clay-silt-sand flow.
c
c Method used:
c
c date : 07-01-2016
c Programmer : R.E. Uittenbogaard
c***********************************************************************
include 'pardef.inc'
include 'dimens.inc'
include 'physco.inc'
include 'timefr.inc'
include 'turcoe.inc'
include 'hydarr.inc'
include 'sedarr.inc'
include 'turarr.inc'
include 'wrkarr.inc'
c
dimension u1 (*),dudz (0:kmaxd),rho (*),
+ phiss (1:kmaxd), solfrc(1:kmaxd), cl2 (1:kmaxd),
+ conlin(1:kmaxd), ssinfy(1:kmaxd), ssinfv(1:kmaxd),
+ actyie(1:kmaxd), actvic(1:kmaxd),
+ xmuwat(0:kmaxd), xmusol(0:kmaxd),phicli(1:kmaxd),
+ phisii(1:kmaxd), phisai(1:kmaxd), phisoli(1:kmaxd)
c
c ********** input parameters ********************
c
phissm = 0.6
ayield = 67191.
powyie = 4.75
bety = 0.2752
watmu = viscou*rhom
Avic = 252.38
powvic = 2.64
betv = 0.2752
shrco = 5000.
c
c
c***************** N E W - S L U R R Y ********************
c **************Vol. Frac SLURRY ******************
c
do k = 1,kmax
    phiss(k) = phisa(k) + phisi(k)
    if (phiss(k).eq.0.0) then
        phiss(k) = 10.e-99
    else
        phiss(k) = phisa(k) + phisi(k)
    endif
c********* phisol(k) from unesco
```

```
      solfrc(k) = phicl(k)/(1.-phisol(k))
c********* Linear concentration sand+silt Eq 2.10
      cl1 = 1./3.
      cl2(k) = ((phissm/phiss(k))**cl1)-1.
      conlin(k) = 1./cl2(k)
      ssinfy(k) = exp(bety*conlin(k))
c ****** Plug length calc, retrieving shear stress at bottom ******
      if (k .eq. kmax) then
         taubot = MAX(1.,rxz(kmax))
      endif
enddo
c
c ************* YIELD STRESS SLURRY ****************
c***** Computation of the yield stress with upwind scheme and numerical switch for plug preserva-
tion, Eq 2.5
c
tyieldplug = 1.
do k=1,kmax
      ku = min(k+1,kmax)
      ki = max(1,k-1)
      if (k .eq. 3) then
         tyieldplug = tyield(ki)
      endif
      safety = 1.050000
      plugl = (tyieldplug*safety)/taubot
      if (k.LE.plugl*kmax .AND. rxz(k).LT.tyield(ki)) then
         tyield(k) = ayield*ssinfy(ki)*solfrc(ki)**powyie
      else
         tyield(k) = ayield*ssinfy(ku)*solfrc(ku)**powyie
      endif
c
enddo
c
c ******* VISCOSITY PARAMETERS SLURRY ********
c
do k = 1,kmax
      ssinfv(k) = exp(betv*conlin(k))
enddo
c
c ******* Equivalent viscosity derived from shear stress for mixture:
c
rhoa = 0.0
do k = 1,kmax
      rhoa = rhoa+rho(k)*thick(k)
enddo
c***** Computation of the viscosity, with the upwind scheme. 2.6 *****
do k=1,kmax
      ku = min(k+1,kmax)
      ki = max(1,k-1)
c
      shear = abs(dudz(k))
      if (shear.eq.0.0) then
         vicmud(k) = 1E4
      else
         shear = abs(dudz(k))
c
```

```
        if (k.LE.plugl*kmax .AND. rxz(k).LT.tyield(ki)) then
            xmuwat(k) = ssinfv(ki)*watmu
            xmusol(k) = ssinfv(ki)*avic*(solfrc(ki)**powvic)
        else
            xmuwat(k) = ssinfv(ku)*watmu
            xmusol(k) = ssinfv(ku)*avic*(solfrc(ku)**powvic)
        endif
c
    xmu (k) = xmuwat(k) + xmusol(k)
    taubh (k) = tyield(k)*(1-exp(-shrco*shear))+xmu(k)*shear
    vicmud(k) = taubh(k)/shear
    vicmud(k) = vicmud(k)/rhoa
    endif
enddo
c
return
end
```

F.1.4. Slurry Yield Stress and Viscosity, Rheological Model 3

```
subroutine mudvic (zeta ,dp ,u1 ,dudz ,rho )
c***********************************************************************
c
c D e l t a r e s S o f t w a r e C e n t e r
c
c Module: Subroutine MUDVIC
c Function: Determine equivalent viscosity (VICMUD) derived from
c rheological model for water-clay-silt-sand flow.
c
c Method used:
c
c date : 07-01-2016
c Programmer : R.E. Uittenbogaard
c***********************************************************************
 include 'pardef.inc'
include 'dimens.inc'
include 'physco.inc'
include 'timefr.inc'
include 'turcoe.inc'
include 'hydarr.inc'
include 'sedarr.inc'
include 'turarr.inc'
include 'wrkarr.inc'
c
dimension u1 (*),dudz (0:kmaxd),rho (*),
+ safrc(1:kmaxd)
c
c ********** input parameters ******************
c
phissm = 0.6
ayield = 7.45E5
powyie = 5.61
yieldk = 0.9/0.6
Bvic = 17.7
visck = 0.75/0.6
shrco = 5000.
c
c**************** N E W - S L U R R Y ****************
c **************Vol. Frac SLURRY ******************
c********* phisol(k) from unesco
do k = 1,kmax
    safrc(k) = phisa(k)/phisol(k)
c ****** Plug length calc, retreiving the bottom shear stress ******
    if (k .eq. kmax) then
        taubot = MAX(1.,rxz(kmax))
    endif
enddo
c************** YIELD STRESS SLURRY ****************
tyieldplug = 1.
do k=1,kmax
    ku = min(k+1,kmax)
    ki = max(1,k-1)
c******Tyield calculation with numerical scheme switch for plug preservation, Eq 2.7****
    if (k .eq. 3) then
        tyieldplug = tyield(ki)
```

```
      endif
      safety = 1.050000
      plugl = (tyieldplug*safety)/taubot
      if (k.LE.plugl*kmax .AND. rxz(k).LT.tyield(ki)) then
          ty1 = ayield*((1-safrc(ki))*(phisol(ki)/
          * (1-safrc(ki)*phisol(ki))))**powyie
          tyield(k)= ty1*((1.-((safrc(ki)*phisol(ki))/
          * (yieldk*phissm))))**(-2.5)
      else
          ty1 = ayield*((1-safrc(ku))*(phisol(ku)/
          * (1-safrc(ku)*phisol(ku))))**powyie
          tyield(k)= ty1*((1.-((safrc(ku)*phisol(ku))/
          * (yieldk*phissm))))**(-2.5)
      endif
enddo
c ******* Equivalent viscosity derived from shear stress for mixture: Eq 2.8
rhoa = 0.0
do k = 1,kmax
      rhoa = rhoa+rho(k)*thick(k)
enddo
c
do k=1,kmax
      ku = min(k+1,kmax)
      ki = max(1,k-1)
c
      shear = abs(dudz(k))
      if (shear.eq.0.0) then
          vicmud(k) = 1E4
      else
          shear = abs(dudz(k))
c
          if (k.LE.plugl*kmax .AND. rxz(k).LT.tyield(ki)) then
              xmu1 = ((safrc(ki)*phisol(ki))/(1.-phisol(ki)))/
              * (1.+((phisol(ki))/(1.-phisol(ki))))
              xmu2 = 1.-xmu1*(1./(visck*phissm))
              xmu3 = (xmu2)**(-2.5)
              xmu(k) = (xmu3)*exp((bvic*(1.-safrc(ki))*
              * (phisol(ki))/(1.-phisol(ki))))*shear
          else
              xmu1 = ((safrc(ku)*phisol(ku))/(1.-phisol(ku)))/
              * (1.+((phisol(ku))/(1.-phisol(ku))))
              xmu2 = 1.-xmu1*(1./(visck*phissm))
              xmu3 = (xmu2)**(-2.5)
              xmu(k) = (xmu3)*exp((bvic*(1.-safrc(ku))*
              * (phisol(ku))/(1.-phisol(ku))))*shear
          endif
c
          taubh (k) = tyield(k)*(1-exp(-shrco*shear))+xmu(k)
          vicmud(k) = taubh(k)/shear
          vicmud(k) = vicmud(k)/rhoa
      endif
enddo
c
return
end
```